Hydrogel-Based Microfluidic System for Cell Culture

by

Michael C.W. Chen

B.Sc., Electrical and Computer Engineering, University of Waterloo, Canada, 2005

A THESIS SUBMITTED IN PARTIAL FULFILLMENT OF THE REQUIREMENTS FOR THE DEGREE OF

MASTER OF APPLIED SCIENCE

in

THE FACULTY OF GRADUATE STUDIES

(Biomedical Engineering)

The University of British Columbia

(Vancouver)

April 2009

©Michael C.W. Chen, 2009

Abstract

Traditionally, cell culture has been done in culture flasks or well plates where the volumes and length scales involved in the culture environment are many orders of magnitude larger than the size scale of individual cells. To better tailor medical care to an individual patient, it may be necessary to carry out genetic, physiological, and biochemical analyses on very small cell samples and to have an *in vitro* cell culture environment that more closely approximates the *in vivo* conditions.

A microfluidic device that integrates both cell handling and long-term 3-D cell culture techniques is presented. The designed microdevice traps cells with alginate, an ionically cross-linking hydrogel, which mimics the extra cellular matrix within our body. To encapsulate the cells, a solution of calcium ions is introduced in parallel with the alginate precursor cell suspension. Alginate hydrogel forms at the interface and as the region of gel grows it traps cells inside. This is a reversible process; the gel matrix can be dissolved and the cells can be released by the addition of ethylene-diaminetetraacetic acid (EDTA), a calcium chelator.

To show that the microfluidic device is reliable for long term mammalian cell culture, hepatocytes and breast tumor cells were cultured within the alginate gel layer inside the microfluidic device for more than two weeks. Hepatocytes were able to form three-dimensional aggregates within the microfluidic hydrogel environment. We further demonstrate the possibility of performing anticancer agent screening within this device. Breast tumor cells seeded in the microchannel were treated with doxorubicin, a common chemotherapy drug. Compared to controls, the doxorubicin inhibited cell proliferation.

In future, this system will have applications in cell-based testing and in studies involving small cell populations, such as cancer cells obtained from needle biopsies of tumors.

Contents

List of Tables

List of Figures

Acknowledgments

I would like to thank Dr. Karen Cheung for her inspiration, encouragement, patience and support over the last two and a half years. I am very fortunate to have this opportunity to work with her.

I would like to thank Dr. Mu Chiao, Dr. Eric Lagally, Dr. Jayachandran Kizhakkedathu and Dr. Boris Stoeber for sharing their lab equipments and being generous with their time and knowledge. I would also want to thank Dr. Helen Burt and John Jackson from UBC faculty of pharmaceutical science for their generous support.

I am also grateful to my dear friends: Vahid Bazargan, Jonas Flueckiger and Madhuja Gupta. This project would not have been possible without their help. We had a wonderful time together here.

Finally, I wish to express my genuine gratitude to my family.

Dedication

To my family

John Chen, Jane Chen and Robert Chen

CHAPTER 1

Introduction

1.1 From Semiconductors to Biomedical Microdevices

BioMEMS stands for *biological microelectromechanical systems*. It can be defined as *microelectromechanical systems* (MEMS) used for biomedical applications or life science. MEMS technology is originally based upon the photolithographic process used to make computer chips [1]. This technology enables production of low-cost, high-functionality devices for everyday use, like printer cartridges for ink jet printing and miniaturized accelerometers for automotive airbags.

BioMEMS promise the production of miniature, smart, and low-cost biomedical devices that could revolutionize clinical practice with improvements to surgical instruments, artificial organs, diagnostic tools, and drug delivery systems [2]. For cell biological studies, microdevices allow uniform nutrient and oxygen diffusion. They are the perfect tools to conduct cell-based experiments. BioMEMS techniques have great

impact on applications like tissue engineering, cell separation and culture devices, and high-throughput drug screening tool and cellular bio-detection [3].

By miniaturizing medical or biological devices, it is possible to work on small sample sizes and consider each cell as a unique identity. BioMEMS could bring the concept of Micro Total-Analysis System (μ-TAS) to reality. μ - TAS integrates devices to create a system to automate complex operations like cell sampling, culture, monitoring and detection.

1.2 Micro Total-Analysis System (μ-TAS)

The concept of Total-chemical-analysis system (TAS) first appeared in the 1980's. The goal was to simplify the analytical steps in chemistry and had samples flown from one step to the other without human intervention [1]. The concept of Micro Total-Analysis System (μ-TAS) was first introduced by Manz et al. in 1990 to describe advantages in chromatography and electrophoretic separation [4]. In 1991, Manz proposed the idea of using photolithographic techniques for producing microdevices for electro-osmotic flow separation. At the same time, Verpoorte microfabricated the first silicon microdevice for cell detection [2].

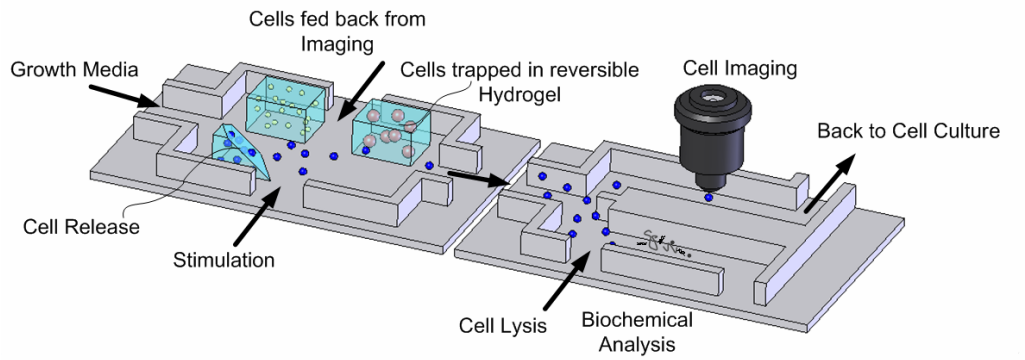

Figure 1.2.1: Micro Total-Analysis System can incorporate 3-D scaffolds for guiding cell growth, and transporting nutrients and reagents. Multiple functionalities for biochemical analysis (such as image-based analysis) can be integrated on a single device. [Courtesy: Jonas Flueckiger]

Most μ-TAS and Lab on Chip devices (LOC) device are based on the concept of microfluidics, which is the study of transport processes in microchannels. These are channels with a hydraulic diameter below 1 mm [2]. Chip-based capillary electrophoresis was one of first devices of this type. Similar to microelectronics, microfluidic technology makes it possible to fabricate highly integrated devices, which incorporate multiple components (valves, mixers, pumps and filters) for performing multiple tasks without human intervention (Figure 1.2.1). Some of the most common applications for μ-TAS and LOC devices include genomics, proteomics, clinical diagnostics, drug discovery and biosensors [5].

1.3 Cell Trapping in Microfluidic Chip

Immobilizing and manipulating cells are the fundamental cell-handling operations (separation, concentration and manipulation), which are required for almost all biological researches [6, 7].

Trapping cells in microfluidic chips poses many challenges because of the complex physical properties of cells. Various trapping mechanisms have been developed Some of the most commonly used methods are electro-osmosis, electrophoresis, dielectrophoresis, optical interference, acoustic standing waves, splitting laminar flows, mechanical obstacles and magnetic forces [6, 7] (Figure1.3,1).

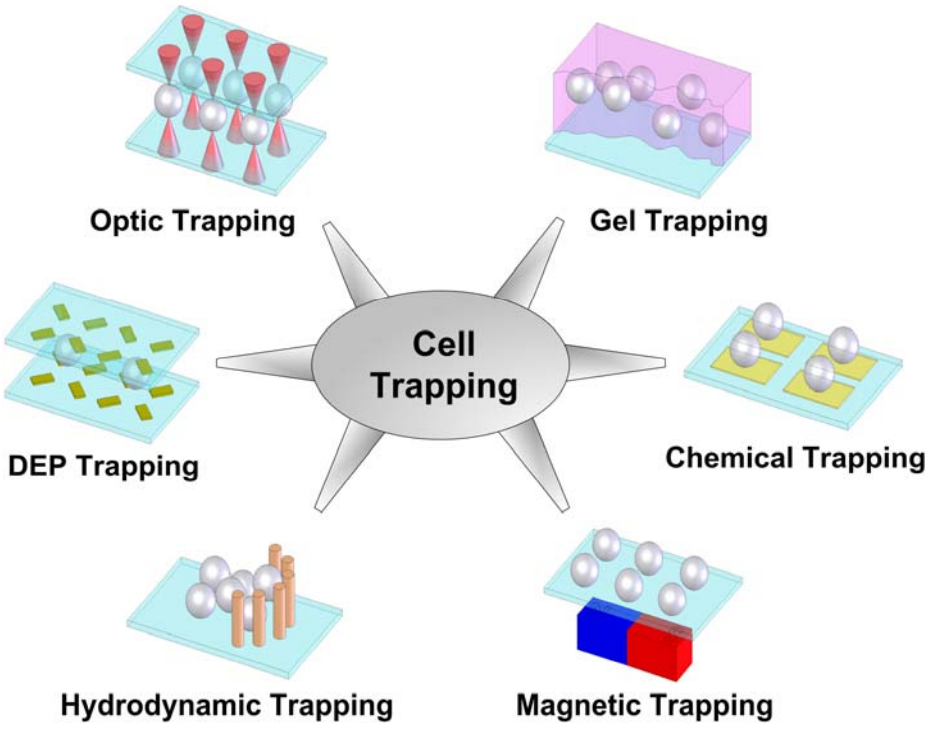

Figure 1.3.1: Cell-immobilization methods

1.3.1 Chemical Trapping

Channel surfaces are modified in topography or chemical composition, providing a discrete location for cell adhesion or protein attachment [7]. In recent years, surface modifications have been integrated with microlithography and microfluidics to achieve high precision cell trapping [8, 9]. In order to achieve an effective trapping surface, the coating material must be highly effective for all deposited cell types. It should also inhibit cell migration and overgrowth. However, there are some drawbacks of surface immobilization methods. They are only applicable to adherent cells, and once attached, the process is often irreversible [7].

1.3.2 Hydrodynamic Trapping

This type of trapping uses variations of surface topography to separate particles from a flow. Mechanical obstacles or barriers are tailored to the size of the particles to be captured, so the obstacles facilitate passage for fluids only [7, 10]. Besides using mechanical barriers, regions of low shear stress can also be used for retaining particles next to the moving fluid [11]. This method has an advantage over other trapping methods for rapid cell immobilization. In addition, these devices are often simple and inexpensive. The shortcomings of this type of device are that contact of the cells with a surface is not avoidable, which might lead to irreversible attachment. Also it is difficult to achieve a single particle deposition in hydrodynamic trapping devices. Array sites are often either empty or filled with aggregates [7].

1.3.3 Dielectrophoretic (DEP) Trapping

Polarizable particles such as cells, viruses, proteins or DNA molecules can be trapped within low-viscosity, low-conductivity solutions using dielectrophoretic trapping [12]. Dielectrophoresis is a phenomenon that uses a non-uniform AC electric field to exert a force on polarized neutral particles. The permittivity and conductivity of the particles and the liquid medium, varies as a function of the frequency of the applied AC field. Depending on the differences between these two values, trapped particles can either experience a positive (move toward the higher field) or a negative (repelled from the high field) dielectrophoretic force [13, 14]. Electric cages can be built that enable a single cell to be trapped within the flowing medium [15, 16]. A drawback of dielectrophoresis trapping is that cells are constantly exposed to strong AC fields, which causes Joule heating and sets up transmembrane voltage. Many conventional cell culture biomaterials such as collagen and alginate are too conductive and viscous to be used in this trapping method [7, 12].

1.3.4 Optical Trapping

An optical trap exerts two forces on a particle. One is the scattering force that drives the particle away from the light source by radiation pressure. The second one is the gradient force that pulls the particle into a high-intensity region of the light beam [7, 17]. Laser and infrared are some of the common light sources that are used in this trapping method [17]. To use optical trapping, particles need to be transparent. In addition, the refractive index of the particle should be different from that of the surrounding medium at the trapping wavelength. However, since each trap requires a

fixed amount of optical power, the number of traps are limited by the available power of the light source [7]. Another shortcoming is that the trapped cell can get severely damaged due to overheating by the light sources [17, 18].

1.3.5 Acoustic Trapping

With acoustic trapping, particles are subject to the mechanical force of a standing acoustic wave field that is generated by integrated ultrasonic transducers [7]. Acoustic force results from different densities and sound speeds between the particles and fluid. The magnitude of the force is linearly proportional to the particle volume and acoustic frequency [19]. This technique has been used for particle concentration, agglomeration and separation [7, 18, 19].

1.3.6 Magnetic Trapping

Magnetic trapping is applicable to diamagnetic particles as long as their magnetic susceptibility is different from that of the suspension [7]. Different configurations of magnetic traps can be fabricated on silicon or glass substrates using photolithography techniques to capture single cells [20]. To achieve high trapping efficiency, the cells can be magnetically labelled and the solution can be modified with paramagnetic ions. However, antigen labelling is an invasive technique and it denaturizes the sample involved [21].

1.3.7 Hydrogel Trapping

Cells immobilized in a polymer matrix are often regarded as being between "contact" and "contact free" immobilization. Hydrogels, in general, are very hydrophilic in nature. For example, agarose has a water content of more than 99 %. Gel trapping allows the liquid medium to have access to the whole cell surface whereas in chemical trapping or hydrodynamic trapping, cells often lean against a flat surface [7]. An advantage of this type of cell entrapment is that it does not require a continuous electromagnetic field or light source which prevents overheating and mechanical stress. Cells can be trapped and then cultured for extensive periods of time [7].

1.4 Traditional Cell Culture and 3-D Cell Culture in Microchannel

1.4.1 Traditional Cell Culture

Traditionally, petri dishes, culture flasks and well plates are used to maintain both non-adherent and adherent cell lines. For adherent cell lines, the cells are attached to the bottom of the culture flask and remain covered by a layer of cell culture media. For non-adherent cell lines, the cells are suspended within the culture medium. It is a complex method involving an array of supplies like petri dishes, pipettes, and conical tubes.

Recently, there has been increased interest in 3-D cell culture, in which cells are embedded in supporting structures that mimic the extracellular matrix (ECM) [22]. 3-D culture is biochemically and physiologically more similar to *in vivo* tissue, but is

technically challenging in terms of maintaining factors such as nutrient and waste exchange.

1.4.2 3-D Cell Culture in Microchannel

The ability to culture and reconstitute tissue structures and functions *in vitro* has a tremendous influence on clinical applications [23, 24].

Within mammalian tissues, cells are supported by a network-like structure, known as the Extra Cellular Matrix (ECM) that give tissues their mechanical strength and helps organize cell-cell communication. Led by cancer researchers, biologists are increasingly excited about 3-D cell cultures, where they have discovered patterns of gene expression and other biological activities that mimic *in vivo* conditions more closely and cannot be observed with traditional 2-D cell culture methods [22, 25].

Cell culture using microdevices has an advantage over traditional culture systems in terms of scale, efficiency and cost [25-28]. For instance, by using a microchip as a culture flask, rapid and secure exchange of culture media and reagents are possible while making continuous microscopic observations. In conventional experiments using a culture flask or petri dish, a long diffusion time is needed for added reagents to reach each cell and localized rapid chemical stimulation is nearly impossible [25, 29]. However, it is possible to realize rapid chemical stimulation with a microfluidic system [30]. In an integrated microfluidic chip, biochemical experiments can be carried out automatically by culture cells with chemical sensors [27, 28, 31].

Microfluidic systems which integrate 3-D cell culture techniques could provide a microenvironment that resembles the physiological environment more closely than can be

achieved by a traditional 2-D culture system. By carrying out experiments at the microscale, precise experimental parameters can be applied efficiently on small cell numbers or even to individual cells. This process will be beneficial in the areas of stem cell research and drug discovery.

Some of the work that has been done with culture cells inside microfluidic devices is listed in Appendix A.

1.4.3 Co-culture Multiple Cell Types

Our body operates as a society or ecosystem whose individual members are cells. Cell-cell interactions are critical to the development of multicellular organisms [32, 33]. Culturing multiple cell types within close proximity of one another has long been used in biological research. For stem cell research, a layer of feeder cells is traditionally co-cultured with the stem cells. The feeder cells provide ECM and specific factors necessary for the maintaining of stem cells in the undifferentiated state without losing pluripotency [34, 35]. Other examples like interactions between endothelial cells and muscle cells affect the expression of regulatory factors such as fibrinolytic and coagulation factors and angiogenic factors [36]. In pathological studies, cell–cell interactions can also implicate diseases like atherosclerosis in cardiovascular disease, denervation atrophy in skeletal muscle and alcoholic cirrhosis in liver disease [9].

1.5 Motivation of this Work

Conventional cell studies are conducted with large populations of cells; therefore measurement can only reflect average cell response values. This can lead to misinterpretation, since some biological mechanisms of a cell are in binary state ("on" or "off") [7]. For example, the majority of existing evidence suggests that, within individual cells, a gene is either maximally expressed or is not expressed at all [37]. Because of cellular heterogeneity, at an intermediate state a cell population will contain one portion in the "on" state and another in the "off" state. The relative numbers of "on" and "off" states often appear as a gradual change in the response of each individual cell. It is necessary to conduct genetic, physiological, and biochemical cell studies on a single cell and with a sufficient number of cells to obtain statistically meaningful data [7].

Traditionally, cell culture has been done with culture flasks, well plates, or petri dishes, which are many orders of magnitude larger than the cellular level. The culture flask is often continuously stirred or refreshed with cell culture medium. This action disrupts the microenvironment and creates stress on the cell due to stirring and oxygen bubbles [25, 38]. Culturing cells within a hydrogel matrix in a microfluidic device allows important factors to accumulate locally forming a stable microenvironment which is closer to *in vivo* conditions. It has been found that cells grow significantly slower in microchannels than in culture flasks [39]. This phenomenon is desirable in drug screening, where repeated measurement is required to detect cell alteration resulting from disease or the application of xenobiotics.

One of the major constraints on the size of *in vitro* tissue engineering is that there is no built-in blood supply; maintaining sufficient circulation of media can be

challenging. Oxygen and other nutrients can only diffuse through short distances before they are consumed [40, 41]. Microfluidic networks can be used for constructing and simulating blood vessels which mimic large-scale physiological properties [40].

In terms of expense, the use of microfluidic devices to conduct biomedical research is more economical compared to traditional cell culture methods. First, only a small amount of reagent and biological sample are needed to perform the experiment because the volume of fluids within the microchannel is very small (usually several nanoliters). This represents a significant cost reduction, especially when expensive reagents are required. Another advantage associated with small sample volumes is that the delivery and removal of soluble biochemical molecules in the extracellular microenvironment can be precisely controlled, which is desirable for highly parallel applications, such as drug discovery, genomics and proteomics [42]. Second, the fabrication techniques used to construct microfluidic devices are compatible with the current photolithography techniques used for microchips and are relatively inexpensive.

Different cell types are often co-cultured in close proximity within the same cell culture environment to achieve *in vivo*-like cell-cell interactions. Cell-cell interactions are important in the physiology of many organ systems such as the vasculature system (smooth muscle cell and endothelium) and the liver (hepatocyte and sinusoidal endothelium) [9]. Besides these interactions, cell-cell interactions are also implicated in the pathophysiology of many diseases. Many of the cellular interactions still remain a mystery [43]. One of the limitations of current co-culture systems is the inability to vary local cell-seeding density independently from the cell number [9]. By incorporating co-culture with cell trapping in micro-fluid chip approach, the accuracy of manipulating cell-

cell interaction can be improved by precisely controlling cell placement inside the cell culture environment.

Unlike other trapping methods such as laser trapping, acoustic trapping, magnetic trapping, and chemical trapping, immobilizing cells in hydrogels does not cause continuous shear stress on cell membranes and gives accurate control over the 3-D extracellular environment. This function can be further expanded to provide *in vitro* cellular co-culture and to better facilitate drug testing.

CHAPTER 2

Alginate Hydrogel Cell Encapsulation

2.1 Applications of Hydrogel

Hydrogels are polysaccharides characterized by high water content and porous polymer networks. They have been used extensively in various applications because of their changing physical properties after exposure to different solvents, ions, pH levels, electric fields, temperatures, or light intensities [44]. The effect of expansion or shrinkage is often utilized to construct artificial muscles or micro-valves in microfluidic systems. Other systems utilize porosity and high flow resistance of the polymer networks for analytical applications such as dialysis, electrophoresis, substance enrichment, and sample separation. Besides the applications mentioned above, hydrogels are also commonly used for cell trapping and drug delivery [44, 45].

2.2 Cell Encapsulation and Cultivation

The human body is comprised of approximately 100 trillion cells, with more than 260 phenotypes. These cells divide, differentiate and self-assemble into tissues and organs [46, 47]. There is always a great need for living cells to restore and maintain the functions of our body.

A variety of 3-D cell culture matrices, or scaffolds, have been developed for tissue engineering applications to restore or maintain tissue and organ functions (Figure 2.2.1) [46]. Unlike traditional cultures on flat surfaces, the 3-D scaffolds not only support cell viability but also metabolic activity and *in vivo* phenotypes.

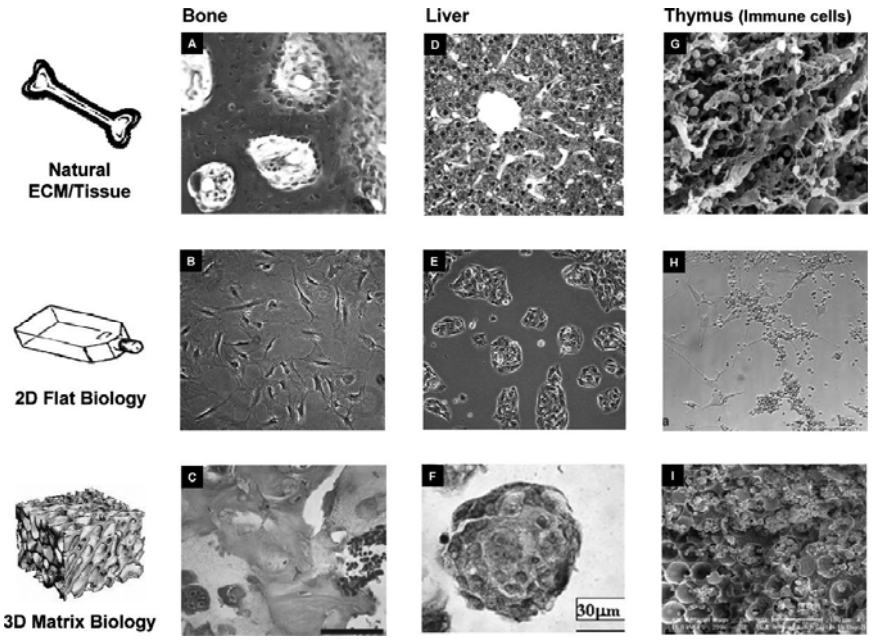

Figure 2.2.1: Different cellular structure formation in 2-D and 3-D scaffolds [48].

2.2.1 Naturally Derived Hydrogel

Naturally derived hydrogels, such as collagen, agarose, and alginate, have frequently been used in tissue engineering because they are either components of or have properties similar to the natural ECM [49].

2.2.1.1 Collagen

Collagen is an attractive material for biomedical applications since it is the main component of natural ECM and comprises 25 % of the total protein mass [49]. Collagen is long fibrous structural protein composed of three polypeptide chains, which wrap around one another.

The mechanical property of collagen fibres and scaffolds can be modified by introducing various chemical crosslinkers, physical treatments, and by blending them with other polymers. Collagen can be naturally degraded by metalloproteases, specifically collagenase, and the presence of cells [50].

2.2.1.2 Agarose

Agar gels are made of polysaccharides derived from seaweed or algae. Agar gels have been used on a daily basis as food thickeners and as a vegetarian gelatine substitute. They also have been commonly used in bacterial cell cultures and in electrophoresis for DNA separation [32].

One of the main components of agar gel is agarose, a linear polymer with a molecular weight of between 106 400 and 243 500 g/mol [51]. The hydrogel is a copolymer consisting of (1,3)-linked β-D-galactose and (1,4)-linked (3-6)-anhydro-α-L-

galactose. Agarose is a thermally reversible gel that solidifies around 35 °C and melts around 70 – 85 °C. The temperature depends on the polymer's molecular weight and concentration [52].

Although agarose has also been investigated as a cell encapsulation material for transplantation, its use in immunoisolation has not yet been demonstrated [53, 54].

2.2.1.3 Alginate (Alginic Acid)

Alginates are polysaccharides derived from seaweed. Similar to agarose, alginate has been commonly used as food stabilizers and thickeners, and as drug-releasing materials. Alginate is an ionically cross-linked gel. It consists of two types of copolymer blocks: (1-4)-linked β-D-mannuronic acid (M units) and α-L-guluronic acid (G units) [55]. The G units can be cross-linked with divalent cations such as Ca^{2+} or Ba^{2+} ion. This is a reversible process. The gel can be dissolved by the addition of chelating agents such as Ethylenediaminetetracetate acid (EDTA).

Alginic acid has been extensively used in cell encapsulation. For example, islet cell transplantation using alginate microspheres has been investigated as an approach for treatment of insulin-dependent diabetes and hepatocyte encapsulation has been investigated in the development of bioartificial livers [56, 57].

2.2.2 Synthetic Hydrogel

Synthetic hydrogels have the advantage of having controllable and reproducible chemistry and properties. They can be reproduced with specific molecular weights,

blocks structures, and crosslinking modes. These conditions, in turn, determine the gel formation and degradation dynamics [49].

Pluronic and *N*-isopropylacrylamide (NiPAAm) are some of the commonly used synthetic hydrogels.

2.2.2.1 Poloxamer

Poloxamer, poly(ethylene oxide)-poly(propylene oxide)-poly(ethylene oxide) (PEO-PPO-PEO), is a reversible tri-block copolymer. It is also known by the trade name Pluronic. Pluronic has been added to mammalian cell culture medium in low concentrations as a surfactant from 0.05-0.1%. The surfactant lowers the surface tension of the medium to prevent cell damage due to shear stress and to improves the efficiency of metabolic transport [58, 59].

The synthetic hydorgel self-assembles into micelles due to the hydrophobicity nature of the tri-block structures, a central hydrophobic PPO block sandwich using two hydrophilic PEO blocks. At higher temperatures, aqueous pluronic solutions undergo thermally activated reversible gel formation. The micelles form into a tightly packed arrangement. The gelling temperature varies with the polymer concentration and its molecular weight. For 15 wt% pluronic F127, the critical solution temperature is around 28 °C [60, 61].

Pluronic F127 has been approved by the Food and Drug Administration (FDA) for drug delivery applications. It has also been used as a tissue-engineering scaffold material for chondrocytes, epithelial cells, and fibroblasts [62, 63]. For better mechanical and chemical stability, pluronic can be modified to add covalent crosslinking [64].

2.2.2.2 N-isopropylacrylamide Polymers (NiPAAM)

N-isopropylacrylamide (NiPAAm) is a temperature-responsive polymer also known as PNIPA, PNIPAAM, PNIPAA or PNIPAm [65]. Similar to pluronic, NiPAAM is also a thermosensitive gel that exhibits a reversible phase transition [66]. In aqueous solutions, NiPAAM has a lower critical solution temperature (LCST) of 32–34 °C. When below the LCST, NiPAAM chains are hydrated and adopt a flexible and extended coil-like structure. Above the LCST, NiPAAM chains become dehydrated and collapse into a tightly packed conformation [67].

NiPAAm has already been used for 3-D culture of chondrocytes and pancreatic islets, and as a carrier for controlled drug delivery [63, 66, 68-70].

2.3 Chemical Structure of Alginate Hydrogel

Alginates (algins, alginic acids) are polysaccharides extracted from brown seaweeds such as *Laminaria hyperborea* and *Lessonia*. The first characterization of alginic acid was done by Stanford (patent 1881) [55]. It consists of two kinds of monomer units: (1,4)-linked β-D-mannuronic acid (M) and (1,4)-linked α-L-guluronic acid (G) (Figure 2.3.1) [55]. These two kinds of monomers are covalently linked in various arrangements along the polymer chain (e.g. -M-M-M-M-, -G-G-G-G- or -G-G-M-M-) (Figure 2.3.2). Alginate is typically composed of 100-3000 building units linked together with molecular weights of between 50 - 100,000 kDa [55].

a) b)

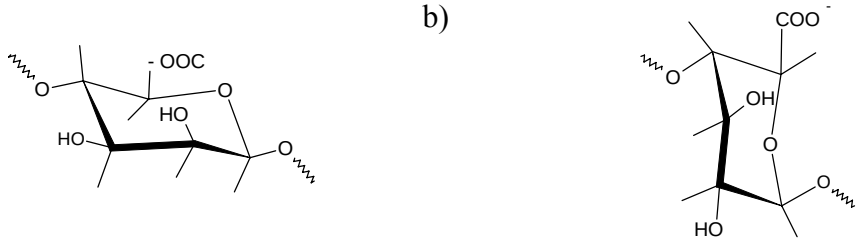

Figure 2.3.1: Monomers of alginic acid: a) (1, 4)-linked β-D-mannuronic acid (M) and b) (1, 4)-linked α-L-guluronic acid (G).

a)

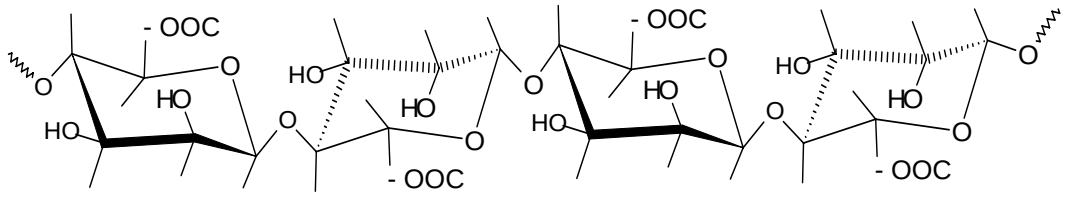

b)

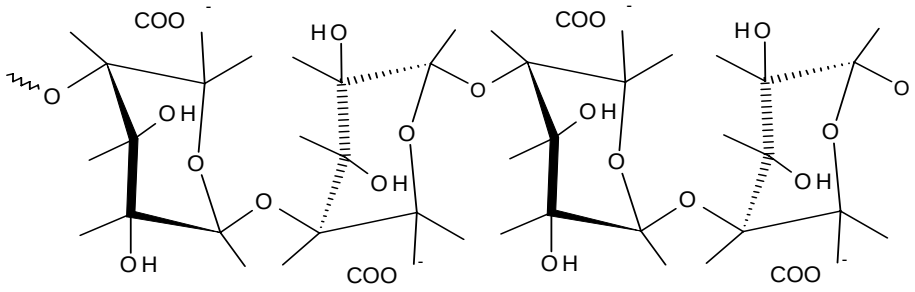

c)

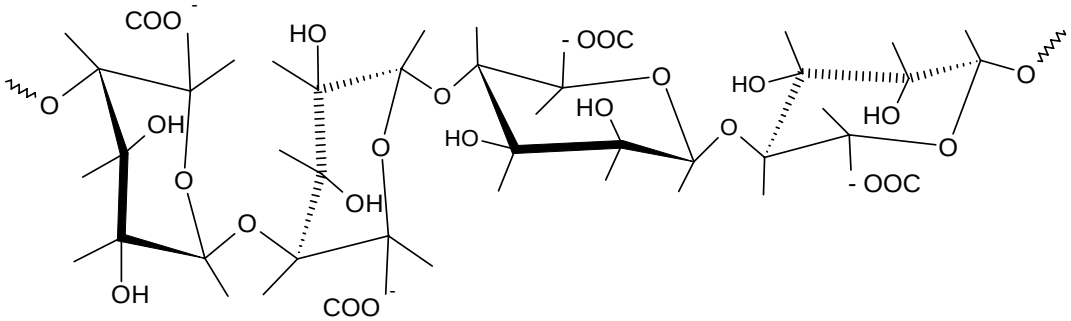

Figure 2.3.2: Molecular structure of alginic acid: a) -M-M-M-M-, poly M segment. b) -G-G-G-G-, poly G segment. c) –G-G-M-M-, mixed segment.

The arrangement of these two components and the relative amount (G/M ratio) depends on the source from which the alginate was derived.

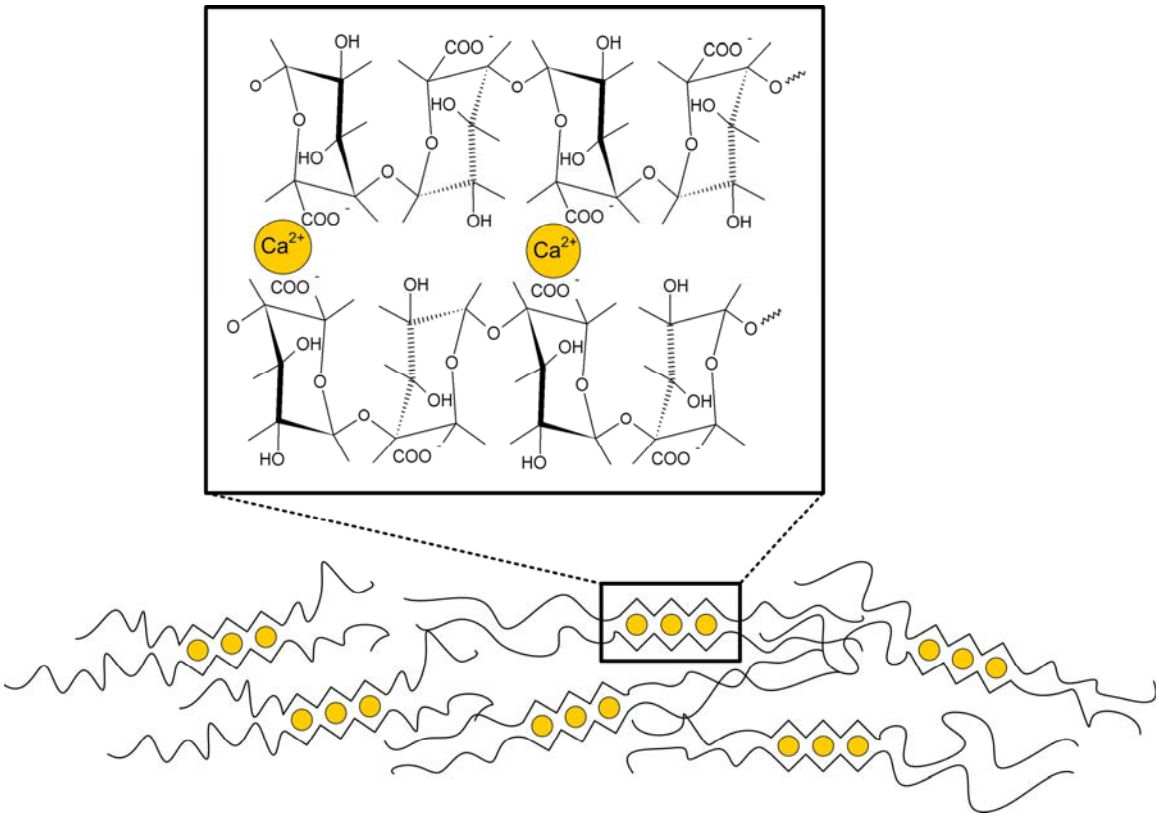

Figure 2.3.3: Bonding sites of Ca^{2+} ion. Only G blocks provide reactive carboxylic bonding sites for the Ca^{2+} ion. The Ca^{2+} ion attaches two different alginate strands together to form solid gel matrixes.

Two G blocks of adjacent polymer chains can be cross-linked with divalent cations, such as Ca^{2+} or Ba^{2+}, through interactions with the carboxylic groups in the polymer chain to form a gel network (Figure 2.3.3). Thus, overall gel stiffness and pole size are dependent on the polymer G/M ratio. High M content alginate chains are more

flexible than high G content alginate chains [4, 55]. The diffusivity within the hydrogel is lower in the high G alginate than in the low G alginate due to a smaller pole size [71].

The reaction between sodium alginate and calcium should be expressed as follows:

$$NaAlg + Ca^{2+} \rightleftharpoons CaAlg + Na^{+}$$

The reaction is very rapid. Calcium alginate forms on the surface almost instantly when the sodium alginate solution comes in contact with the Ca^{2+} ion.

2.4 Mechanical Properties of LF120M Sodium Alginate

The alginate used for this experiment was the LF120M type sodium alginate from FMC Biopolymer, Norway. The G/M ratio is around 35-45/55-65 %. With 1.0 wt% solution, the viscosity is around 150 mPa·s at 20 °C [72].

Alginate solutions are shear-thinning, non-Newtonian fluids. The viscosity decreases with increasing shear rate. The viscosity is dependent on solution concentration, polymer chain length, and solution temperature. At similar concentrations, the shorter the polymer chains the lower the viscosity. The viscosity also decreases with increases in temperature.

For mammalian cell culture, all labwares or materials used need to be sterilized to prevent infection and contamination. One of the most common methods of sterilization is autoclaving. Following the biology protocol, all solution used for the experiment, which includes the LF120M alginate solution, was heated to 121 °C for 20 minutes to inactivate all bacteria, viruses, fungi, and spores [73]. Alginic acid is a covalently-linked

long chain polymer. By autocalving, the polymer chain will be broken and the viscosity will be lowered. The polymer chain analysis showed that before and after autoclaving, the average molecular weight (Mn) of LF120M changed from 140,500 to 83,470 g/mole (measured with Gel Permeation Chromatography). The measured result was consistent with the viscosity measurement shown in Figure 2.4.1.

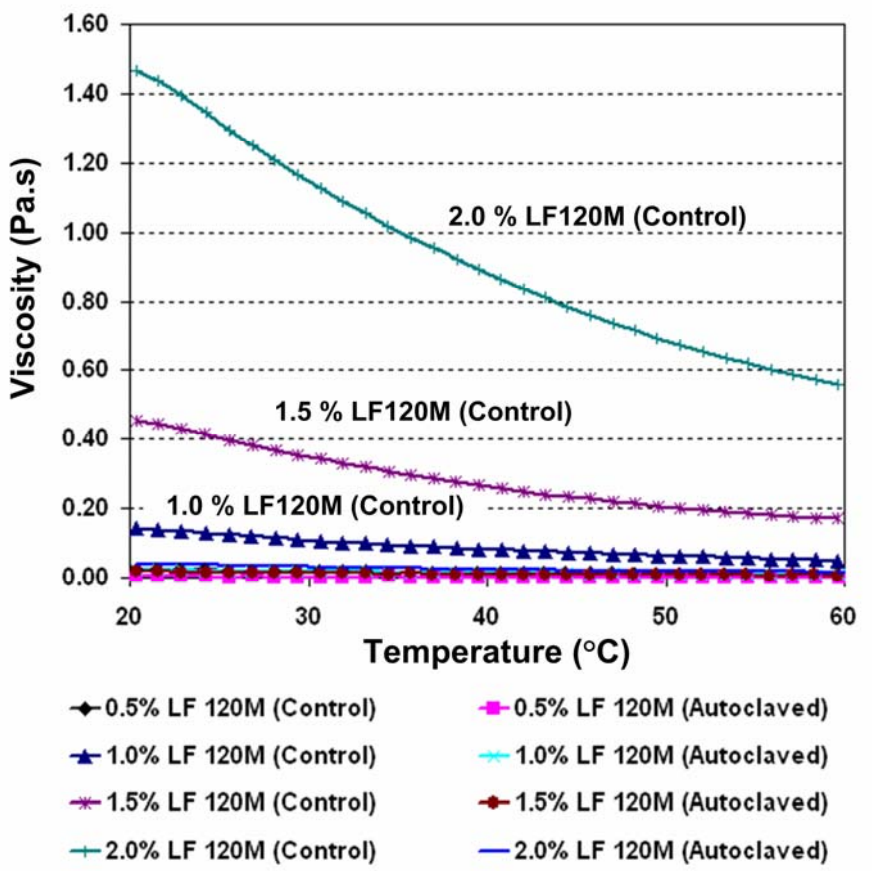

Figure 2.4.1: The viscosity of 0.5 wt%, 1.0 wt% 1.5 wt% and 2.0 wt% LF120M alginate solutions from 20 °C to 60 °C was measured with a Bohlin C-VOR rheometer. Each alginate solution was prepared in two different conditions: un-autoclaved and autoclaved at 17 psi and 120 °C for 20 minutes. After autoclaving, the solution was noticeably less viscous.

2.5 Alginate Gel Stability

It has been found that gel strength may vary with the kind of divalent cation used in the following order: $Pb^{2+} > Cu^{2+} = Ba^{2+} > Sr^{2+} > Cd^{2+} > Ca^{2+} > Zn^{2+} > Co^{2+} > Ni^{2+}$ [74]. However, in applications involving immobilization of living cells, toxicity is a limiting factor in the use of most ions, and only Sr^{2+}, Ba^{2+} and Ca^{2+} are considered nontoxic for these purposes.

A long-term alginate gel stability test was carried out. In this test, 1.5 wt% alginate solution was bought in contact with 40 mM and 100 mM of the $CaCl_2$ solution. Gel degradation could be affected by changes in polymer molecular weight (MW) [75], which can be altered during the sterilization process. Therefore, two of the most common sterilization protocols, autoclaving and UV sterilization, were incorporated as part of the test condition. A 200 μm wide gel slab was first formed inside the microfluidic channel and the channel was filled with a F12K cell culture medium. The microfluidic chip was placed inside the incubator at 37 °C and 5 % CO_2 level. The cell medium inside the channel was changed three times a week. The experiment showed that the LF120M gel type is very stable under these cell culture conditions. There was no sign of gel dissolution throughout the two-week period from visual measurements (Figure 2.5.1). However, the mechanical strength of alginate gel is expected to degrade over time [53].

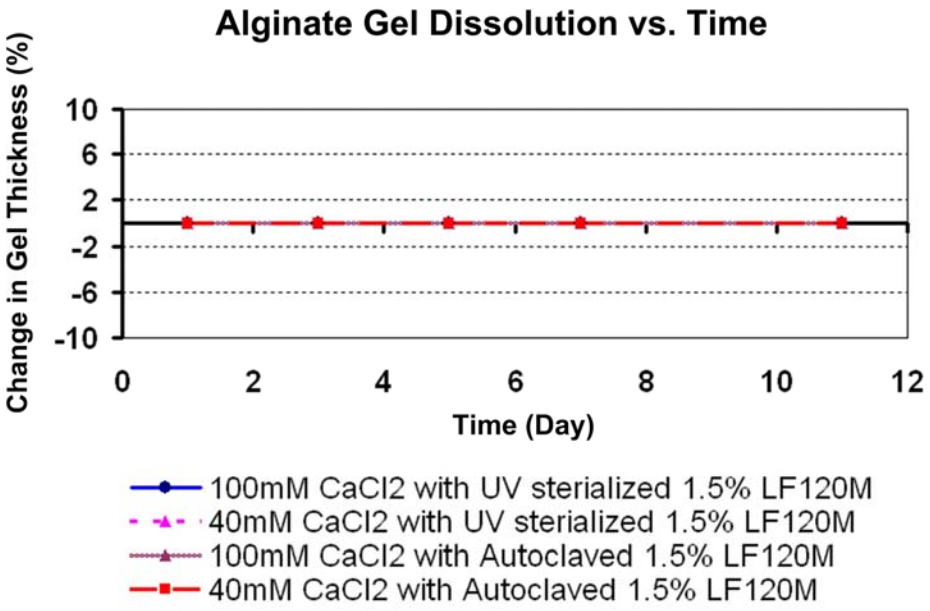

Figure 2.5.1: Stability of alginate in microchannel. The change in alginate gel layer thickness was measured every second day for 11 days. Alginate solutions were pre-treated with two different sterilization protocols: a) autoclaved at 121 °C for 20 minutes or b) exposed to UV light for 2 hours. 100 mM and 40 mM $CaCl_2$ solutions were used for each test condition. We found no signs of gel dissolution (0% change in gel thickness) from visual measurements.

CHAPTER 3

Microfabrication Technology

3.1 Polydimethlsiloxane (PDMS) Microfluidic Chip

In recent years, microfluidic systems have attracted a lot of scientific and industry attention. Early development is mainly based on conventional semiconductor materials and fabrication technology intended for integrated circuits. Using these technologies and materials is costly and imposes many limitations on fabrication and testing. Several alternative technologies using organic polymers have been investigated, one of which is polydimethylsiloxane (PDMS) [76-78].

Besides the advantages of being biocompatible, permeable to gas, and inexpensive, PDMS is also transparent to visible and UV light wavelengths ranging from 230 nm to 700 nm. This is ideal for biological applications since most of the fluorescence markers and the UV lights used for sterilization (~ 265 nm) are well within that range [77, 79]. In addition to these, PDMS has a low curing temperature (<100 °C), which can be easily achieved by conventional oven.

In combination with photolithography technology, 3-D PDMS microchannels can be made easily and rapidly by the replica moulding method. This technique is cost-effective, fast, and simple. A microchannel design can be turned into an actual device within 24 hours. Typically, 3-D channels are formed by exposing both PDMS layers to oxygen plasma and then bonding them immediately to a flat surface after the plasma treatment (see section 3.2) [78].

3.1.1 Chemical Structure and Property of PDMS

PDMS is one of the most commonly used silicon-based organic polymers. The chemical formula of PDMS is $(H_3C)_3SiO[Si(CH_3)_2O]_nSi(CH_3)_3$, where n is the number of the repeating monomer $[SiO(CH_3)_2]$ [80]. The structure of PDMS is shown in Figure 3.1.1.

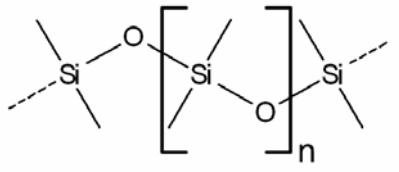

Figure 3.1.1: The backbone structure of PDMS

3.1.2 PDMS Curing

PDMS is cured by an organometallic crosslinking reaction between a base and a crosslinking agent [81]. A 10:1 weight ratio of base and crosslinking agent is typically used [82, 83]. The base, with a length of about 60 monomers, consists of a linear oligomer containing vinyl groups ($-HC=CH_2$) at the terminations [84]. The crosslinking

agents, with about 10 building blocks, sometimes have a hydrogen atom attached to the Si atom instead of a methyl group. This bonding site is designated as R in Figure 3.1.2. The curing agent also contains a platinum-based catalyst that catalyzes the addition of the Si-H bond across the vinyl groups, forming Si-CH_2-CH_2-Si linkages [81, 84].

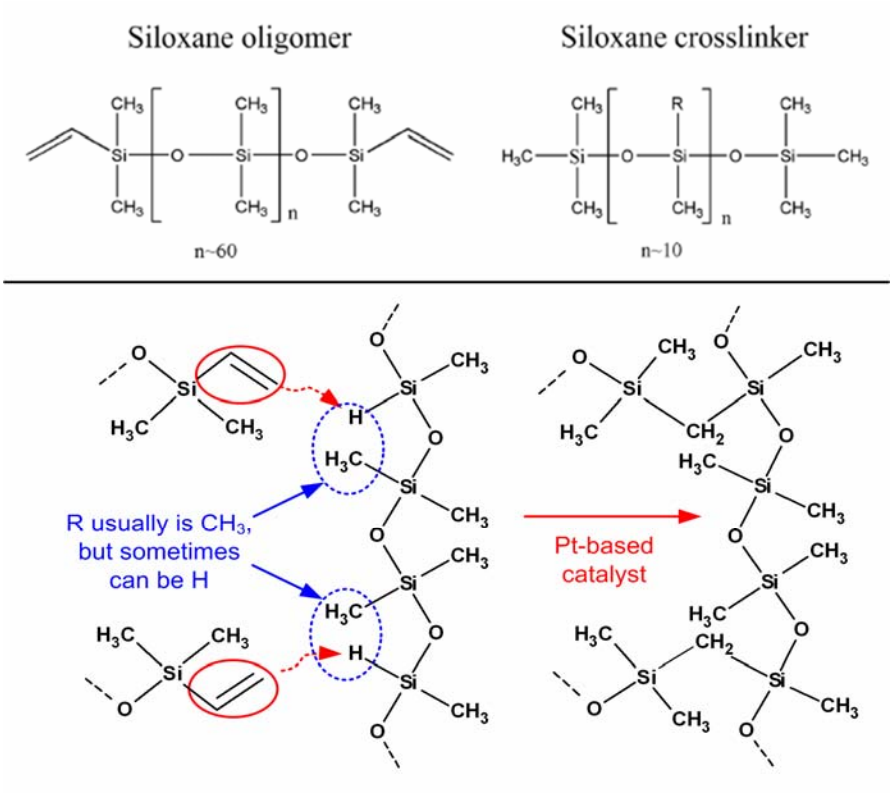

Figure 3.1.2: PDMS curing. The crosslinking agent consists of a siloxane oligomer with a length of about 10 units. At some of the bonding sites (R), the silicon atom has a hydrogen atom attached to it instead of a methyl group. The hydrogen atom will then react with the vinyl group of the base.

The properties of the cured PDMS are dependent on the ratio between the base and curing agent. The higher the ratio of the curing agent added, the harder the cured

PDMS becomes because more cross-linked elastomer is formed. After curing, the top and bottom of the PDMS layer remain smooth and flat.

For proper curing, the base and crosslinking agent need to be thoroughly mixed. The weighted PDMS is mixed with an AR-250 mixer from Thinky for five minutes and cured over a master in an aluminum foil dish. Dow Corning Sylgard 184 PDMS can be cured over a wide range of times and temperatures, varying from ~48 hours at room temperature to 10 minutes at 150 ºC [85]. The crosslinking time can be shortened with higher curing temperatures.

3.1.3 Diffusivity of PDMS Chip

3.1.3.1 Oxygen Supply

Oxygen supply is one of the most important parameters for cell culture. Because PDMS is highly porous, and microbioreactors have a high surface area to volume (SAV) ratio, the oxygen supply to the cultured cells from the atmosphere is sufficient; hence, there is no need to use an oxygenated culture medium [86]. The oxygen supplied by diffusion through the PDMS layer can be estimated with Fick's first law:

$$J = -D_{PDMS} \frac{\Delta C_{O_2}}{\Delta x} \tag{3.1}$$

where Δx , ΔC_{O_2} and D_{PDMS} denote the thickness of the PDMS chip, the oxygen concentration difference across the PDMS layer, and diffusivity of oxygen through the PDMS layer. D_{PDMS} is estimated as 4.1×10^{-5} cm^2/s [87, 88] and Δx equals 4 mm as measured. The typical oxygen concentration in a tissue culture medium is 0.22 μmol/ml,

assuming all oxygen is consumed by the cultured cells inside the channel so ΔC_{o^2} equals 0.22 μmol/ml [86, 89]. Based on these parameters, J is estimated to be 2.25×10^{-5} μmol/cm^2·s. The fabricated channel has a surface area of 0.1 cm^2. The amount of oxygen diffusing through this PDMS microfluidic device is calculated to be 1.353×10^{-4} μmol/min.

The oxygen consumption rate of MCF-7 human breast tumor cell type (6 nmol/min per 1million cells) [90] is used as an estimate for LCC6/HER2 breast tumor cell type used in this experiment.

Since the initial number of cells cultured in this microfluidic device is from 500 to 1000 cells (section 5.2.1), the estimated oxygen supply is more than an order higher than the oxygen consumption by the cultured cell lines. It can be assumed that a sufficient amount of oxygen can be supplied to this device by simple diffusion at the initial stage. As the cell proliferates, the culture medium needs to be circulated through the culture chamber to ensure sufficient oxygen is provided to the cells.

3.1.3.2 Nutrient Supply

Besides oxygen, the second most important nutrient in the cell culture is glucose. It provides the source of energy for metabolism. Even though PDMS is highly oxygen permeable, the same cannot be said about glucose. The permeability of PDMS (a highly hydrophobic polymer) to glucose is very low [91, 92]. Given that glucose is water soluble, one of the possible explanations is due to the hydrophobic nature of PDMS. The permeability of water into PDMS is generally considered very low [93]. Based on this

finding, the circulation of culture media through the microchip is essential for long-term cell culture.

Nutrient supply through continuous perfusion is discussed and demonstrated in section 5.2.3.

3.2 PDMS Bonding

The PDMS moulding process provides three of the four walls necessary for forming an enclosed channel as shown in section 4.4.2.2. The fourth wall is provided by bonding the PDMS replica to a flat surface. Bonding of a PDMS-based device is simpler than what is required for glass or silicon because high temperatures, pressures, and voltages are not required [94]. The adhering process can be reversible or irreversible [76].

3.2.1 Reversible PDMS Bonding

Reversible bonding occurs when a flexible PDMS piece is in contact with a flat surface making a weak van der Waals attraction [76, 95]. This method is fast and occurs at room temperature. The sealing is watertight but cannot withstand high fluid pressure (< 5 psi) [95].

3.2.2 Irreversible PDMS Bonding

One of the most common techniques for irreversible PDMS bonding to another flat surface is by oxygen plasma treatment. The flat surface can be either PDMS, glass, silicon, quartz, polystyrene, polyethylene or silicon nitride [76, 81].

PDMS contains repeating units of $[SiO(CH_3)_2]$. The methyl groups, $–CH_3$ at the PDMS surface are turned into silanol groups, –OH, when exposed to oxygen plasma. Since the silanol groups are polar in nature, they will make the treated PDMS surface temporarily hydrophilic. When these silanol groups are brought in contact with those on another surface, they condense and form a covalent O–Si–O bond after the loss of water molecules (Figure 3.2.1). This covalent bond is irreversible [76, 81, 95, 96].

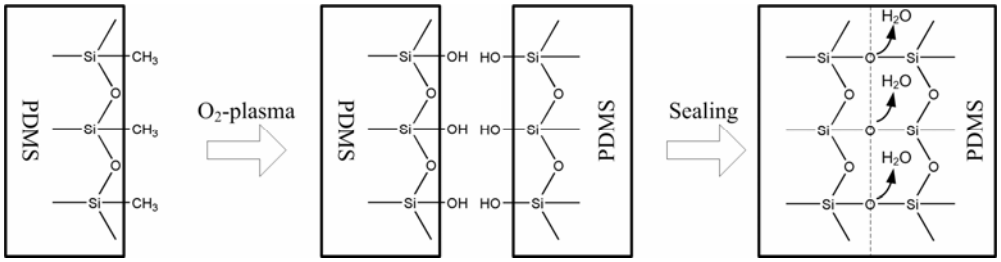

Figure 3.2.1: PDMS-PDMS bonding. After exposure to oxygen plasma, the methyl groups $–CH_3$ at the PDMS surface are turned into silanol groups –OH. When these silanol groups are in contact with one another, they condense and form a covalent O–Si–O bond after the loss of water molecules. A similar process can be applied between a PDMS surface and another flat surface made of either glass, silicon, quartz, polystyrene, polyethylene or silicon nitride [81].

The bonding strength is affected by the RIE power and exposure time during plasma treatment. At low power levels, the kinetic energy of ions incident on the substrate reduces. Low power level also reduces the electron acceleration within the plasma environment leading to a reduction in the radical density. As a result, less active sites (Si-OH groups) are available for surface bondage. With higher power levels, there

is an increase in the ion bombardment thus damaging the siloxane backbone. Overexposure may also cause an increase in silanol bond density and surface chain scission reactions, resulting in surface reorientation and cracking [95-97]. The damage is unrecoverable. The same can also be said about exposure time.

After the oxygen plasma treatment, PDMS becomes hydrophilic. However, hydrophobicity recovers if the treated samples are left in the air. The recovery mechanism is not yet fully understood. Some of the possible reasons are migration of a low molar mass species from the bulk to the surface, reorientation of polar groups at the surface into the bulk, condensation of silanol groups at the surface, external contamination of the treated surface, changes in surface roughness, and loss of volatile oxygen-rich species to the atmosphere [81, 96]. The surface wettability can be considered one of the indicators of bonding strength. A contact angle below 5 degrees is a general requirement for good bonding [95]. This implies that the bonding process should be carried out as soon as possible.

3.3 SU-8 Photolithography

Polymer micromolding is a common way to make microchannels because of the ease of processing, low cost, and bio-compatibility [98]. The moulds often require sub micron resolution and high-aspect-ratio. EPON SU-8, an epoxy-based negative photoresist, originally developed by IBM and sold by Shell Chemical, is ideal for this application [99, 100]. It has low molecular weight and can be spin-coated as very thick films up to 500 μm in a single coat. The photoresist can also assemble structures with thickness of up to 2 mm [81]. Similar to other types of negative photoresists, SU-8 has

good adhesion to various substrates such as Si, GaAs, InP, and glass. Additionally, it exhibits excellent thermal and chemical stability. Figure 3.3.1 shows the chemical structure of SU-8.

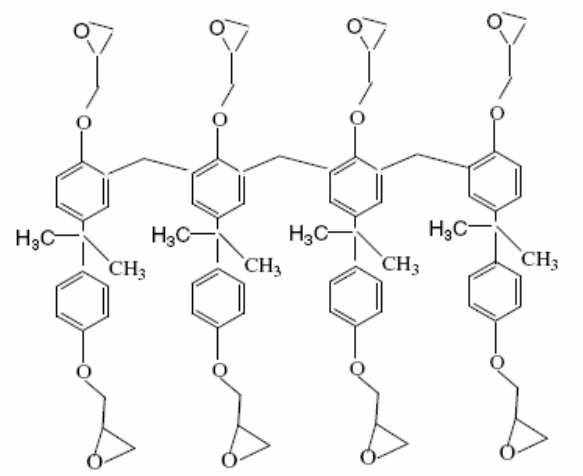

Figure 3.3.1: Molecular structure of SU-8. SU-8 is a highly functionalized molecule with 8 epoxy groups. After exposure to ultraviolet light, e-beam or x-ray, the epoxy resist will form a highly structured cross-linked matrix [101].

SU-8 belongs to the category of chemically amplified photoresists. Chemical amplification increases the sensitivity to the exposure energy. In the process, acid released by the exposure radiation diffuses during the post exposure bake step. The acid renders surrounding polymer soluble in developer [102, 103]. A single acid molecule can catalyze many deprotection reactions; hence, fewer photons or electrons are needed [104]. Acid diffusion is important not only to increase photoresist sensitivity, but also to ease edge roughness.

The absorption of SU-8 in the UV spectrum is very low, thus allowing the epoxy resin to achieve high aspect ratio; aspect ratio > 20 by using UV light in the 365 to 436 nm range, and >80 by using electrons and x-rays. Exposure introduces a high level of cross-linking density, converting the SU-8 photoepoxy into a strong polymer [99, 100, 103]. SU-8 can be dissolved by solvents such as most ketones, toluene, and diacetone alcohol.

The SU-8 patterning procedures are listed below [81, 100, 103, 105]:

1. **Wafer Preparation:** The wafers are cleaned with a RCA-1 cleaning procedure. Si wafers are placed in the *Piranha solution*, a 3:1 mixture of sulphuric acid (H_2SO_4) and hydrogen peroxide (H_2O_2). When finished, the wafers are thoroughly rinsed with DI water. The cleaned Si wafers go through a dehydration bake to eliminate any moisture trapped inside the substrate. The Si substrate can also be cleaned with oxygen plasma. This treatment would also increase the adhesion of the photoresist to the wafer.
2. **Spin coating SU-8 photoresist:** To have a uniform layer of epoxy, the SU-8 photoresist is spun for at least 40 sec. Because SU-8 2075 from MicroChem is highly viscouse, the wafer must go through a ramping step before reaching the final spin speed. The thickness of the coating depends on the spin speed and viscosity of the epoxy.
3. **Soft bake:** The soft bake evaporates the solvent and cures the epoxy before exposure. This prevents the substrate from sticking to the mask. The baking time varies according to the thickness of the feature. Mild temperature ramping is required to prevent bubbling of the resist film.

4. **Exposure:** UV radiation is used to initiate the cross-linking of the SU-8 photoresist. The exposure time has to be adjusted depending on the coating thickness. The exposure pattern is defined by the mask, which defines which areas of the resist surface will be exposed to radiation and those that will be covered.
5. **Post Exposure Bake (PEB):** SU-8 is belongs to the category of chemically amplified photoresist. The PEB catalytically completes the photoreaction initiated during exposure and reduces mechanical stress formed during soft bake and exposure.
6. **Development:** Development involves the washing away of the non-polymerized SU-8. The developer solution is made of PGMEA (propylene glycol methyl ether acetate). The development time is dependent on the thickness of the feature. The developed wafer is washed with isopropanol and blow-dried with nitrogen gas.
7. **Hard Bake:** Hard bake may be applied after development to improve thermal, physical, and chemical stability. Because of the different thermal expansion coefficient between resist and substrate, gentle temperature ramping and slow cooling are required to prevent cracking.

CHAPTER 4

Microfluidic Chip Design

4.1 Drag and Laminar Flows

A PDMS-moulded channel is often rectangular in shape. In order to approximate the flow through the rectangular channel (where the height and width are comparable), the concept of hydraulic diameter D_h is used. The hydrodynamic diameter is given by:

$$D_h = \frac{4 \times A}{P_{wet}} \tag{4.1}$$

Hydrodynamic diameter allows engineers to approximate flows though irregular channel shapes as those flows through channel with circular cross section. P_{wet} stands for *wetted perimeter*, which is the perimeter of the channel that is in direct contact with the flow, while A is the cross-section area where the flow goes through. If the channel is completely filled, P_{wet} and A are simply the diameter and cross-section area of the channel [106].

For flows in a long straight channel with a constant cross-section, Reynolds number, the ratio of the inertial forces to the viscous forces, is a good indication of whether the flow is laminar or turbulent [106-108]. The Reynolds number is given by:

$$\mathrm{Re} = \frac{\rho D_h u}{\eta} = \frac{D_h u}{v} \tag{4.2}$$

As discussed above, D_h is the hydrodynamic diameter. u is the mean flow velocity of the flow in the channel, η is the dynamic viscosity of the fluid, v is the kinematic viscosity, and ρ is the density of the fluid.

Table 4.1-1 lists the relationship between the Reynolds number and flow profile for circular pipe flow.

Table 4.1-1 Reynolds Number. It can be used to determine if flow is laminar, transient or turbulent. The information is for circular pipe flow.

Re < 2000	**Laminar**
2000 < Re < 4000	**Transition (Turbulent or Laminar)**
Re > 4000	**Turbulent**

For our application, most of the solutions used have properties similar to water (dynamic viscosity = 0.001 Pa·s, density = 1,000 kg/m^3). The designed microchannel was 90 μm high, 800 um wide and 1000 um long, which gives the D_h of 161.80 μm. The mean flow velocity of the injected solutions was controlled at around 200 μm/sec.

With this information, the Reynolds number can be calculated ($\mathrm{Re} = 0.03236 \approx 10^{-2}$). With a Reynolds number <<1, the flow profile remains laminar as shown in Figure 4.1.1.

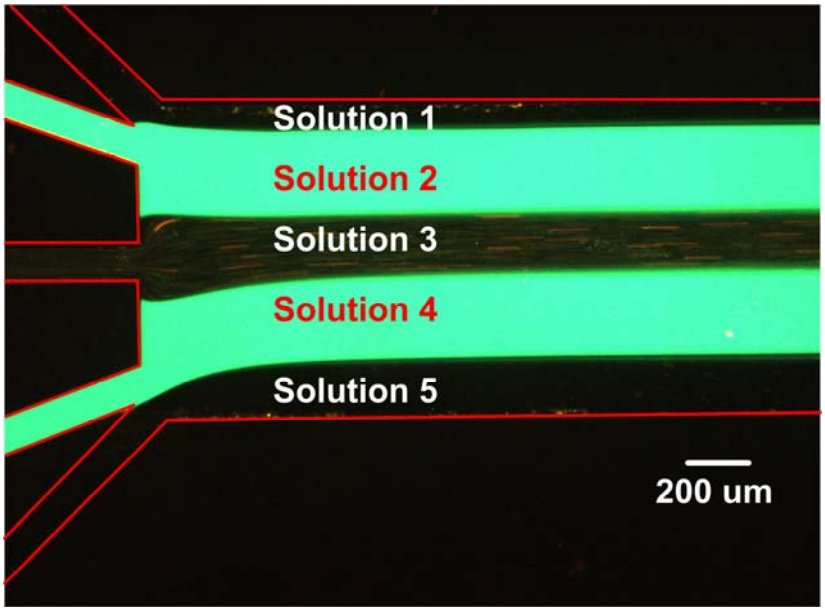

Figure 4.1.1: Laminar flow in the microfluidic chip. By applying appropriate settings (mean flow velocity ≈200 um/sec and solutions with dynamic viscosity similar to water), we can create multiple streams of laminar flow inside the microfluidic device.

4.2 Cell Trapping

By using the phenomenon that an alginate solution will form a 3-D gel matrix after contact with the Ca^{2+} ion, we can trap various cell types inside. The microfluidic chip contained a minimum of three inputs: 40 mM $CaCl_2$ solution, 40mM EDTA solution and 1.0 wt% alginate solution.

The input ports were connected to a pneumatic flow control unit (see section 5.2.2). Because of a much higher viscosity of 1.0 wt% alginate solution compared to the $CaCl_2$ solution at room temperature, $CaCl_2$ was injected at a higher flow rate than alginate to keep the interface near the center of the channel.

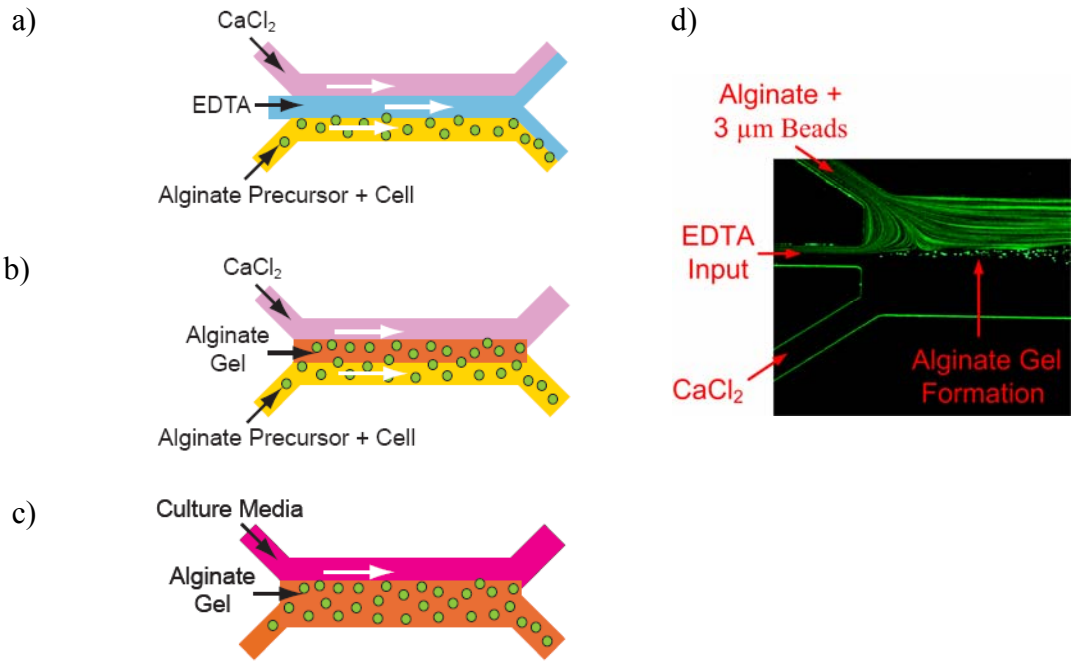

Figure 4.2.1: Operation principle. a) Cells were suspended in alginic acid (1.0 wt% LF120M buffered in tris-HCl). We used the other two inlets for EDTA and $CaCl_2$. At the loading step, a laminar flow of 40 mM EDTA was used to separate the Ca^{2+} ion from contacting with the alginate flow. b) After the EDTA flow was suppressed, the 40 mM Ca^{2+} ion solution was brought in contact with the alginate phase. The gel matrix started to grow from the boundary into the alginate stream with cells trapped inside. c) Once the gel formation step was completed, cell medium was introduced into the channel. d) The actual picture taken from the microfluidic device with 3 µm fluorescence beads added to the alginate solution.

The cell suspension was prepared with 1.0 wt% LF120M alginate solution and culture media. At the initialization stage, EDTA was used as a separation fluid to prevent unwanted gel formation and channel clogging. Once the steady state was reached, EDTA flow was suppressed and the alginate solution was brought in contact with the Ca^{2+} ion. The gel matrix started to form at the boundary as the gel slab grew toward the alginate flow stream with the cells trapped inside.

All solutions, except culture media, were prepared with 50mM tris-HCl buffer solution with a 7.8 pH level and passed through a 5.0 μm Millex syringe filter (Ireland) to remove particulates during preparation before autoclaving.

After the cells were trapped, the culture medium was introduced into the channel for long-term cell culture. The whole cell-trapping process is shown in Figure 4.2.1.

4.3 Diffusion and Gel Growth

4.3.1 Gel Formation

Depending on the degree of polymerization, the average molecule weight of alginate is in the rage of 50 - 100,000 kDa, and the molecule weight of the Ca^{2+} ion is 40.08 Da. Since the molecule weight of the alginate polymer is much heavier than the Ca^{2+} ion, the gel formation was controlled by the speed in which the Ca^{2+} ion diffuses from the contact interface through the alginate gel block and reacts with the alginate to form new gel layers (Figure 4.3.1).

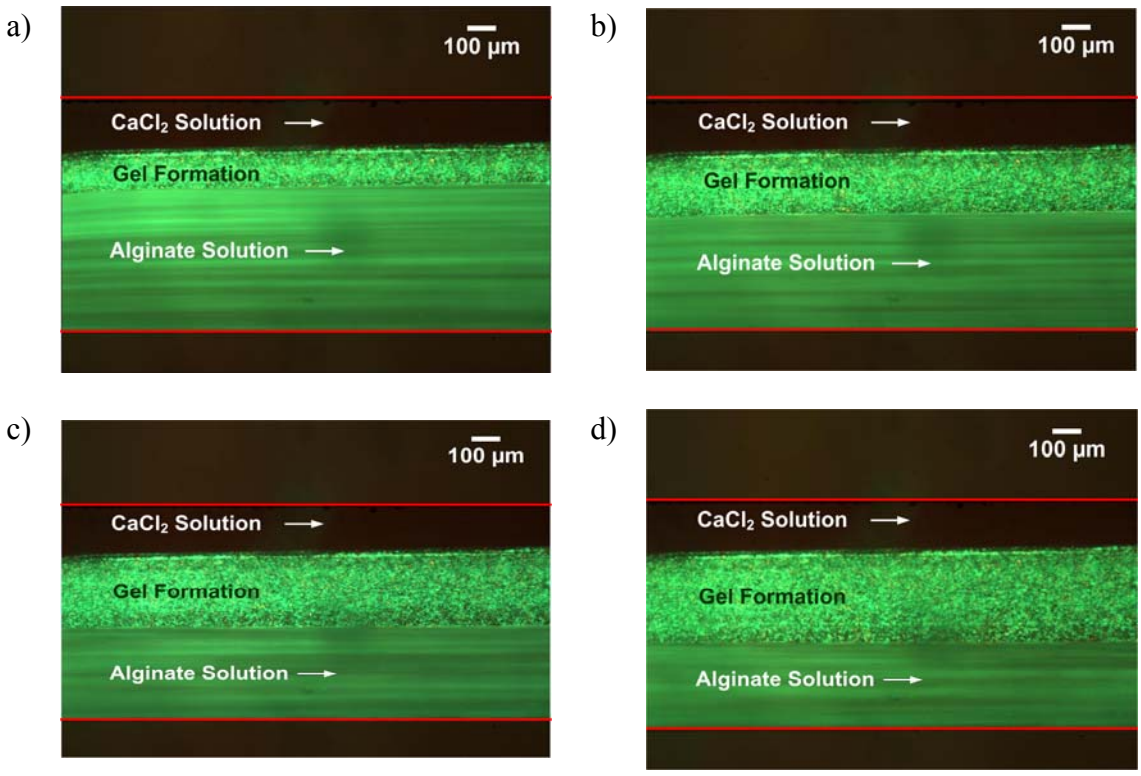

Figure 4.3.1: Gel formation a) 10 seconds, b) 30 seconds, c) 50 seconds, and d) 70 seconds after alginate phase was brought in contact with $CaCl_2$. The picture shown is done with 1.0 wt% LF120M alginate gel with 40 mM $CaCl_2$ solution. 0.7 µm fluorescent beads were added to the alginate solution as an indicator.

The relation between the formed gel thickness and time is shown in Figure 4.3.2, where the x-axis represents the time in seconds and y-axis represents the formed gel layer thickness in micrometers. The result of the graph can be explained with Fick's first Law:

$$J = -D\frac{\Delta C}{\Delta x} \tag{4.3}$$

where J is the mass flux and Δx represents the distance that the Ca^{2+} ion is diffusing through. D is the diffusion coefficient of Ca^{2+} ion in the newly formed gel layer and ΔC is the concentration gradient between the calcium stream and alginate stream. Since

we assume all the Ca^{2+} ions are consumed during gel formation (zero concentration at gel-alginate boundary), ΔC will equal the calcium solution concentration (cbulk($CaCl_2$)).

If we assume gel growth rate is slow compared to diffusion times of ions in aqueous solution and we have approximately a linear concentration gradient of free Ca^{2+} ions (plus the ones bounded to alginate, but they don't count for the diffusion calculation) across the gel layer, the quantity of Ca^{2+} ions that diffuses is:

$$\frac{dnCa^{2+}}{dt} = D\frac{cbulk(CaCl_2)}{\Delta x} \times A \tag{4.4}$$

A is the cross section area where the calcium ions diffuse through. The quantity of Ca^{2+} needed to make a new layer of gel depends on the thickness of the new layer:

$$dnCa^{2+} = dx \times A \times q \tag{4.5}$$

q is the volume density of Ca^{2+} binding sites. By rearranging equation (4.4) and (4.5), and combining all constants into p. Following expression for gel growth rate can be derived:

$$\frac{dx}{dt} = \frac{p}{x} \tag{4.6}$$

The constant p takes the form of diffusion constant. A higher ion concentration (cbulk($CaCl_2$)) means a larger p value, which results in faster gel formation.

Equation (4.6) can only be considered as an approximation. For a more accurate model, the diffusion time of calcium ion in alginate gel and the effect of convection should not be ignored ($D \approx 7.92 \times 10^{-10} m^2/s$ at 25°C in aqueous solution [109]).

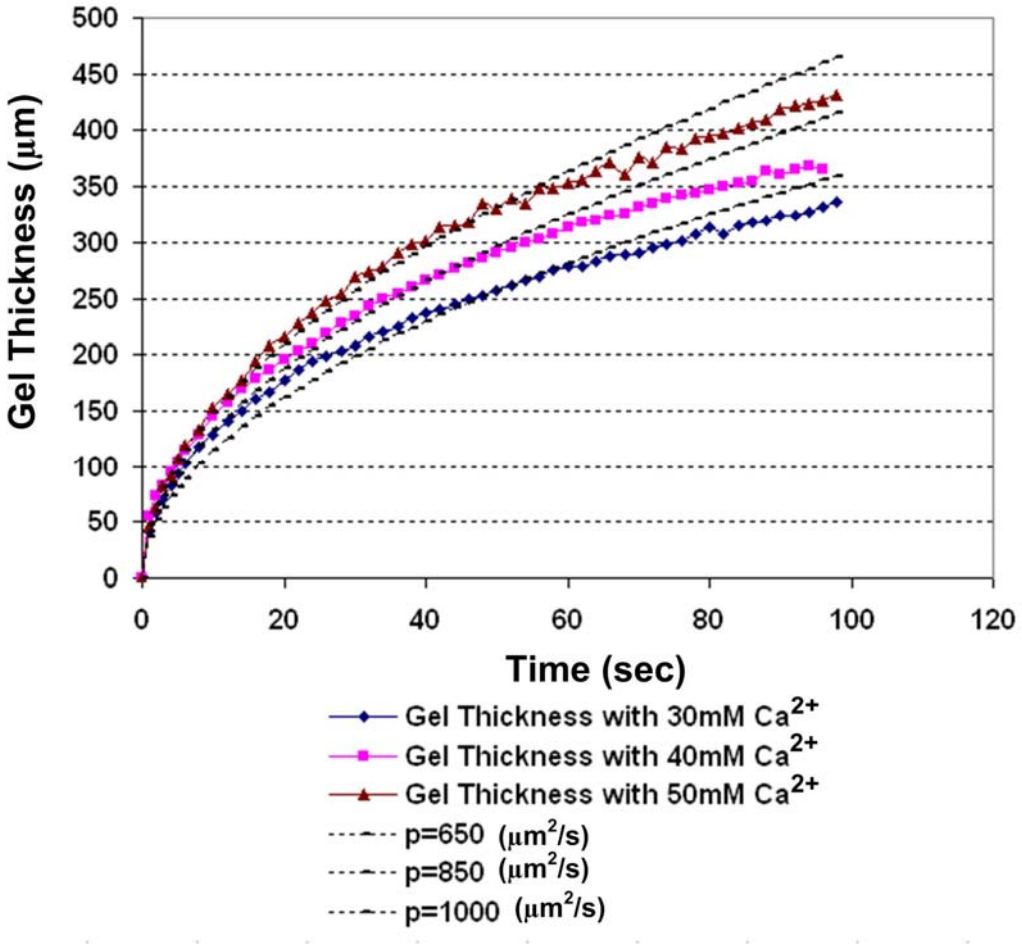

Figure 4.3.2: Alginate gel growth rate increased with higher Ca^{2+} ion concentrations. The 1.0 wt% LF120M solution was prepared with 50 mM tris-HCl pH 7.8 buffer solution. The growth rate decreased with increasing gel thickness.

4.3.2 Gel Dissolving

The goal of this project was to design a microfluidic device that can perform reversible cell trapping. After cells are trapped and cultured inside the alginate gel, they can be released by reintroducing EDTA back into the channel. EDTA is a strong chelating agent which binds to metals ions (Ca^{2+}) via four carboxylate and two amine groups. By reintroducing EDTA, the chelating agent will deprive the calcium ion and

dissolve the alginate gel.

Unlike the gel formation, where the calcium ions diffused through the gel block and formed new gel layers at the opposite flow stream, EDTA dissolved the gel block at the EDTA / gel slab interface. If we maintained a continuous flow stream of EDTA solution, the gel block was dissolved at a constant rate. As the EDTA concentration increased, the dissolving rate increased (Figure 4.3.3). The dissolving rate can be fitted in a straight line:

$$\frac{dx}{dt} = -r \tag{4.7}$$

dx/dt represents the change of gel thickness over time and r is the gel dissolving rate.

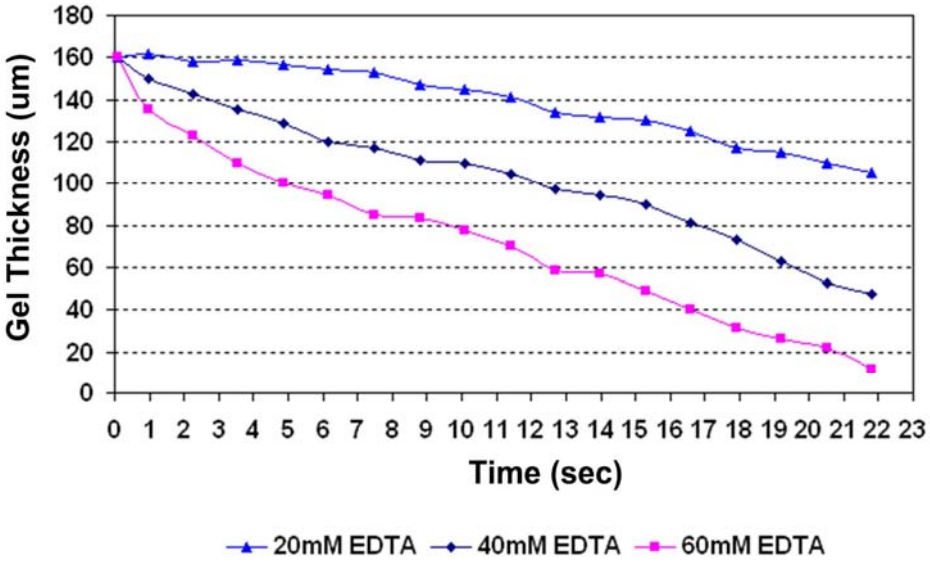

Figure 4.3.3: Alginate gel dissolving rate. Alginate gel can be dissolved by reintroducing EDTA, a chelating agent, back into the channel. A 160 µm gel layer was preformed within the channel for this test. The experiment was done using various concentrations of EDTA solution, which were buffered with tris-HCl. The average flow speed of EDTA stream was ≈150 µm/s.

4.4 Microfluidic Chip Design Realization

4.4.1 Chip and Mask Design

There are two main considerations for designing the fluidic chip: main channel dimension and the number of inlets. The device was designed for trapping and long-term culture of mammalian cell lines, LCC6/HER2 breast cancer cells, HMVEC endothelials, HepG2 hepatocytes, and HFL1 fibroblasts. The cell size varied from 10μm to 40μm in diameter. Since LCC6/HER2 and HepG2 cell lines proliferate and form 3-D clumps inside the gel matrix (section 5.3), the channel height was designed be at least 3 to 4 times the size of the used cell line to prevent clogging, minimize shear stress and provide enough cell culture space. The width of the channel was intended to fit the microscope viewing window and prevent channel collapsing.

There were two types of channel patterns used. One had three independent inputs and the other one had five independent inputs. The patterns are shown in the figure below (Figure 4.4.1).

a) b)

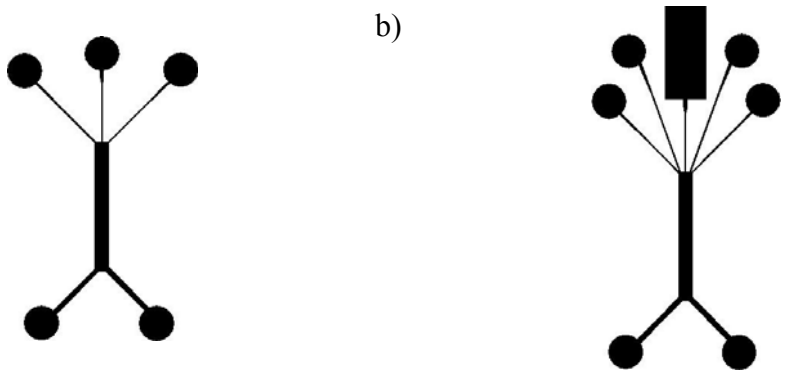

Figure 4.4.1: Channel design: a) 3 input and b) 5 input design used in this project. The main section of the channel was 800 µm wide, 90 µm high and 1 cm long.

The 3-inlet design was mainly used for gel characterization such as gel forming and dissolving rate measurement. The 5-inlet design was used for single cell type or multiple cell type co-cultures.

4.4.2 Micro-Fabrication Process

4.4.2.1 SU-8 Master Mould

The designed microfluidic device with minimum features of 100 μm,was fabricated in the AMPEL nanofabrication facility, University of British Columbia (UBC).

Because SU-8 is highly transparent to i-lines (365 nm), the exact wavelength provided by the cleanroom mask aligner, the patterned sidewall can be very vertical for thicknesses of up to 100 μm. The epoxy also exhibits excellent chemical stability, adhesive strength and resistance against stress corrosion [110]. It is the ideal patterning material to use as the master mould for our PDMS chip.

For our fabrication process, the following cleanroom equipment and material was used:

- **Canon PLA-501F double-side 100 mm mask aligner:** It is designed to work with 4" wafers. The light source was a Hg lamp (USHIO 250W, Super High Pressure Mercury Lamp) with the wavelength at i-lines (365 nm).
- **Laurell WS-400B Spin Processor:** The spinner provides automated ramping functions with a maximum spin speed of 8000rpm. It is ideal for photo-resist coating.
- **Trion Plasma Enhanced Chemical Vapour Deposition (PECVD):** The machine comes with a 300 watt, 300 kHz bottom powered electrode. It was used for the wafer cleaning process and PDMS bonding with a glass substrate.

For mould fabrication, we used the standard SU-8 fabrication process mentioned in section 3.3. SU-8 2075 from MicroChem, USA was chosen because of its ideal operating characteristics for a feature height of around 100 μm. The recipe used for fabrication is shown in Appendix B.

4.4.2.2 PDMS Channel

The PDMS used was the Sylgard 184 from Dow Corning. The fabrication process followed the procedure discussed in section 3.1. The base and crosslinking agent (10:1 ratio) were thoroughly mixed before pouring onto the master. Before placement inside the oven, the samples were placed inside desiccators for removing air bubbles created during pouring.

Dow Corning Sylgard 184 PDMS can be cured over a wide range of temperatures as discussed in section 3.1.2. For our experiment, the PDMS was placed inside the oven

at 50 ºC for 24 hours. The curing temperature was set at a lower temperature to prevent the SU-8 pattern from cracking due to the different thermal expansion coefficient between the SU-8 pattern and Si wafer.

Based on experience, the PDMS was cured within 2 hours at 50 ºC. Applying a longer baking time was to ensure thorough curing and prevent uncured PDMS chain effects biocompatibility (section 5.1.2). For PDMS-glass bonding, the Trion PECVD machine located in the UBC cleanroom was used. The microchannel fabrication process is shown in Figure 4.4.2 and Appendix B

The completed chip is shown in Figure 4.4.3. The finished chip was 1.5 cm wide, 2.5 cm long and 0.3 cm high, which fits perfectly into standard 6-well plates.

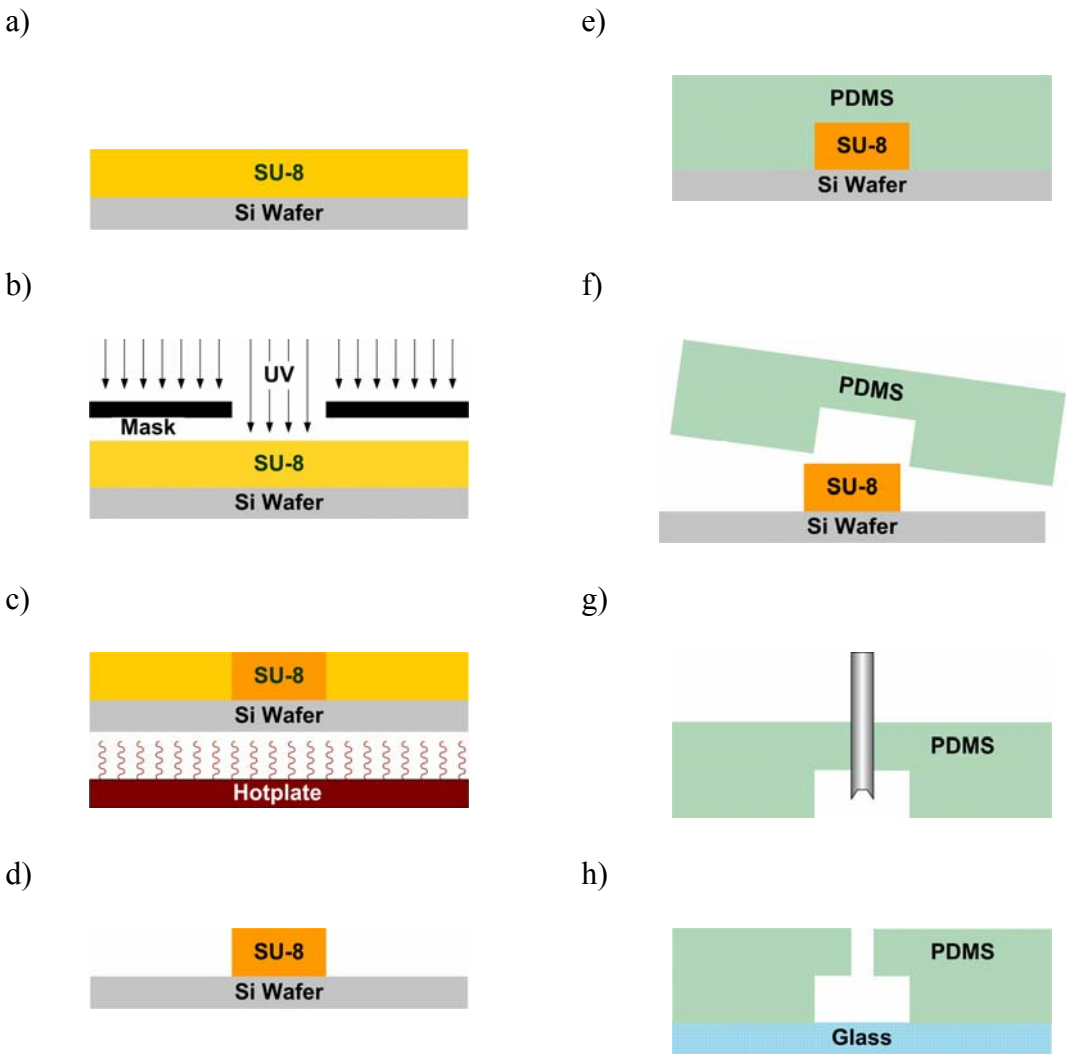

Figure 4.4.2: The fabrication process of the microfluidic chip: a) spin coating photoresist, b) UV exposure, c) post exposure bake, d) developing, e) PDMS curing, f) mould release, g) punch input and output holes, and h) PDMS-glass bonding.

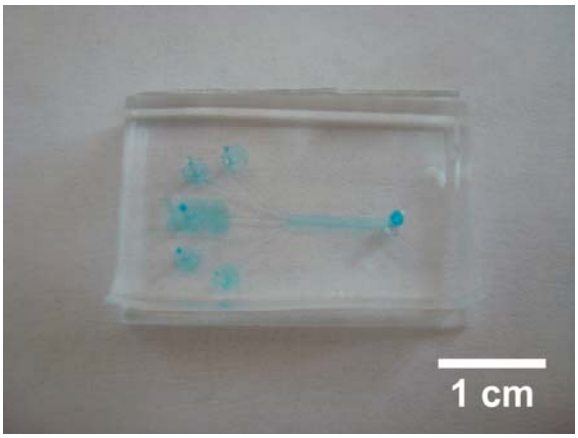

Figure 4.4.3: The finished chip was 1.5 cm wide, 2.5 cm long and 0.3 cm high with a main microchannel that was 800 µm wide, 90 µm high and 1 cm long. The channel was injected with blue dye for visualization.

4.4.3 Polyethyleneimine Coating (PEI)

Hydrogels typically have weak adhesion to surfaces; the same can be said about calcium alginate on glass substrate [44]. When gel adhesion is weak, bending and shifting of the gel slab is observed. This uncontrolled gel movement is undesirable during various stages of the experiment.

The shifting of the gel wall causes a leakage flow of the calcium solution between the gel and channel wall, which results in an irregular gel shape during gel formation. Here, the culture media needs to be circulated through the culture chamber for long periods of time; a weak gel-surface linkage causes cell samples to be flushed out in the middle of the experiment. At the end of the research stage, alginate gel was dissolved and cells are released in a controlled manner. Instead of a gentle release, weak adhesion causes samples to be washed away in a sudden burst.

In order to prevent the problems mentioned above, improving adhesion between the alginate gel and glass surface was necessary. It can be done by coating the surfaces with a thin layer of polyethyleneimine (PEI).

PEI is a cationic, non-toxic organic polymer, which is commonly used in DNA analysis and transfection of eukaryotic cells [111-113]. It is water soluble and has a strong affinity for protons due to a large number of nitrogen atoms of amino groups [114, 115]. The basic chain structure of PEI is $[-CH_2-CH_2-NH-]_n$. In aqueous solutions, the nitrogen atoms of amino groups combine easily with H^+ to form $[-CH_2-CH_2-NH_2^+-]_n$. The chemical structure is shown in Figure 4.4.4. Since alginate is negatively charged, there is a strong interaction between positively charged, PEI-coated surfaces and alginate gel layers [44].

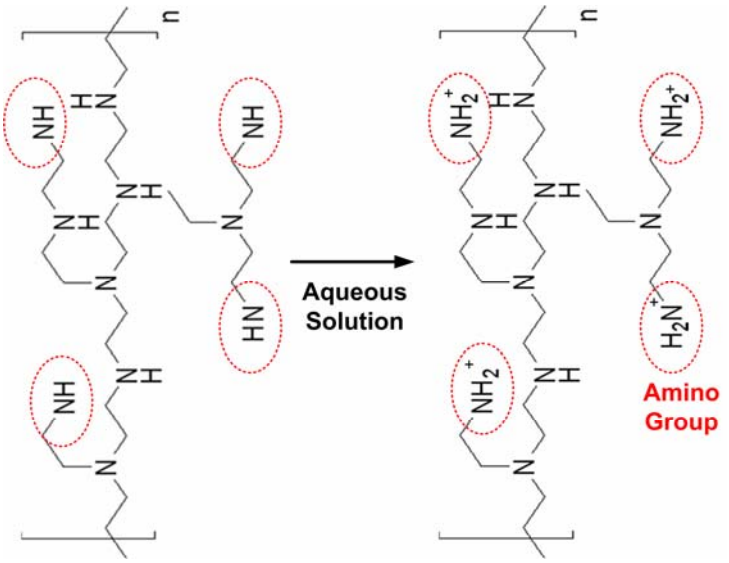

Figure 4.4.4: Molecular structure of PEI. The basic chain structure of PEI is $[-CH_2-CH_2-NH-]_n$. In aqueous solutions, the nitrogen atoms of amino groups combine with H^+ to form $[-CH_2-CH_2-NH_2^+-]_n$.

For coating the sample, an aqueous solution of 0.5 wt% PEI (50 % (w/v), MW 750,000, Sigma Aldrich) and 1 M NaCl (the addition of salt into polyelectrolyte system causes deposition in thicker layers of polyelectrolyte chains [116]) was prepared and used to fill the channel for 24 hours following the bonding of the microfluidic chip. Afterward, the channels were thoroughly rinsed with water with a syringe pump at the rate of 0.01 ml/min for 20 min. The excess PEI solution was removed; otherwise, it would cause polymerization of the alginate solution during the experiment (Figure 4.4.5).

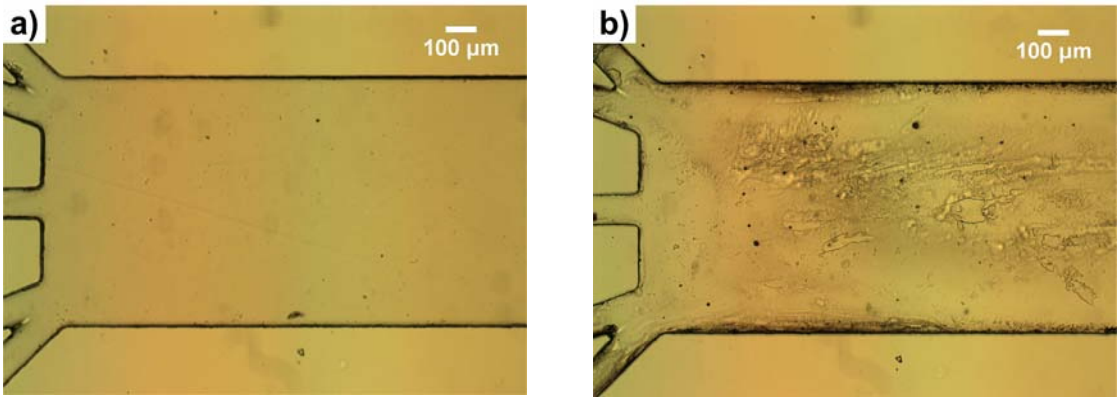

Figure 4.4.5: Excess PEI solution cause alginate solution to polymerize. After coating, the microchannel needs to be thoroughly rinsed with water. a) Thoroughly rinsed PEI-coated channel and b) not rinsed PEI-coated channel filled with 1.0 wt% alginate.

Because PEI is positively charged (polar) in nature, contact angle measurement becomes a good indication of the PDMS surface treatment. After the coating procedure, the PDMS surface turns from being hydrophobic to hydrophilic. The immobilization of PEI on PDMS surface may due to the result of van der Waals interaction [117]. The contact angle measurement is shown in Figure 4.4.6. The interaction between PEI and

glass surface is expected to be ionic (glass is a negatively charged surface) [118]. Because glass substrate is strongly hydrophilic by default, the same measurement cannot be done with the PEI-coated glass surface.

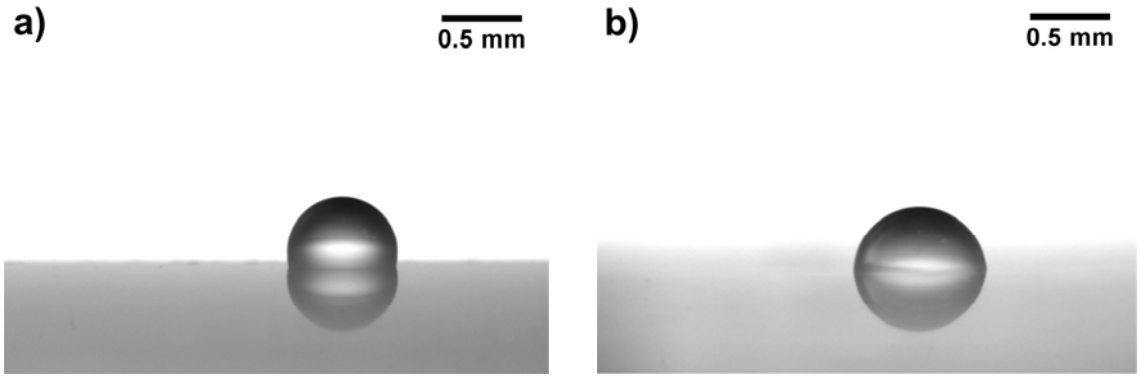

Figure 4.4.6: The static contact angle measurement shows that the original a) hydrophobic PDMS surface (contact angle 90° – 110°) changes to being b) hydrophilic (contact angle 70° – 80°) after PEI coating.

It is expected that the polymer layer degrades with each gel formation and dissolution process; the surface treatment has to be renewed [44]. Quantitative analyses on the polymer degradation in cell culture media have been tried; there is no observable static contact angle difference between coated and non-coated surfaces. However, a dynamic contact angle difference can be observed even after the PEI-coated PDMS slab is submerged in cell culture media and incubated for 48 hours. Because culture media contains more than 30 nutrients, ions, and proteins, the actual explanation for why no static contact angle difference can be observed remains unknown. Since all the microfluidic chips can only be used once, renewing the surface coating is never considered.

CHAPTER 5

On-Chip Cell Culture

5.1 Biocompatibility Test

5.1.1 Food Dye Coloring

For visualizing flow profile, FD&C Blue No.1 and Red No. 40 food coloring were added to the EDTA and $CaCl_2$ solutions.

Blue no. 1, also known as Brilliant Blue FCF, is a synthetic food colorant derived from coal tar [119]. The dye is water soluble with maximum absorption at about 630 nm [120]. The dye is certified as a safe additive in the European Union and United States and is often found in dairy products such as ice cream and soft drinks [121].

Red no. 40, which also goes by Allura Red AC, is a water-soluble synthetic food dye. Its maximum absorbance is around 503 nm [122]. Similar to Blue no. 1, Red no. 40 is also derived from coal tar. It is approved by the European Union and by the Food and

Drug Administration in the United States for use in puddings, dairy products, beverages, and confections [121].

To ensure that the food coloring did not affect the cell viability during the experiment, a biocompatibility test was carried out using HFL1 fibroblast cells. The experiment set up is shown in Figure 5.1.1 and summarized in the following steps:

1. Prepared HFL1 cell suspension with concentration of 1 million/ml.
2. Dispensed 100 ml suspension into each well, resulting in a total of 100,000 cells per well.
3. Added 1.5 ml of culture medium (Ham's F12K) in each well.
4. Added 25 µl of food coloring in each well.
5. Placed the 6-well plate inside the incubator (5 % CO_2 at 37 °C)
6. Performed cell viability readings every 24 hrs, 48 hrs, and 72 hrs.

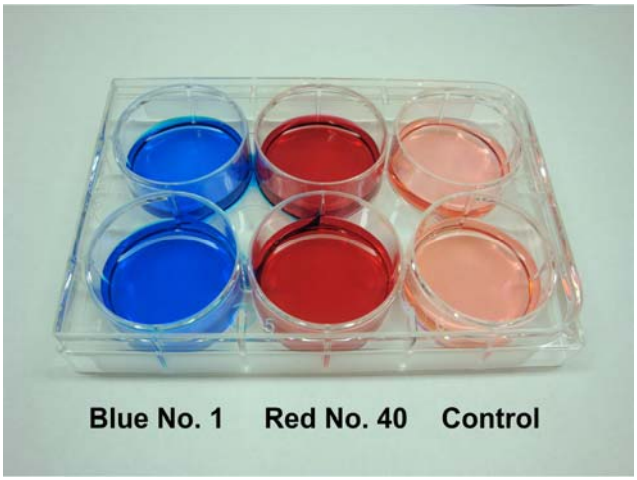

Figure 5.1.1: Experimental setup of food dye compatibility test. Each well contained 1.5 ml of culture medium and 100,000 HFL1 fibroblasts. The 6-well plate contained one control group and two experimental groups with 25 µl of Blue No.1 and Red No. 40 food dye.

The biocompatibility test ran for three days. The cells were removed from each well and live/dead assays were performed with trypan blue. More information about live/dead assays is discussed in section 5.2.4. The test showed that the food colors used did not affect cell viability (Figure 5.1.2).

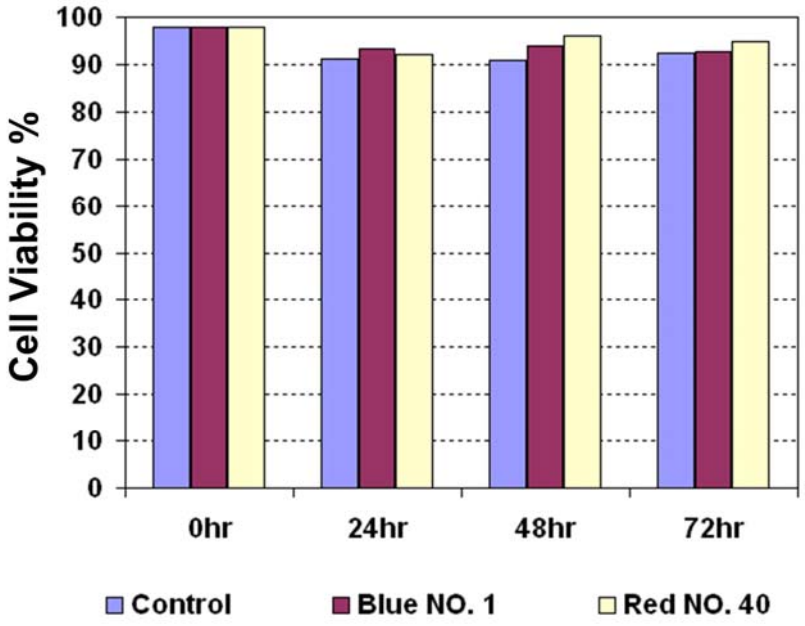

Figure 5.1.2: Cell viability reading using trypan blue after cells were exposured to food coloring.

5.1.2 PDMS Curing

PDMS is well known as an excellent soft material for soft lithography. It is especially known for its biological usage due to its low curing temperature, fast curing, and non-toxic nature [85, 123]. However, uncured PDMS elastomer is very sticky and viscous to work with.

At the beginning of the experiment, the cell viability inside the microfluidic channel was unexpectedly low. We suspected that the PDMS base and curing agent may seep out from not fully cured PDMS sidewalls. To find a proper curing time for PDMS moulding, a series of biocompatibility tests related to PDMS curing were carried out.

A sequence of PDMS pallets were made from 6-well culture plates with various curing times at a 50 °C curing temperature. The PDMS was cured at lower temperature than specified by the PDMS datasheet (50 °C instead of 80 °C) to prevent the SU-8 pattern from cracking due to different thermal expansion coefficient between the SU-8 layer and the Si substrate. The curing time of PDMS pallets was from 1-13 hours. The experimental set up was similar to the one carried out with food coloring shown in the previous section. It is described below and shown in Figure 5.1.3:

1. Prepared HFL1 cell suspension with concentration 1million/ml.
2. Dispensed 100 ml suspension into each well with a total of 100,000 cells per well.
3. Added 1.5 ml of culture medium (Ham's F12K) in each well.
4. Pre-cured PDMS pallet was plated inside the well.
5. Placed the 6-well plate inside the incubator (5 % CO_2 at 37 °C)
6. Performed viability every 24 hrs, 48 hrs, and 96 hrs with trypan blue (see section 5.2.4 for more information about viability assay).

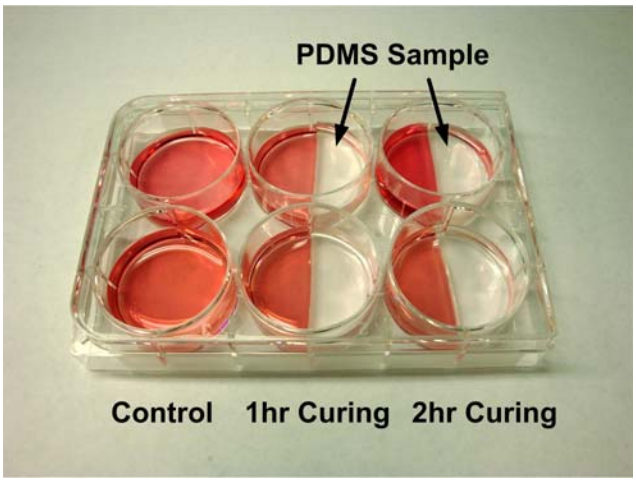

Figure 5.1.3: Experimental setup of PDMS curing compatibility test. The cured PDMS disks were placed inside a 6-well plate, pre-seeded with 100,000 HFL1 fibroblast cells. Each plate contained 2 wells of control group for comparison.

From the experiment, it was been found that there is a significant drop of cell viability with PDMS at a 50 °C curing temperature when curing time is less than three hours (Figure 5.1.4). This result gives a good reference for setting up proper fabrication protocols.

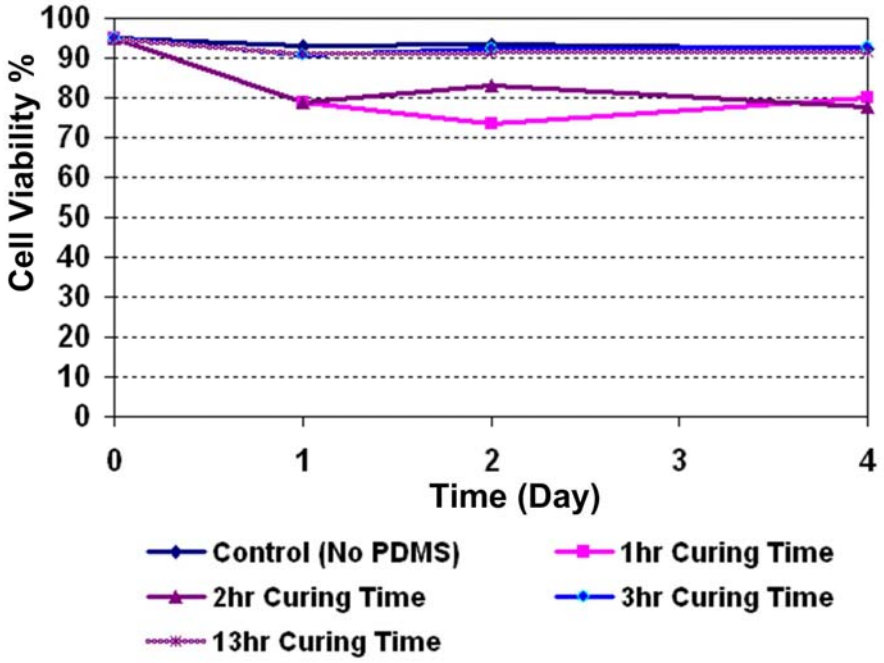

Figure 5.1.4: Cell viability reading over four-day period. There is a noticeable difference of cell viability for PDMS when curing is less than three hours at 50°C.

5.2 Experimental Setup

For each set of the experiment, six to ten cell-loaded microfluidic chips were prepared. The setup for the experiment had to enable easy access to the device so the cell-loading process could be repeated from chip to chip efficiently. It was expected that the whole cell-trapping process would be completed within one and half hours; otherwise, cell sedimentation and aggregation would affect the distribution of cells inside the channel. Exposing microfluidic channels to the outside environment for extensive periods of time would also increase the chance of contamination.

5.2.1 Cell Counting

The number of cells trapped inside the microfluidic device is highly dependent on the cell concentration of the alginate-medium cell suspension. For cell counting, we used a standard hemocytometer (Bright-Line, Canada).

a) b)

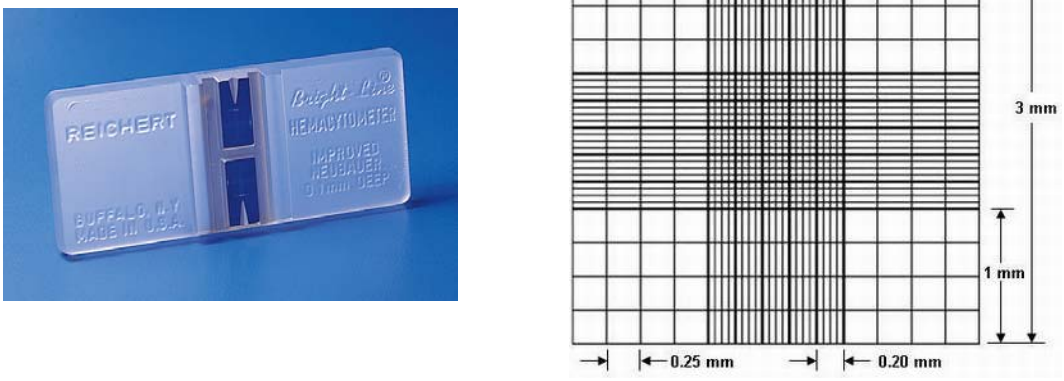

Figure 5.2.1: Hemocytometer: a) Improved Neubauer hemocytometer. b) Under the microscope view, the hemocytometer has nine large squares. The center square is subdivided into 25 squares and each of these is divided again into 16 squares.

A hemocytometer is a thick glass plate, which fits onto the stage of a microscope. There are several designs of hemocytometers available: Burker, Fuchs-Rosenthal and Neubauer. The one used was the improved Neubauer, the most common type used today (Figure 5.2.1). Under the microscope view, the improved Neubauer-type hemocytometer has nine large squares with 1 mm sides. The center square is subdivided into 25 squares and each of them divided again into 16 0.05 × 0.05 mm squares (Figure 5.2.1). With the cover slip on, the volume of each of the nine large squares is $1 \times 1 \times 0.1 = 0.1\ mm^3$. After obtaining the average cell count from each of the 9 large squares, we multiplied by

1 x 10^4 to obtain the number of cells per millilitre. The expected error associated with cell counting using the hemocytometer is around 10% [124].

It is desirable to trap around 1000 cells inside the microchannel for viability and drug testing. For Hep G2 and LCC6/HER2 cell lines, the seeding density is also adequate for forming 3-D spheroids (section 5.3.2 and 5.3.3).

From experience, for trapping 1000 cells inside the gel slab (300 µm wide × 90 µm high × 1 cm long) within the designed microchannel (800 µm wide × 90 µm high × 1 cm long), 10 million cells/ml of initial alginate cell suspension was needed (Figure 5.2.2).

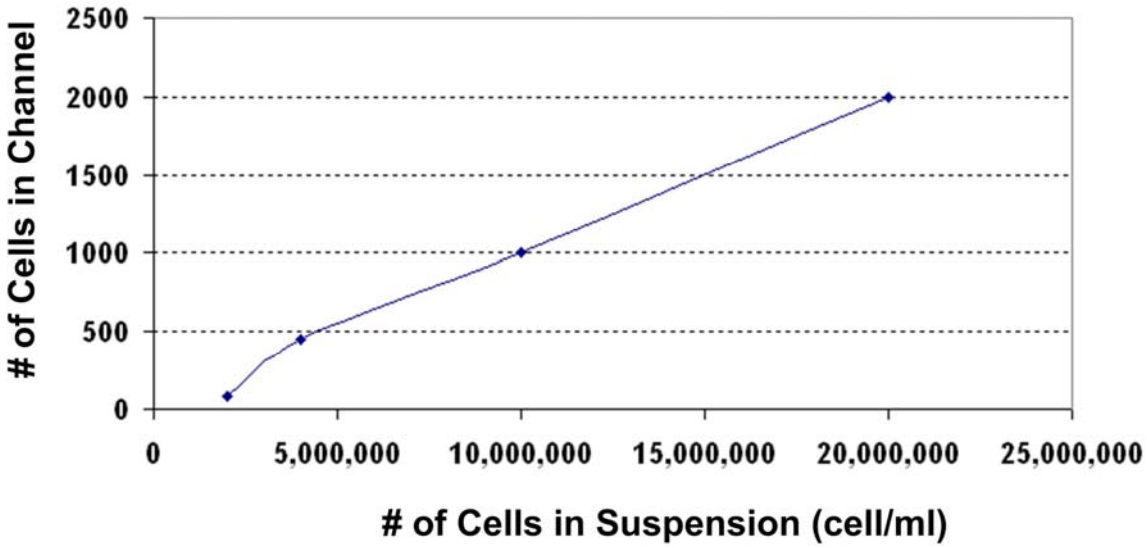

Figure 5.2.2: Number of trapped cells vs. initial cell suspension concentration. The number of trapped cells in the gel layer (300 µm wide × 90 µm high × 1 cm long) varied linearly with initial cell concentration in the alginate solution. The experiments were carried out with 40 mM $CaCl_2$ solution, 1.0 wt% LF120M alginate solution.

Besides the initial cell suspension concentration, the number of cells trapped in the gel layer was also highly dependent on other variables such as cell sedimentation, the formation of cell clumps and alginate gel growth rate. At high gel forming rate, the cell density inside the gel layer would be closer to the initial cell concentration of the alginate cell suspension. The lower the gel forming rate, the less likely the cells would be trapped.

For the Hep G2 cells, 20 to 25 minutes after the preparation of cell suspension, cells started to sediment and form aggregates. The longer the experiment was carried out, the less evenly distributed was the cell inside the gel layer.

5.2.2 Pressure-driven Fluid Flow Control System

A syringe pump or peristaltic pump is often used for applications requiring precision transport of fluid. However, due to the mechanical design of both types of devices, it is difficult to apply gradual changes to independent channels. Severe pulsations can also be observed at a low flow rate (nl/min range). To overcome this problem during the cell loading process, the flow of the liquid was controlled by a high-precision pressure regulator (MFCS-8, Fluigent) as shown in Figure 5.2.3. The MFCS-8 has eight independently controlled channels with the smallest pressure step of 25 μBar and a deviation of less than 1%. Pressure can be adjusted from 0 bar to 1 bar.

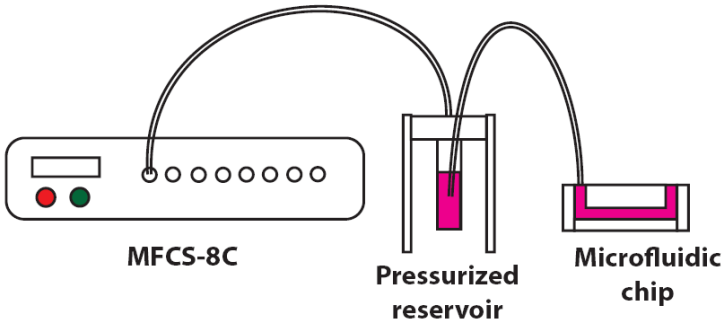

Figure 5.2.3: MFCS-8 high precision pressure regulator

The flow rate inside the microfluidic channel was also strongly dependent on the tubing used. With soft elastic tubing, one may have a slow response time, or at the other extremity, rigid tubing could cause leakage at connection points. From experience, Tygon tubing (0.020" ID, 0.060" OD) was found to be ideal for our purpose (Figure 5.2.4).

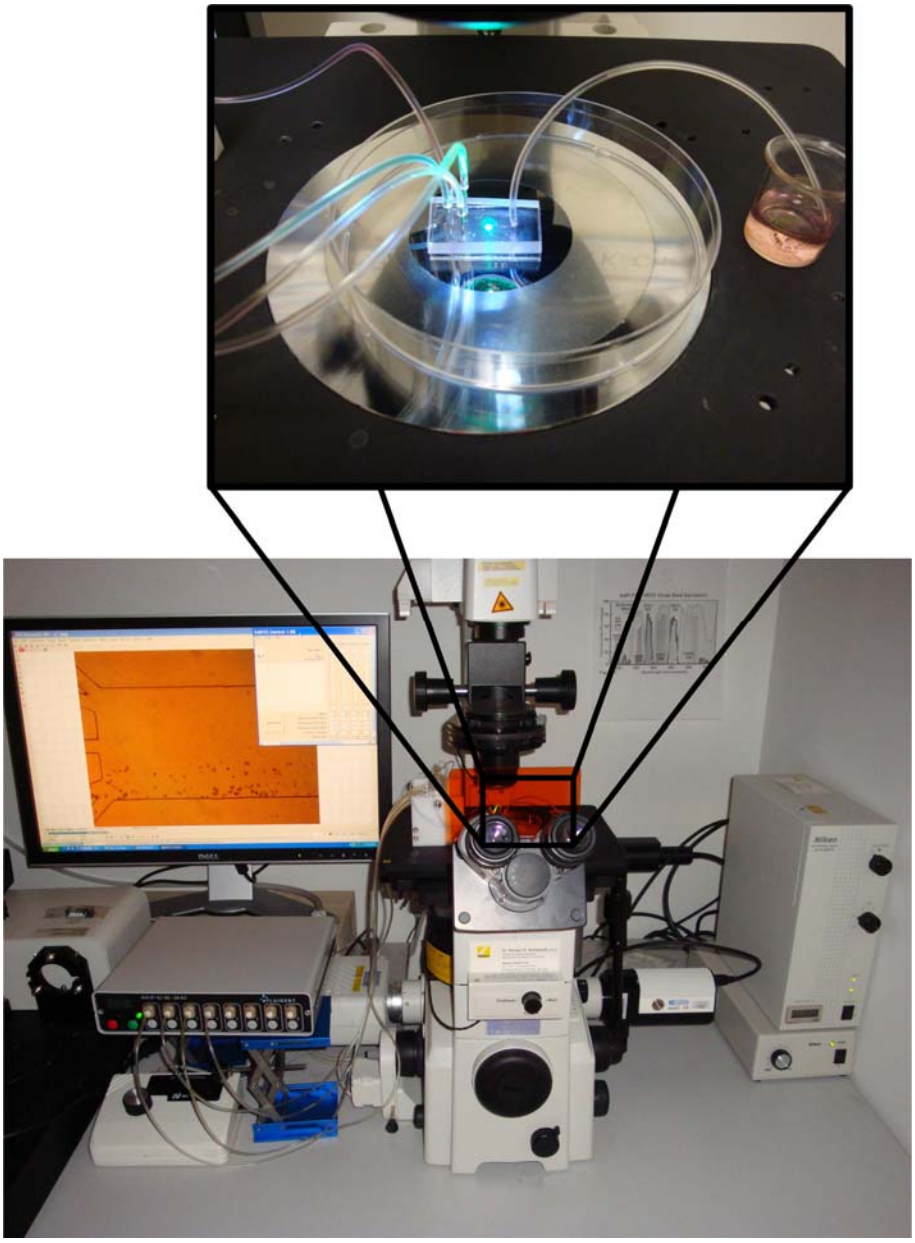

Figure 5.2.4: Experimental setup during cell-loading process. It was done with the MFCS-8 pressure control device and Nikon TE2000-U fluorescence microscope.

5.2.3 Nutrient Circulation

Even though PDMS is highly porous and there is enough oxygen supplied to the cells by simple diffusion [125], there may not be enough glucose or other nutrients to

permeating through the PDMS layer as mentioned in section 3.1.3.2. To overcome this problem, a syringe pump was used to continuously supply culture mediums through the micro-bioreactor.

To further demonstrate the need for a continuous supply of nutrient through the culture chamber, LCC6/HER2 cells were loaded into four identical microfluidic chips and divided into two test conditions. One set of microfluidic chips was connected to a syringe pump and circulated with DMEM culture medium at a rate of 0.3 μl/min; the other set of microfluidic chips was in the static condition (the channel was pre-filled with medium and there was no circulation provided). All test chips were submerged in the DMEM cell culture medium with inlet and outlet blocked. All microchips were loaded with 200 to 300 cells in alginate gel inside the microchannel. From the experiment, we found that cell viability dropped significantly after 3 days in the static condition, where no nutrient was supplied and no waste was removed (Figure 5.2.5). This result supports the assumption that, without circulation, cells will die due to lack of nutrients and accumulation of waste generated from metabolism.

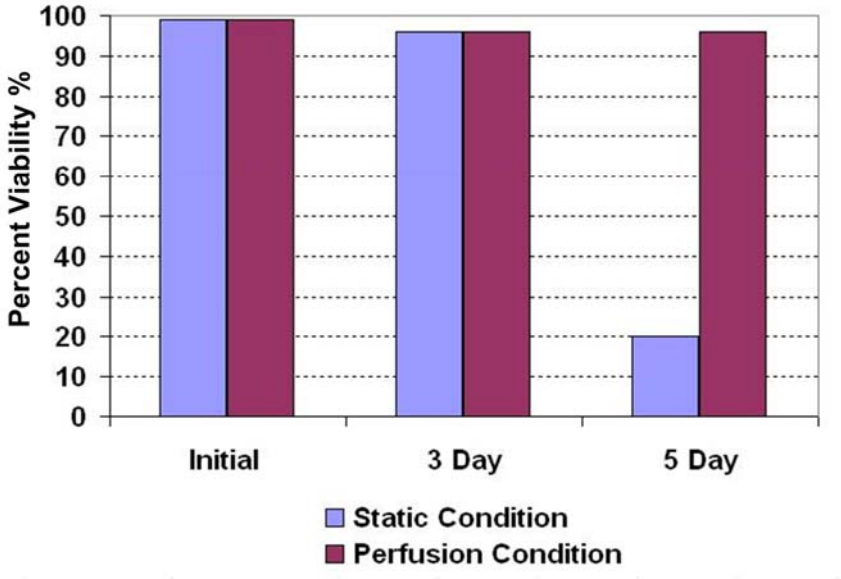

Figure 5.2.5: Cell viability comparison between the static condition and perfusion condition (continuous supply of nutrient at a rate of 0.3 µl/min). We found that, without circulation, cell viability dropped significantly as predicted.

Besides the above reasons, perfusion cell culture also provides a more stable culture environment due to the continuous supply of nutrients and removal of waste. Continuous perfusion, in combination with 3-D culture with multiple cell types, can provide a microenvironment that mimics the structure and composition of a blood vessel [40, 126]. This brings a whole new dimension to drug testing.

For circulating the fluid, the Tygon tubing purchased from Fisher Scientific was connected to the pre-drilled access holes on the PDMS chip. The syringe pump was set at the withdraw motion to prevent contamination from the tubing and provide easy access to waste removal. Since fresh mediums never came in contact with the tubing for extended periods of time, the biocompatibility of Tygon tubing was not a concern. The

size of the syringe was chosen to be as small as possible to minimize the pulse flow generated by the syringe pump (Figure 5.2.6).

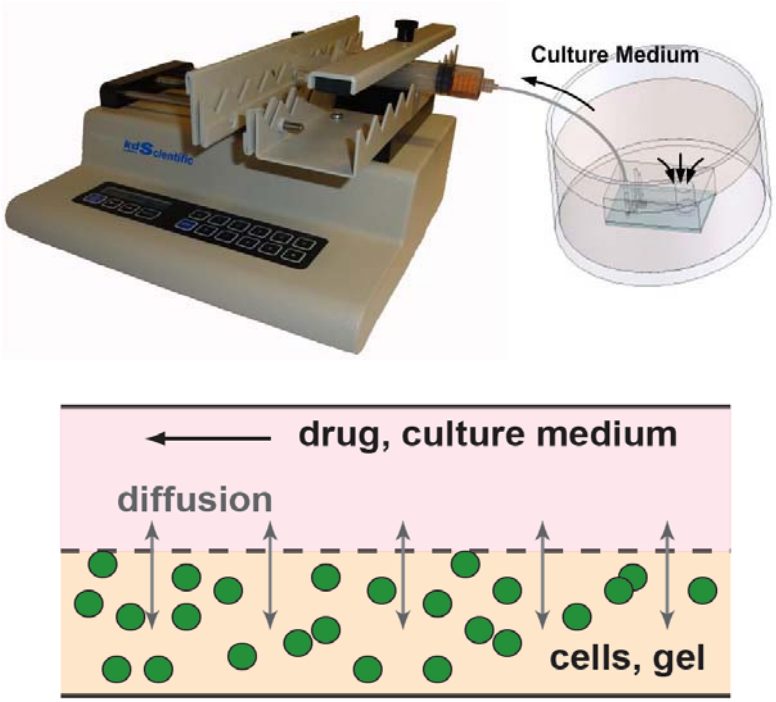

Figure 5.2.6: Syringe pump was used to continuously supplied culture media to the chip. The pump was set at the withdraw motion. The chips were placed inside the incubator to maintain a stable microenvironment.

Glucose is the major energy source for cell metabolism and the main component of all culture medium. The flow rate of the culture medium was determined by the rate of cell glucose consumption. Based on literature research, the average glucose consumption rate for mammalian cells is $\sim 5 \times 10^{-4}$ µg/10^3cells/min [127]. In DMEM, the glucose concentration is 4500 mg/L. When the DMEM culture medium was flowing through the channel at the rate of 0.3 µl/min, as it was in the experiment, the glucose was supplied at

a rate of 1.35 μg/min. If we assume 1000 cells were seeded inside the channel, the glucose supply rate was more than three orders higher than the rate of average cell consumption.

The syringe pump was set at a higher withdraw rate than the average nutrient consumption rate needed by the cells to ensure the continuous supply of culture medium (Channel blockage and tubing leakage may occur during long-term cell culture experiments).

5.2.4 Live/Dead Assay

Viability is a measure of the metabolic state of a cell population, which indicates the proportion of live, metabolically active cells in a culture. The cell viability may be determined from simple assays such as dye exclusion where the loss of viability is determined by membrane damage [124].

5.2.4.1 Trypan Blue

For cell viability testing, trypan blue is one of the most common vital stains used. The assay is derived from toluidine, that is, any of several isomeric bases, $C_{14}H_{16}N_2$. It has a very deep, blue color. Live cells or tissues with intact cell membranes will not be colored; however, the dye will traverse the dead cell membrane. As a result, the dead cells appear as a distinctive dark-blue color under white light. Trypan blue dye only stains the dead cells and excludes the live cells. This is also called the Dye Exclusion Method. It is fast and effective.

The dye is very stable under room conditions. For taking the reading, an equal volume of trypan blue was added to a cell suspension. The dye is poisonous. Therefore, the result had to be interpreted within 2 to 3 minutes; after that, all the cells would begin to take up the dye [124].

5.2.4.2 Live/Dead Viability/Cytotoxicity Kit

Trypan blue gives instant result, but the samples can only be interpreted once, which is extremely inefficient. In a later stage of the experiment, a new assay from Invitrogen was used.

The live/dead kit from Invitrogen contained two color dyes, calcein AM and ethidium homodimer-1 (EthD-1). Calcein AM (ex ~495nm, em ~515nm) was retained within live cells and EthD-1 (ex ~495nm, em ~635nm) was excluded by the intact plasma membrane of live cells [128]. Live cells were identified by the presence of ubiquitous intracellular esterase activity, which turns the non-fluorescent cell-permeate calcein AM to an intensely fluorescent calcein. In this case, the live cell showed a green fluorescence color and the dead cell nucleolus showed a red fluorescence color [128]. Unlike trypan blue, this assay is not lethal to the cell. The sample can be re-dyed in the future, as necessary.

For dying the microfluidic chip, 4 μM of EthD-1 was prepared with PBS and 2.5 μM of calcein AM was mixed right before the experiment. The reagent was injected into the channel with a syringe and incubated for 45 minutes.

The reagents needed to be stored below -20°C. Calcein AM is susceptible to hydrolysis when exposed to moisture, so the solution needed to be freshly prepared

before use. EthD-1 is stable in a moisture environment. A stock EthD-1 solution was prepared with PBS beforehand, which has a shelf life of up to one year under frozen conditions [128].

5.3 Cell Viability

5.3.1 HFL1 Fibroblast Cells

Fibroblast is a type of cell that synthesizes the extracellular matrix and collagen, the structural frameworks for animal tissues. It is the most common cell within connective tissues in animals. The main function of fibroblasts is to maintain the structural integrity of connective tissues [33].

Fibroblasts are among the most widely used cells in laboratory cultures due to the relative ease in maintaining them and low bio-safety level [124]. To first test out the reliability of this culture technique, we trapped ~300 human HFL1 fetal lung fibroblasts (ATCC, USA) in the microchannel. For comparison, the same cell line was also cultured inside alginate gel beads (350 μm diameter) and in a typical culture flask as control groups (Figure 5.3.1).

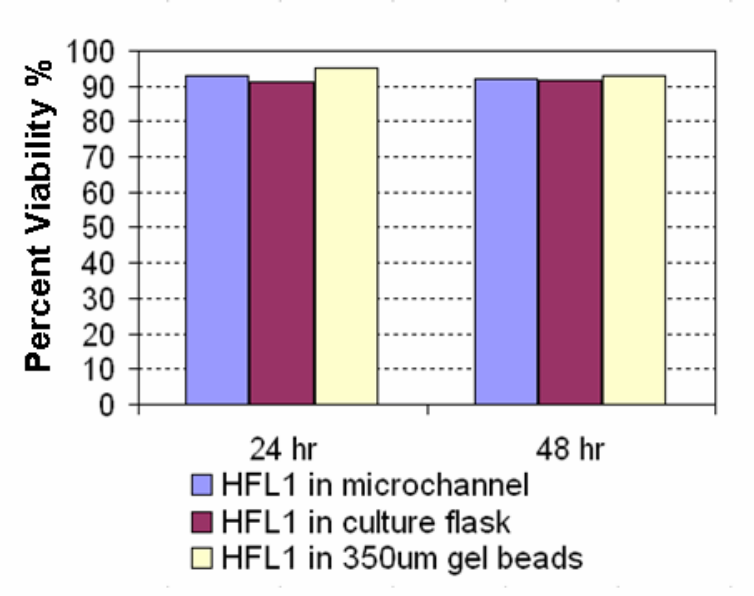

Figure 5.3.1: HFL1 cell viability comparison. The cell viability inside the microchannel was as high as cell culture inside the Petri dish and alginate gel beads.

For culture HFL1, we used Ham's F12K medium (Invitrogen USA) supplemented with 10% Fetal Bovine Serum (FBS), 100 units of Penicillin and 100 μg of Streptomycin. For cell culture inside the microchannel, Ham's F12k medium was continuously fed through the device. The setup of the experiment is shown in section 5.2.3. The syringe pump was set with a withdrawing rate of 0.3 μl/min.

The cell viability is observed every 24 hours for 2 days. From the results, we proved that the cell viability inside the channel was as good as other cell culture techniques (Figure 5.3.2).

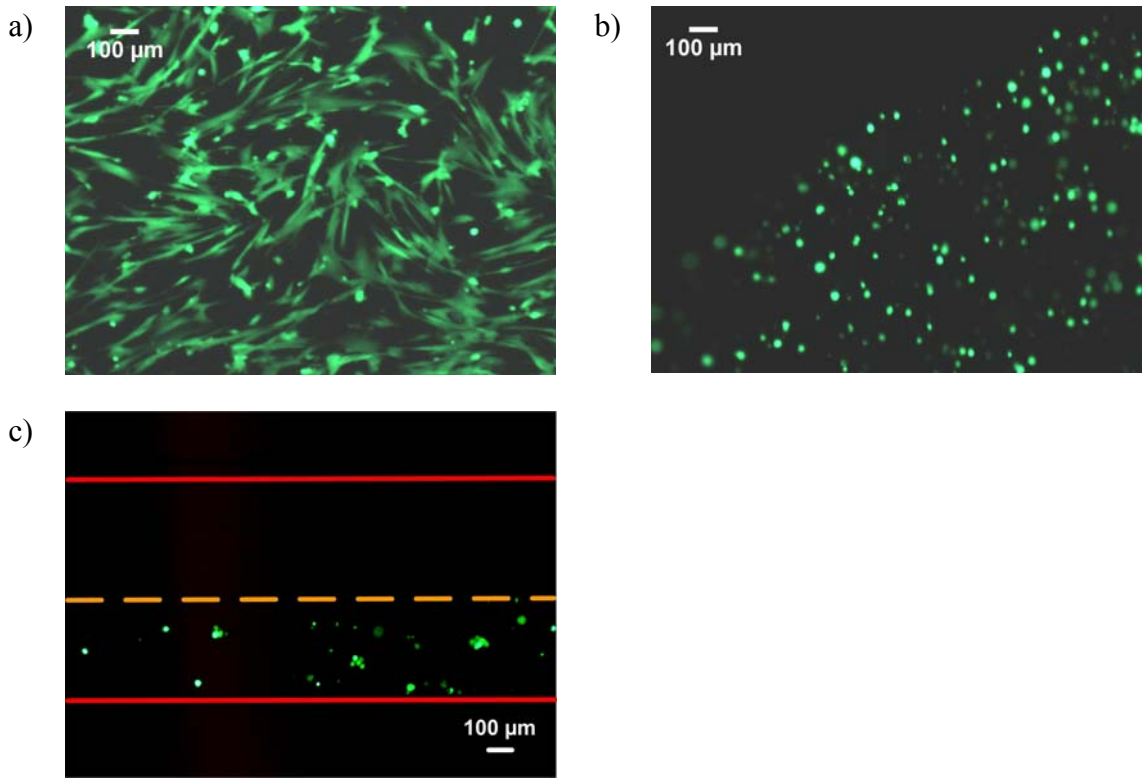

Figure 5.3.2: HFL1 cellular shape: a) In a typical culture flask, HFL1 extended out and adhered to the bottom of the plate. b) The HFL1 cells were in spherical shapes inside the alginate beads. c) Similar spherical structures also appeared inside the microchannel,

5.3.2 Hep G2 Hypatocyte Cells

The Hep G2 cell line was originally derived from human liver tissue [129]. The cells secrete a variety of major plasma proteins (e.g. albumin, alpha2-macroglobulin, alpha 1-antitrypsin, transferrin and plasminogen), which are often used as an indicators for studying metabolic functions [33, 130] since liver is the main organ associated with drug detoxification. To explore drug metabolism and toxicological testing, a cell culture that simulates *in vitro* models of liver is required [129].

Isolating hepatocytes using 2-D culture techniques has posed a great challenge based on the fact that the cell line often shows loss of viability and metabolism activity [131, 132]. When culture hepatocytes using hydrogels, the cells form spheroids and possibility retain expressions of liver markers (such as albumin) and their ability to respond to peroxisome proliferators [132]. It is a more stable, attractive tool for further investigation of the acute phase and other hepatocellular responses. To further improve the *in vitro* model, we demonstrated the possibility of 3-D culture the Hep G2 cell line inside the microdevice.

The hepatocyte cell line was cultured inside the channel for 2 weeks. Hepatocytes are much smaller than fibroblasts in terms of cell size. They also grow much faster. For the experiments, we managed to trap 500 to 1000 cells inside a 300 μm wide x 90 μm high x 1 cm long gel slab.

For the Hep G2 culture, the growth medium used was Minimal Essential Media α (MEM α) (Invitrogen, USA) supplemented with 10% FBS, 100 units of Penicillin and 100 μg of Streptomycin. The setup was the same as the one used for the HFL1 fibroblast in section 5.3.1. The culture medium flowed flowing through the microchip at a rate of 0.3 μl/min.

For comparison, we cultured the same batch of cells in 350 μm alginate beads and in a culture flask along with the cells in the alginate gel layer inside the channel (Figure 5.3.3).

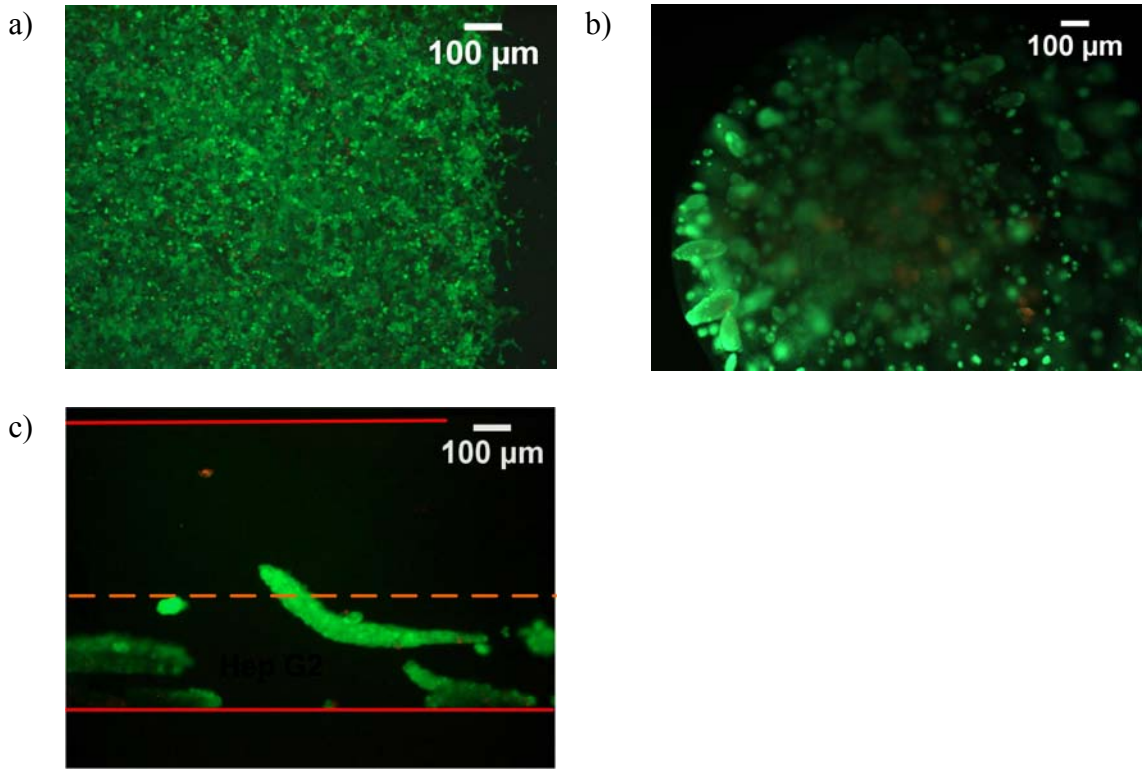

Figure 5.3.3: Hep G2 cellular shape: a) In a typical culture flask, the Hep G2 cell line only formed a 2-D structure at the bottom of the plate. b) After 6 to 7 days, the HepG2 cell line formed spheroids inside the 350 µm alginate beads. c) Similar 3-D spheroids were also observed inside the microchannel after 6 days.

We observed that the Hep G2 started to form spheroids in the gel beads and microchannel on the 5th day of the experiment. As time went by, the cell proliferated and the spheroids grew in size (Figure 5.3.4).

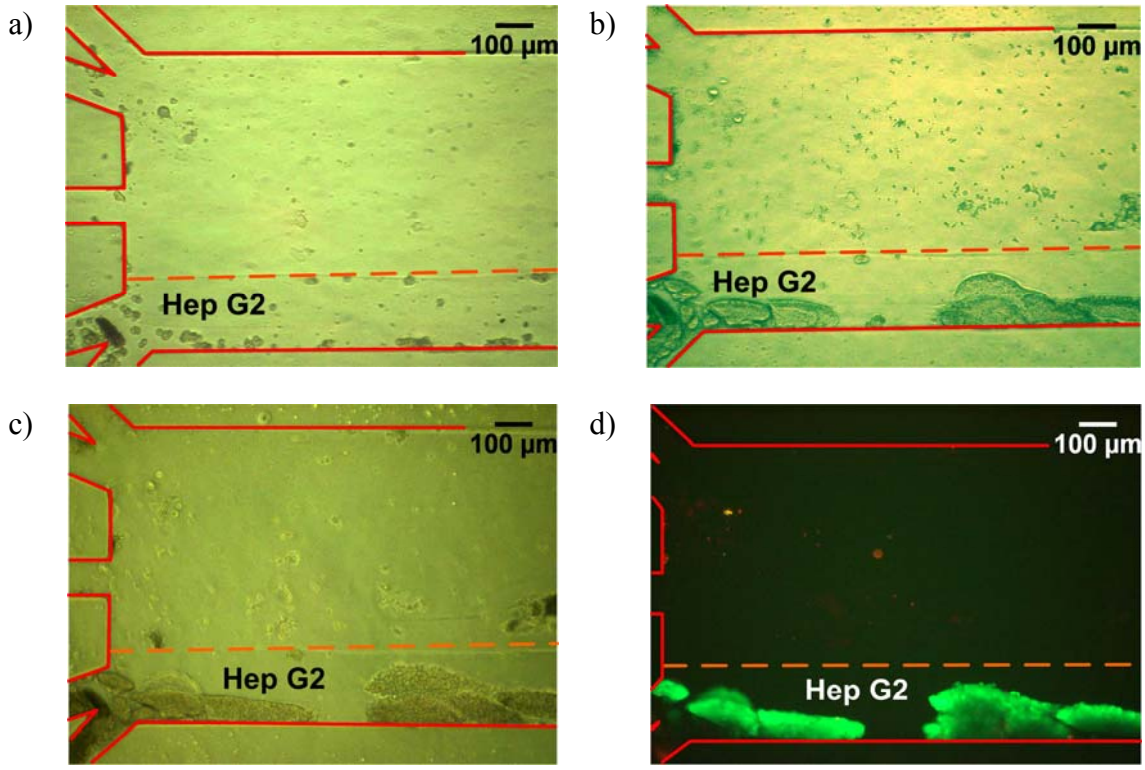

Figure 5.3.4: The Hep G2 cell line inside the microchannel forms 3-D spheroids. Pictures were taken throughout the experiment. a) The first day of the experiment. b) 1 week into the experiment. c) 2 weeks into the experiment. d) At the end of the experiment, the cells were dyed with the live/dead kit. The result shows that more than 95% of the cells were alive.

The experimental results are shown in Figure 5.3.5. From the results, we can say that, for long-term culture, the cell viability inside the channel is as high as traditional 2-D culture flask and 3-D alginate beads culture techniques.

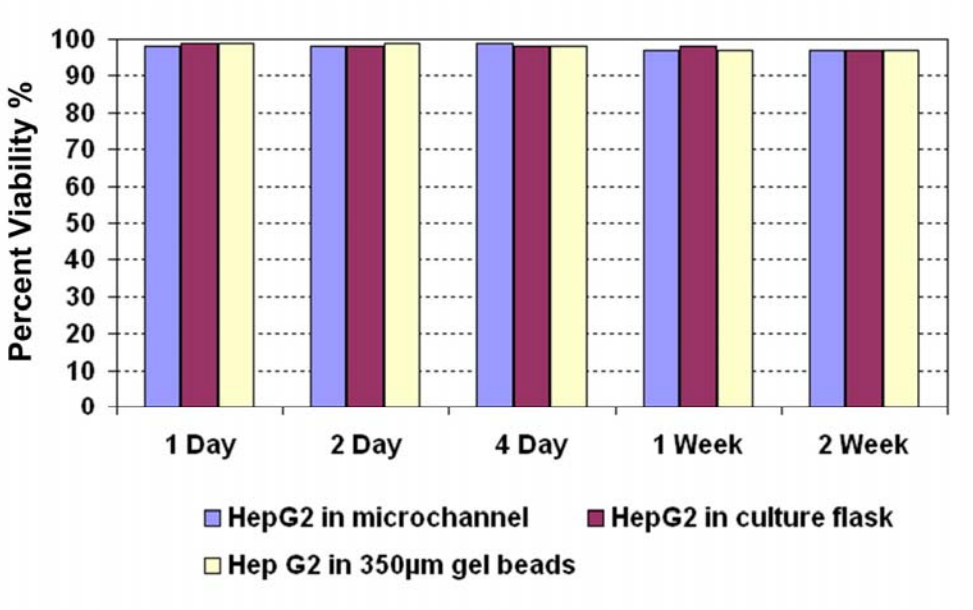

Figure 5.3.5: Hep G2 cell viability comparison. The cell viability inside the microchannel is as high as cell culture inside a petri dish and alginate gel beads.

5.3.3 LCC6\HER2 Breast Cancer Cells

Malignant neoplasm, known by most people as cancer, is a disease in which a group of cells display uncontrolled growth (division beyond the normal limits), invasion (intrusion onto the adjacent tissues), and sometimes metastasis (spreading to other locations in the body via lymph or blood). According to the American Cancer Society, more than 7.6 million people in the world died from cancer during 2007 and breast cancer is the number one cause of death for female cancer patients [133, 134].

There is great interest in cancer drug development. To make the microfluidic device feasible for drug testing, we first needed to demonstrate that it is feasible to culture cancer cells inside the microdevice for extensive periods of time. In this case, we

used LCC6/HER2 breast cancer cells. Similar to hepatocytes, breast cancer cells also formed spheroids inside the gel matrix after 5-7 days (Figure 5.3.6).

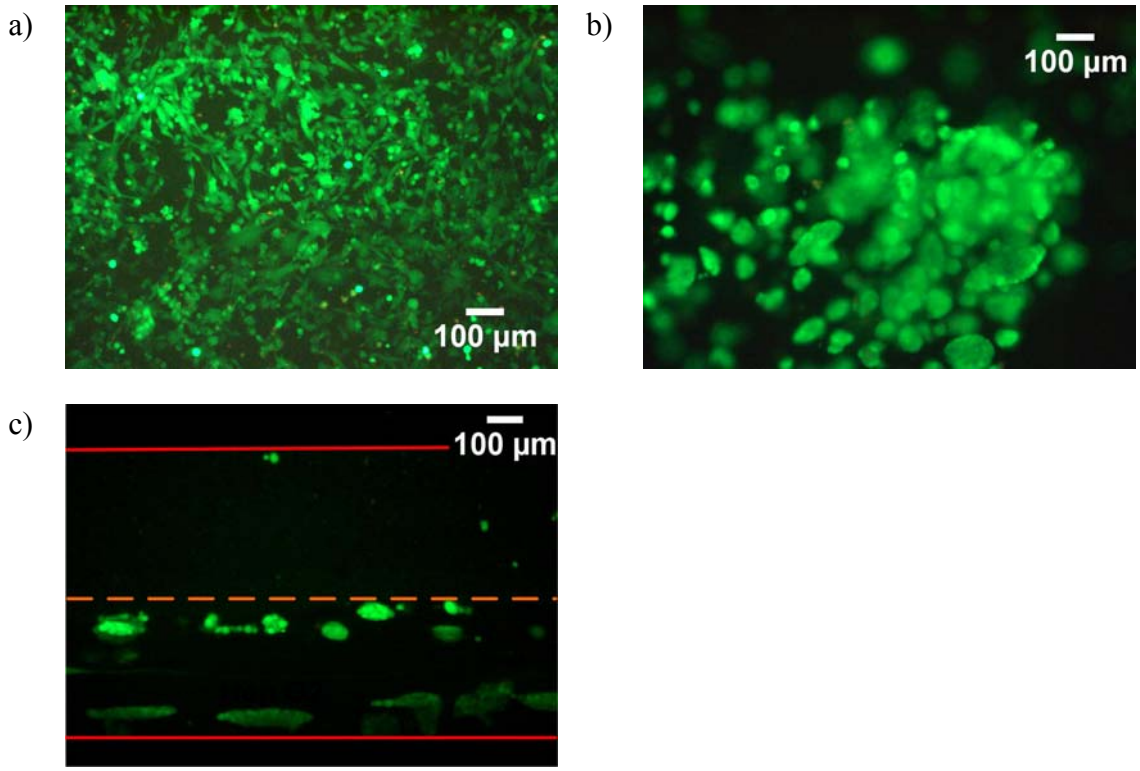

Figure 5.3.6: LCC6/HER2 cellular shape. Similar to hepatocyted a) the LCC6/HER2 cell line only formed a 2-D structure at the bottom of the plate. b) After 5 to 7 days, the LCC6/HER2 cell line formed spheroids inside the 350 µm alginate beads. c) 3-D spheroids also formed inside the microchannel.

We cultured the LCC6/HER2 cancer cell line for 3 weeks. Starting on the 6th day, the cancer cells started to form spheroids. Throughout the experiment, the cells proliferated and the spheroids grew in size (Figure 5.3.7).

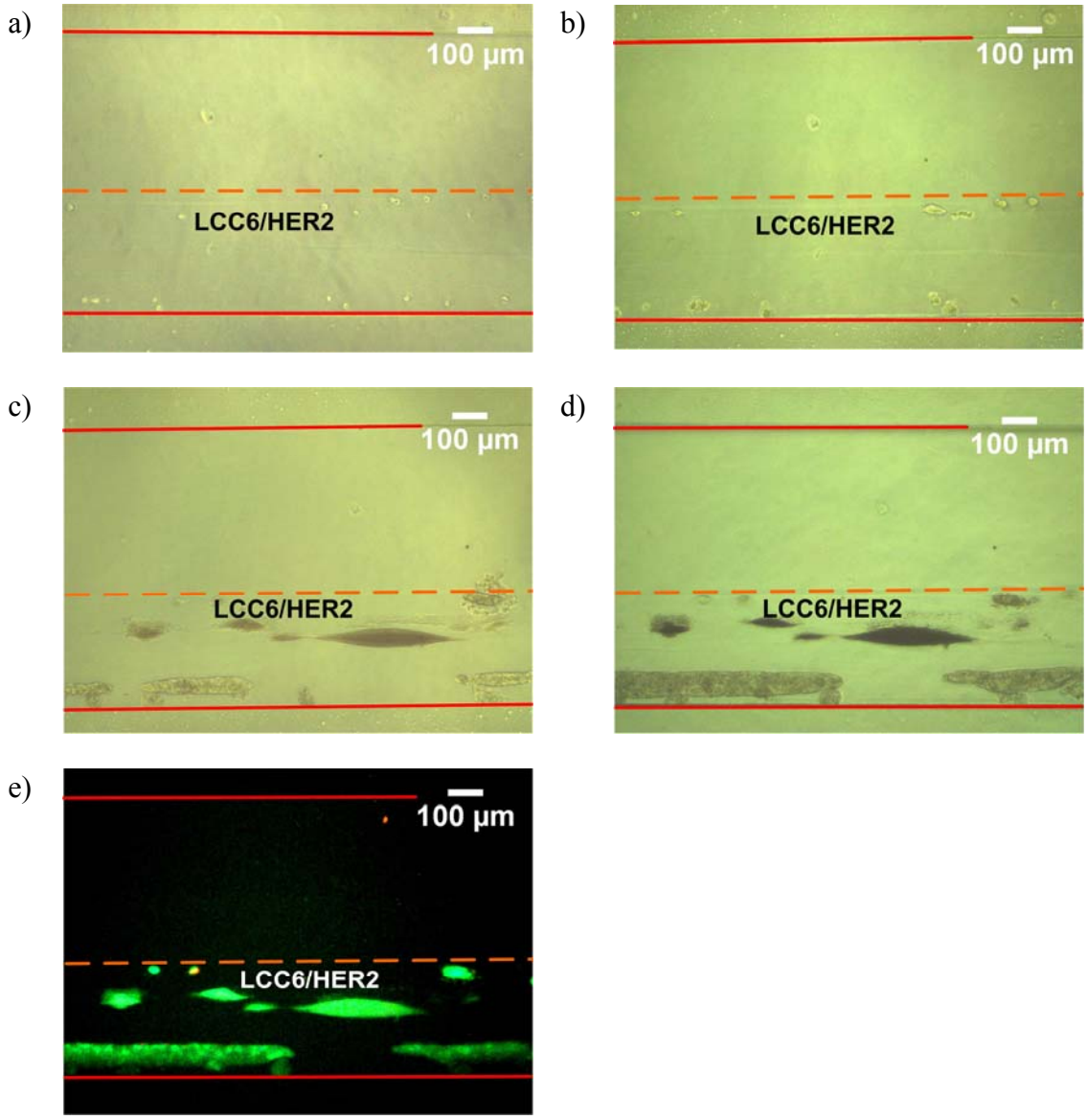

Figure 5.3.7: The LCC6/HER2 cells proliferated and formed 3-D spheroids inside the gel layer. Pictures were taken throughout the 3-week experiment. a) The first day of the experiment. b) 1 week into the experiment. c) 2 weeks into the experiment. d) 3 weeks after the start of the experiment. e) At the end of the experiment, the cells were stained with the live/dead kit. The result shows that more than 95% of the cells were alive.

The experimental results are shown in Figure 5.3.8. The cell viability inside the microchannel was consistently over 90% throughout the 21 days. In terms of cell viability, the 3-D microchannel culture technique was as reliable as the typical culture technique in the culture flask or 3-D culture inside alginate gel beads. Based on this result, we could precede to cancer drug screening (section 5.6).

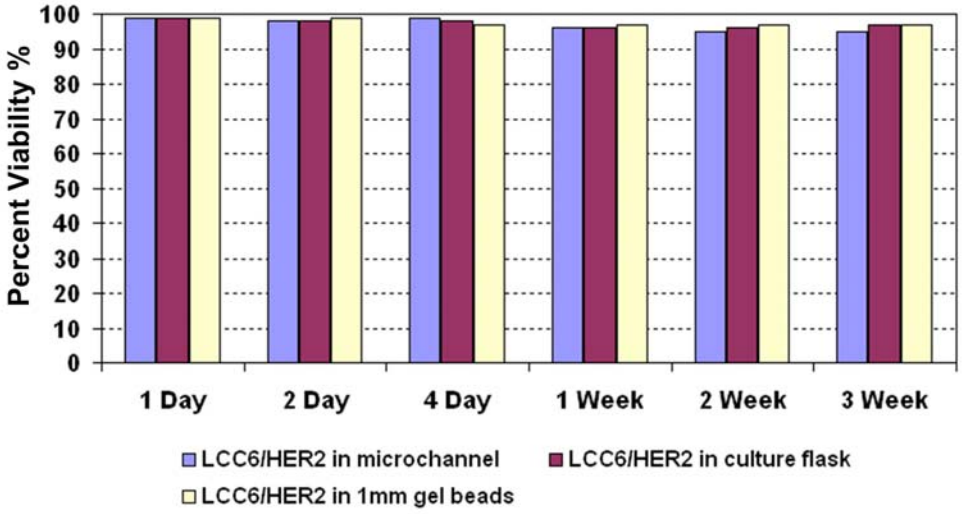

Figure 5.3.8: LCC6/HER2 cancer cell viability comparison. The tumor cells were cultured inside a microdevice for 3 weeks. The result shows that the cell viability was more than 90% consistently throughout the experiment.

5.4 Co-culture

By manipulating the fluid flow, we achieved separate gel formation at two boundaries close to the channel sidewalls or multiple stacked adjacent layers. This allowed different cell types to be cultivated in close proximity in the same cell culture environment (see Figure 5.3.9, Figure 5.3.10).

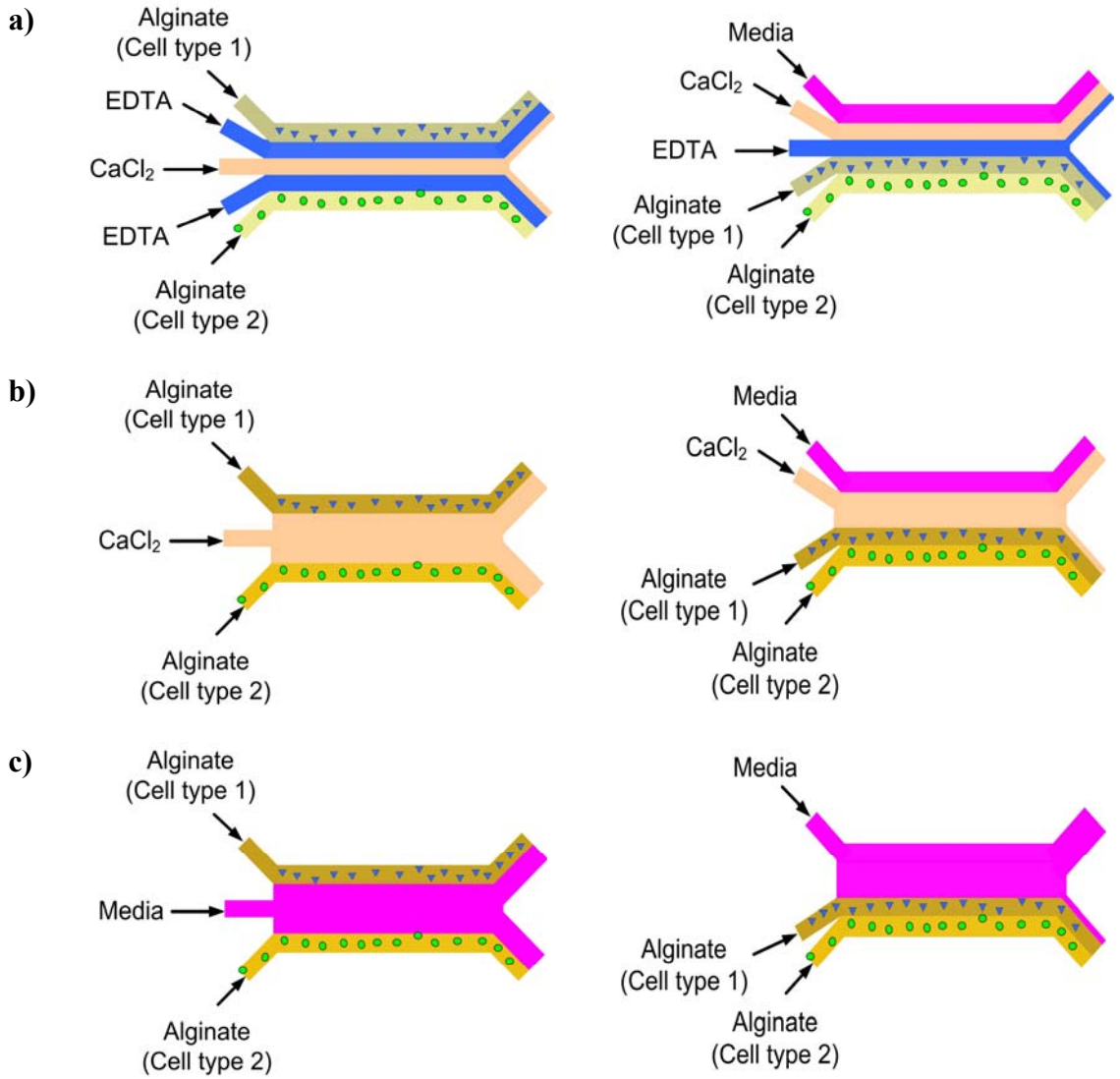

Figure 5.3.9: The trapping process for co-culture two cell types simultaneously. a) Different cell types were mixed in two separate alginic acid solutions. We used the interior and central inlets for EDTA and $CaCl_2$. This was the initialization step. A laminar flow of EDTA was used to separate the Ca^{2+} and alginate flows prior to gel formation. b) After the EDTA flow was suppressed, the Ca^{2+} ion solution came into contact with the alginate phase. The gel started to grow from the boundary towards the alginate stream with cells trapped inside. c) Once the gel formation was complete, the inlet flows were switched to culture medium for long-term cell culture.

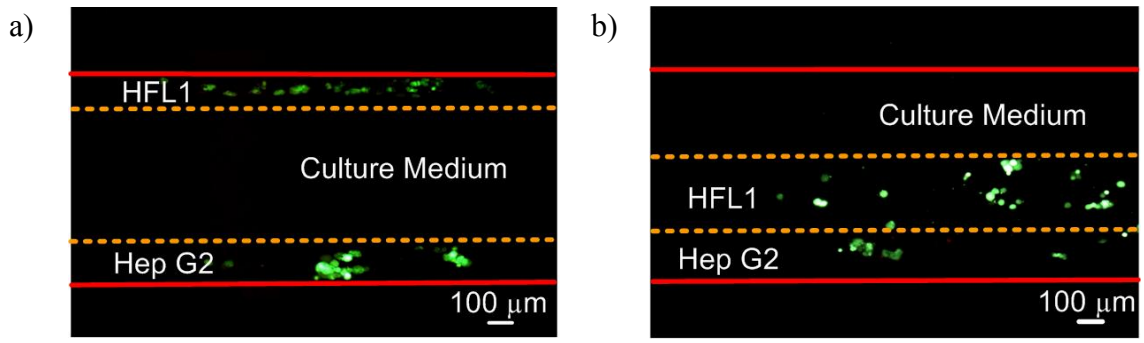

Figure 5.3.10: Co-culture HFL1 and Hep G2 cells. Cells were individually cultured inside microfluidic devices: a) two separate regions or b) adjacent layers. Cell viability was measured using a LIVE/DEAD Viability/Cytotoxicity Assay Kit immediately after gel formation. The live cells showed an intense uniform green fluorescence.

5.5 Cell Releasing

To demonstrate the possibility of releasing cells from the microchip, we first cultured 1000 to 2000 Hep G2 cells inside the microfluidic device for 48 hours and gently injected 40mM EDTA solution to dissolve the alginate gel. Two control groups were prepared side by side with this experiment. One had Hep G2 cells cultured inside typical culture flasks. Another set of Hep G2 cells were trapped inside alginate beads with diameters from 350 µm to 1 mm.

A 0.5 cm diameter reservoir was created at the end of the channel to accommodate the dissolved cell suspension. The cell suspension was then pipetted out into a 12-well plate and cultured for 5 days (Figure 5.3.11).

a)

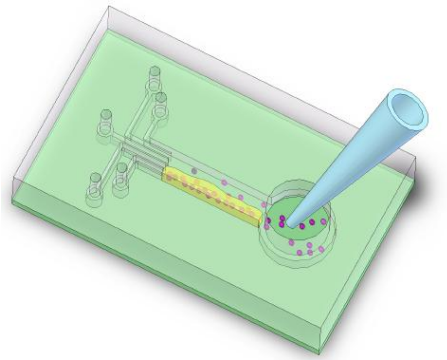

b)

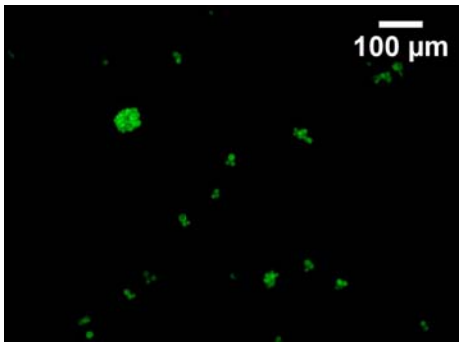

Figure 5.3.11: Cell releasing: a) To retrieve the cells trapped inside the microfluidic device, a 0.5 cm reservoir was created at the end of the channel to accommodate the released cell suspension. b) The majority of Hep G2 Cells remained alive 5 days after releasing.

We found that cell viability was much higher with the one released from the channel than the one released from alginate beads (Figure 5.3.12). From cell releasing experiments using alginate beads, it has been found that the cell viability is highly dependent on the concentration of EDTA solution used and the length of time cells are in contact with the EDTA solution. The longer the cells are in contact with the EDTA solution and the higher the EDTA solution concentration used, the lower the cell viability. It only takes 15 to 20 seconds to release the cells from the channel using 40 mM EDTA solution, but it will take 1 hour to 1.5 hours to release the cells form 1 mm 1.0 wt% alginate gel beads. This shows another advantage of culture cells inside the microchannel.

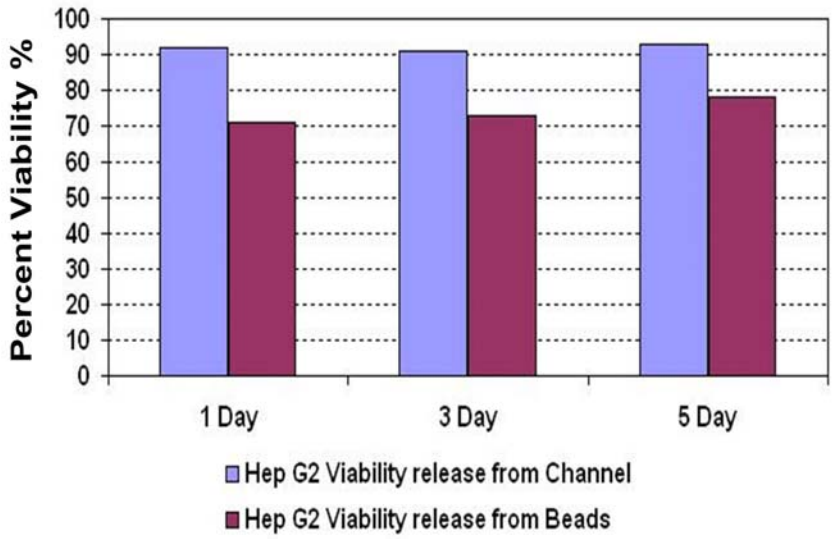

Figure 5.3.12: Cell releasing viability comparison. The cell viability was noticeably higher when releasing from the microchannel than releasing from the beads due to the shorter exposure time to EDTA.

5.6 Drug Testing

Unfortunately, oncology has one of the poorest records for investigational drugs in clinical development, with success rates that are more than three times lower than those of cardiovascular disease [135]. Anticancer drug targets can be classified into two categories: essential and non-essential. Essential means that at least one vital cell type in the body depends on the target for survival. Drugs that target essential functions most likely have very narrow therapeutic windows. Drugs that target essential genes always have the risk of serious side effects. On the contrary, our body has much higher tolerance for drugs that target non-essential proteins. However, the efficacy of non-essential drugs is limited. Another challenge with drug treatment is that essential and non-essential genes are very difficult to discriminate within mammals [135].

Cancer drug development faces many challenges. However, microfluidic technologies that can carry out tests based on a single cell or have access to a more detailed picture of cell abnormalities bring new possibilities to drug development.

For the experiment, we used doxorubicin (Dox) generously provided by Dr. Helen Burt, UBC Faculty of Pharmaceutical Sciences.

5.6.1 Doxorubicin (Dox)

Doxorubicin (Dox), also known as adriamycin or hydroxydaunorubicin, has a chemical formula of $C_{27}H_{29}NO_{11}$ (Figure 5.3.13) and MW of 543.52 g/mol. Dox has peak excitation and emission wavelengths at 480 nm and 550 nm respectively. Dox is a common chemotherapy drug used in treatment for many types of cancer [136, 137]. For chemotherapy, Dox is normally given by injection into a vein through a canula. The treatment is given in sessions over a few months. Possible side effects may include hair loss, nausea, vomiting, and lowered resistance to infection.

The exact mechanism of doxorubicin is complex and still somewhat unclear. What is known is that it interacts with DNA by intercalation and inhibits biosynthesis [137]. It also has been reported to interact directly with the cell membrane and to inhibit the unwinding of DNA for replication [138]. This phenomenon would inhibit cell growth.

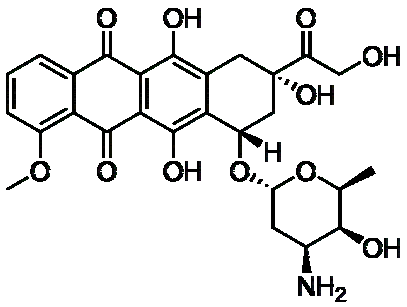

Figure 5.3.13: The molecular structure of doxorubicin (Dox).

The ability of doxorubicin to interfere with the growth of LCC6/HER2 breast cancer cells was later determined through both fluorescence and confocal microscopes (section 5.6.4).

5.6.2 Drug Diffusion in Alginate Gel

Lacking any non-invasive techniques to measure the concentration of Dox inside the microfluidic device during drug testing, a low concentration of the fluorescent dye, Rhodamine B, was introduced to evaluate cross channel diffusion. Rhodamine B is a commonly used hydrophobic fluorescent dye in biotechnology applications such as fluorescence microscopy, flow cytometry, and ELISA. The chemical structure of the fluorescent dye is shown in Figure 5.3.14. The peak excitation and emission wavelength of Rhodamine B dye are 540nm and 625nm [139]. With the chemical formula, $C_{28}H_{31}ClN_2O_3$, and molecular weight of 479.01 g/mole, it is comparable with Dox in terms of molecular size. We used Rhodamine dye to simulate Dox for measuring the diffusivity because it is less toxic and safer to use.

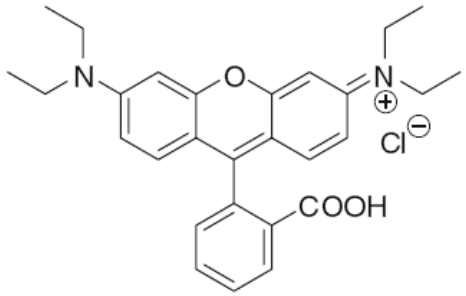

Figure 5.3.14: Structures of Rhodamine B ($C_{28}H_{31}ClN_2O_3$) [140].

The intensity of the Rhodamine B dye in the channel was used to correlate with the dye concentration, which represented the drug concentration (Figure 5.3.15).

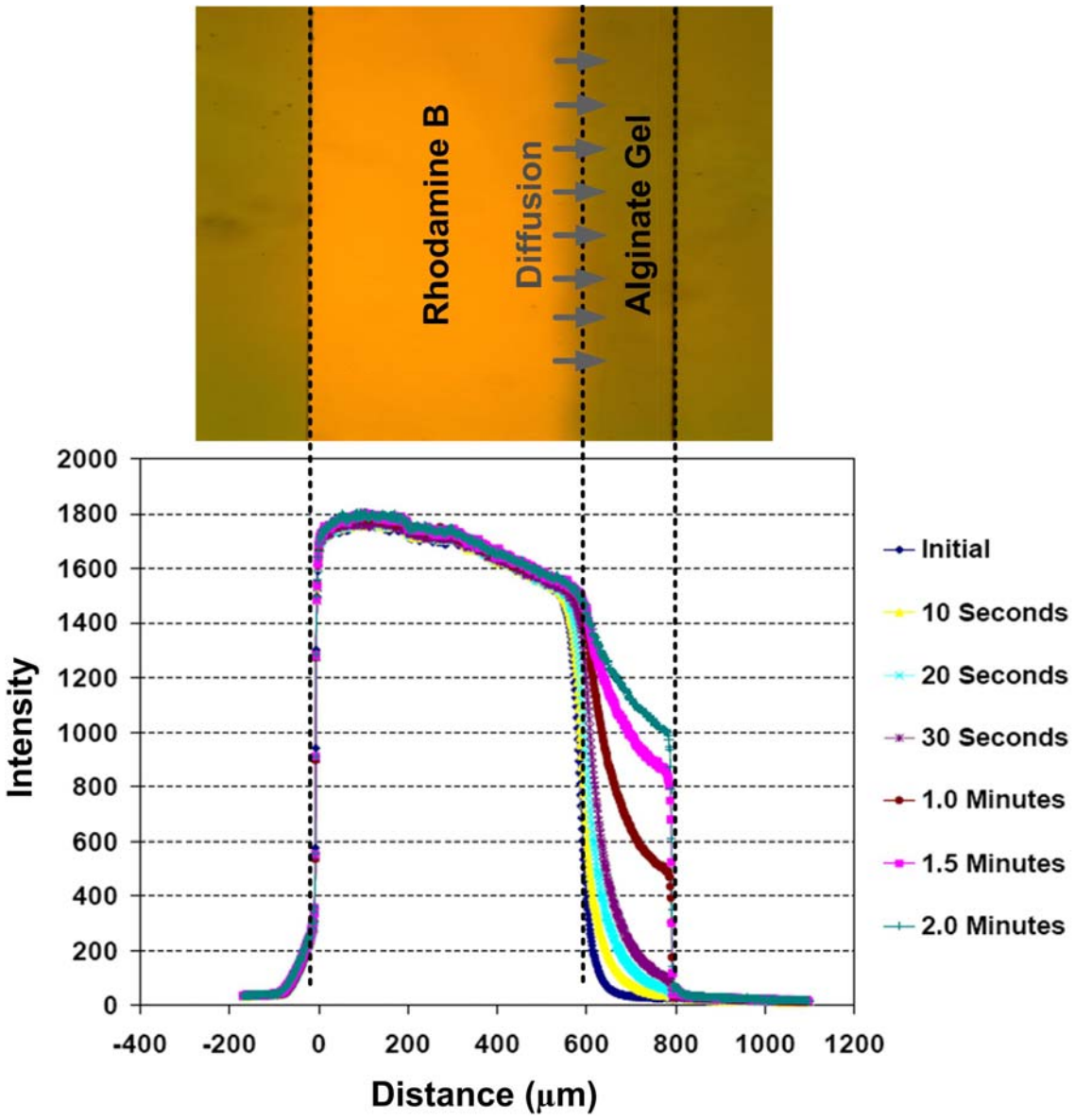

Figure 5.3.15: Diffusion time measurement of Rhodamine B through alginate gel layer. A 200-µm gel layer was formed inside the channel. 500 µM Rhodamine B was injected at a rate of 3 µL/min into the channel at room temperature to simulate Dox (cancer drug). The intensity of the fluorescence signal can be used to determine the dye concentration to show the amount of dye diffusing into the gel layer across the channel. Since Rhodamine B has a similar diffusion coefficient as Dox, it is a close approximation to the delivery of cancer drugs to the breast cancer cells.

To estimate the diffusion coefficient of Rhodamine B, we can use Fick's second Law:

$$c(x,t) = c_0 erfc\left\{\frac{x}{2\sqrt{Dt}}\right\} \tag{5.1}$$

With boundary condition:

$$c(x,t=0) = 0 \tag{5.2}$$

$$c(x=0,t) = c_0 \tag{5.3}$$

$$c(x=\infty,t) = 0 \tag{5.4}$$

where $erfc(q)$ is known as the complementary error function, which can be written as:

$$erfc(q) = \frac{2}{\sqrt{\pi}}\int_q^{\infty} e^{-t^2} dt \tag{5.5}$$

With the channel height equal to 90 μm, Gel width equaled to 200 μm, and original Rhodamine B concentration equal to 500 μM. Based on the measured data (Figure 5.3.15), the diffusion coefficient in alginate gel ($\approx 5.0\times10^{-10} m^2/s$) at room temperature, which is very similar to the diffusion coefficient of Rhodamine B in aqueous solution ($\approx 3.6\times10^{-10} m^2/s$) at 21.5°C [140].

5.6.3 Drug Diffusion through PDMS Chip

To have precise control over the drug testing condition, it is necessary to ensure that tumor cells only in contact with the Dox solution passing through the channel. Because the PDMS chip is porous and submerged in the Dox solution, we need to make certain that Dox does not diffuse through the chip and reach cells inside. Similar to

section 5.6.2, we replace Dox with Rhodamine B for measuring the diffusion rate of Dox though PDMS.

For determining the diffusion speed, a PDMS pallet is submerged in 500 μM Rhodamine B solution. The diffusion distance (the distance Rhodamine B diffuse from the edge of PDMS block towards the center of the PDMS pallet) is measured through fluorescence microscope for 2 weeks (Figure 5.3.16). Because of the hydrophobic nature of Rhodamine B, hydrophobic attraction is expected between the dye and the PDMS bulk [141].

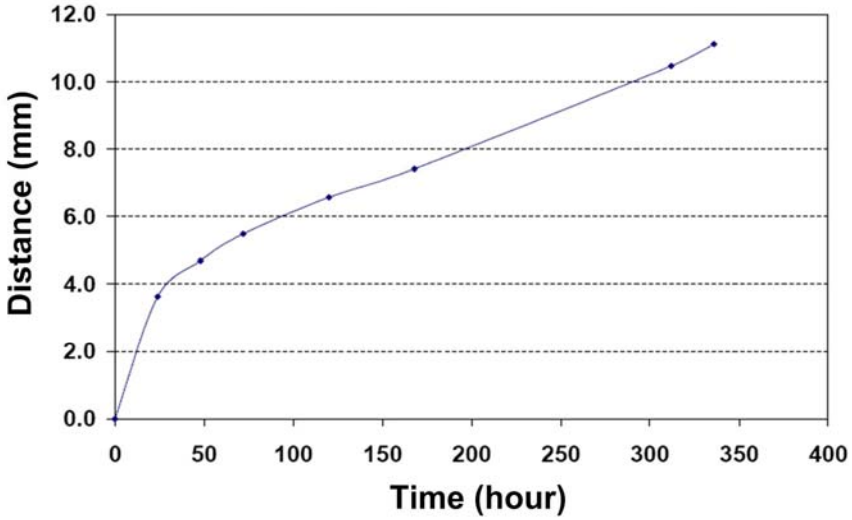

Figure 5.3.16: Diffusion distance of Rhodamine B through PDMS block over two weeks at room temperature.

Using Fick's second law of diffusion (5.1), we estimate the diffusion coefficient $D \approx 2.5 \times 10^{-11} m^2 / s$. Base on the geometry of the designed microfluidic device, it will take more than four days for the fluorescent dye to reach the main section of the channel.

5.6.4 Control Group

To ensure that all the nutrient consumed by the cells inside the microfluidic device was provided by the withdrawing motion of the syringe pump, four different control groups were test: submerged in culture medium flowing with culture medium, submerged in culture medium flowing with PBS, submerged in PBS flowing with culture medium, and submerged in PBS flowing with PBS. The microfluidic chip was placed inside the six-well plate with fluid drawn from a separate well through PTFE tubing (Figure 5.3.17). Tygon tubing is more flexible and easier to use, but biocompatibility is always a concern. For the case where supplements were required to flow through, PTFE tubing was used.

For the four different control cases, cell viability was observed after 72 hours using the Live/Dead kit purchased from Invitrogen. The result showed that with the continuous feeding of nutrients, the cell viability remained stable and above 90%. With the two cases of feeding only with PBS, the cell viability dropped significantly below 5% (Figure 5.3.18).

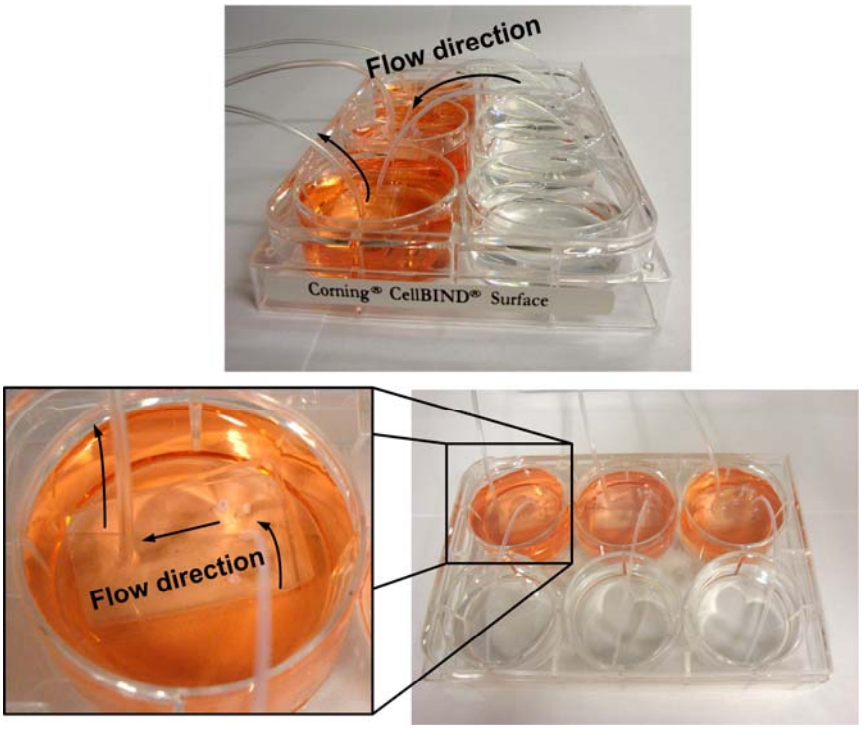

Figure 5.3.17: Control experiment before drug testing. The microfluidic chip was submerged in culture medium or PBS with culture medium or PBS flowing through from a separate well connected with PTFE tubing. In this case, the cell culture chip was submerged in culture medium with PBS flowing through.

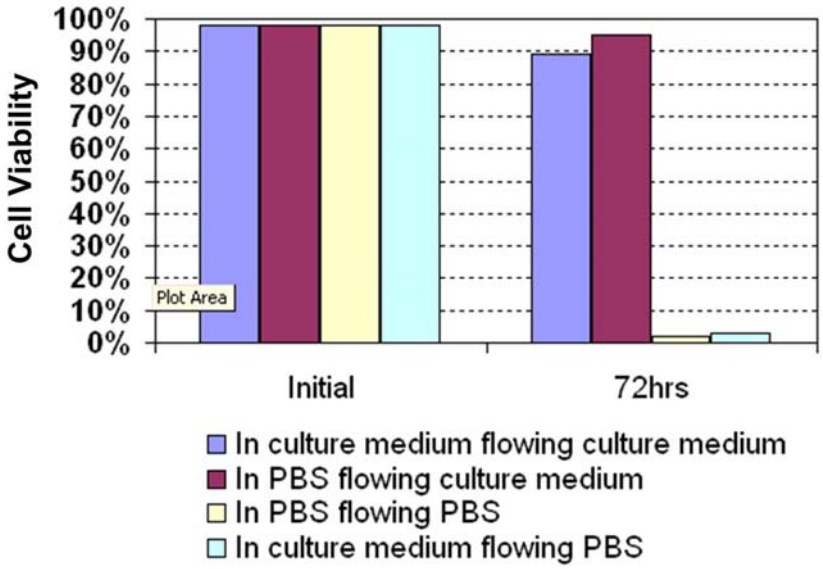

Figure 5.3.18: Control experiment result. The cell viability remained above 90% for the two cases with the continuous feeding of the nutrients. For the two cases involving feeding with only PBS, the cell viability dropped below 5%. The result was taken after 72 hours.

5.6.5 Experimental Result

For drug testing, the Dox solution was prepared with 0.2% DMSO and DMEM culture medium. The cells were first loaded in the channel and incubated for 24 hours with a circulation of drug-free culture media. After 24 hours, the drug-free culture media was replaced with 0.8 μM and 1.5 μM of the Dox solution. The drug solution was continuously perfused through the channel at a rate of 0.3 μl/min.

The Dox concentration (0.8 μM and 1.5 μM) was previously determined from the MTS assay, where the cells were encapsulated in 50 μl 1.0 wt% alginate gel beads. Each gel bead contains about 2500 cells. The IC 50 for Dox with the LCC6/HER2 cell line in

alginate beads was determined to be 0.4 μM. At this concentration, the drug was 50 % effective in inhibiting cell proliferation.

From drug encapsulation research, it has been found that alginate (negatively charged) have a strong ability to accumulate positively charged Dox [142, 143]. For this reason, the drug concentration used was 2 to 3 times higher than the IC 50 (0.8 μM and 1.5 μM) to insure enough Dox can reach the tumor cell.

Two control groups were prepared: one with the typical DEMEM culture medium and the other one feeding with DEMEM and 0.2% DMSO (all drug solutions were prepared with 0.2 % DMSO). Each channel contained 500 to 1,000 cells. The set up was the same as the one mentioned in section 5.2.3. Cell viability readings were taken every 24 hours for 3 days after introducing the cancer drug (Figure 5.3.19).

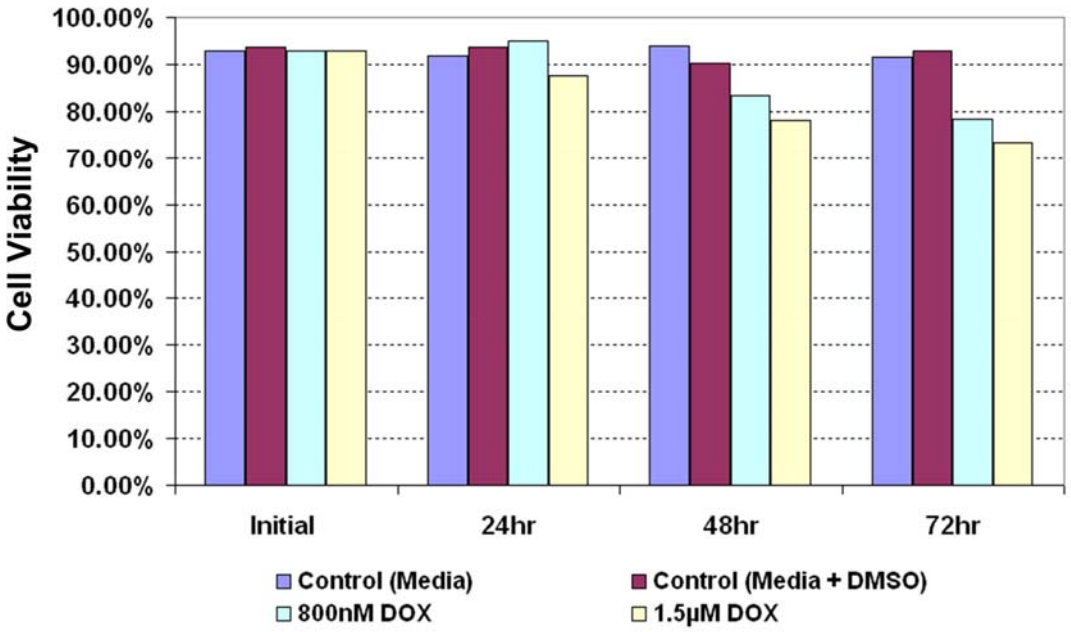

Figure 5.3.19: Cell viability reading for Dox drug testing. The viability reading was taken every 24 hours for 3 days after introducing 0.8 μM and 1.5μM Dox to the cells.

From the results, we found that cell viability gradually lowered after 48 hours. Dox did not kill the cell on contact but stopped the cells from proliferating. Therefore, the effect of the drug can only be observed after 24 hours. Additional pictures were taken that show that the LCC6/HER2 cell line formed spheroids in the control chip with 0.2 % DMSO, but the same structure could not be observed after contact with 0.8 µM Dox (Figure 5.3.20, Table 5.3-1). The experimental procedure is shown in Appendix D.

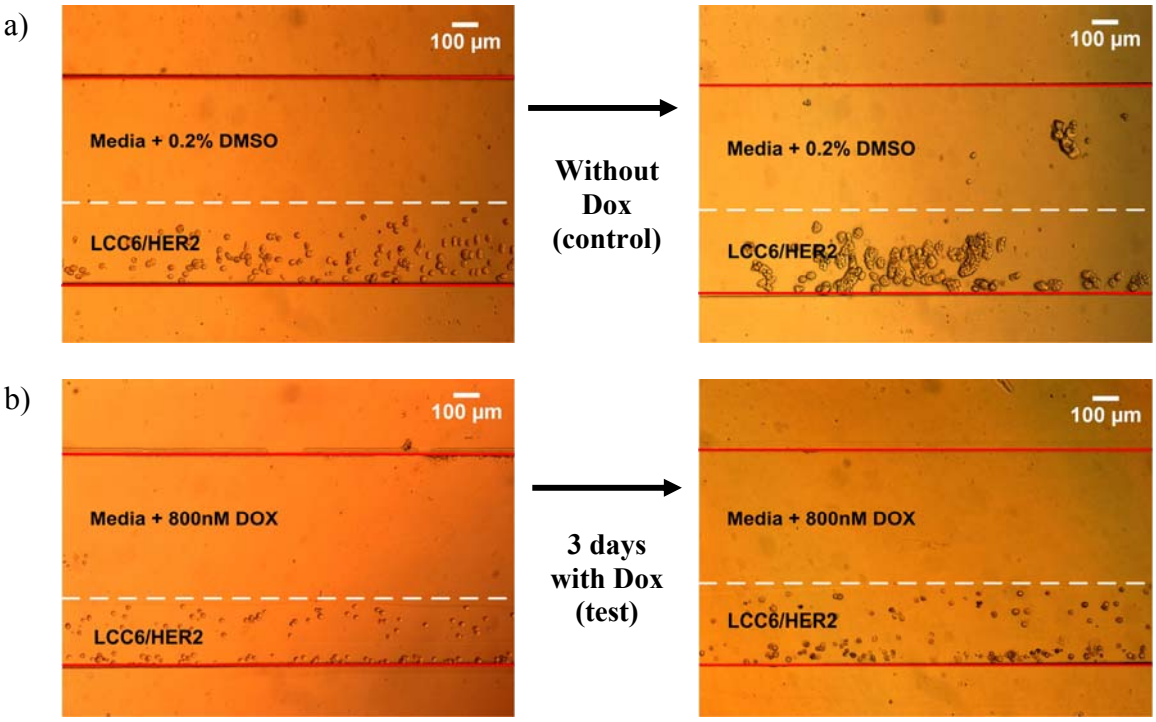

Figure 5.3.20: Drug testing result: a) The LCC6/HER2 cell line formed spheroids in the control chip with 0.2 % DMSO 5 days into the experiment. b) Dox stopped the cells from proliferation so 3-D spheroid structures could not be observed after contact with 0.8 µM Dox.

Table 5.3-1 Cell proliferation after 72 hours treatment.

	Control	0.8 μM Dox	1.5 μM Dox
Increase in Cell Number	>150%	~0%	~0%

CHAPTER 6

Conclusion

6.1 Summary

In this project, we have designed a microfluidic device, which is capable of reversible trapping of mammalian cell lines using alginate, ionic cross-linking hydrogel, in combination with Ca^{2+} ions. In the microfluidic device, cells are cultured in ECM-like structures. With alginate gel trapping, nutrients had access over the whole surface of the cell and the immobilization process occurred under mild conditions at room temperature. Because the microfluidic device is made with PDMS and glass (transparent to most of the fluorescent marker), it is compatible with many biological imagining techniques.

In order to provide enough nutrients to the cultured cells and remove metabolic waste, culture media was continuously fed to the microchip with a syringe pump to provide a stable microenvironment for long-term cell culture. We have also demonstrated the possibility of co-culture two cell types (HFL1 and Hep G2) in separate gel layers. Continuous perfusion, in combination with 3-D culture with multiple cell

types, can provide a microenvironment that mimics the structure and composition of a blood vessel.

Various mammalian cell lines were successfully cultured within a microfluidic device for long periods of time. The HFL1 cells have successfully cultured for over 48 hours. The Hep G2 and LCC6/HER2 cells were cultured for more than 2 and 3 weeks with cell viability of more than 90%. After culture the cells for more than 5 days, hepatocytes (Hep G2) and breast cancer cells (LCC6/HER2) formed 3-D spheroids. The 3-D structures have a greater resemblance to the cell behaviour in the *in vivo* conditions and could only be observed when the cell lines were cultured within the gel matrix.

In the last part of the project, we demonstrated the possibility of performing cancer drug testing within the microfluidic device. LCC6/HER2 breast cancer cells were first cultured within the microdevice for 48 hours. 1.5 μM and 800 nM of the cancer drug, Dox, were introduced to the cells. Dox inhibited the unwinding of DNA thus stopping the cells from proliferation. Dox did not kill the cell on contact so the effect of the drug could only be observed after 24 hours. The observed result agrees with the prediction.

6.2 Future Work

Current experimental results are limited to cell viability reading and manual cell counting. Due to the dimension of the designed device it is nearly impossible to perform conventional MTS assays using a plate reader. Future work would focus on applying MTS or similar assays within the microfluidic device to investigate cellular activities during Dox drug testing.

MTS (3-(4,5-dimethylthiazol-2-yl)-5-(3-carboxymethoxyphenyl)-2-(4-sulfophenyl)-2H-tetrazolium) is a colorimetric assay for viable cells. The dye is cleaved to a colored product by the activity of dehydrogenase enzymes and this indicates levels of mitochondrial activity in cells. The color development is proportional to the number of metabolically active cells [124, 144]. It is one of the most commonly used assays to evaluate cellular activity.

To further expand the function of the microfluidic device, we are looking into the possibility of incorporating microvalves into the existing device. With an integrated valve system, the flow profile of the culture media and cancer drug, and the seeding position of the cultured cell types can be more precisely controlled to simulate human blood vessels.

Bibliography

[1] E. Verpoorte and N. F. De Rooij, "Microfluidics meets MEMS," *Proceedings of the IEEE*, vol. 91, pp. 930- 953, 2003.

[2] S. S. Saliterman, *Fundamentals of BioMEMS and Medical Microdevices*. Bellingham, Washington USA: Wiley Interscience, 2006.

[3] V. Senez, T. Yamamoto, B. Poussard, T. Fukuba, J. M. Capron, and T. Fujii, "Evaluation of electric impedance spectra for single bio-cells in microfluidic devices using combined FEMLAB/HSPICE simulated models," *Monthly Journal of Institute of Industrial Science, University of Tokyo*, vol. 56, pp. 97-100, 2004.

[4] J. West, M. Becker, S. Tombrink, and A. Manz, "Micro total analysis systems. Latest advancements and trends," *Institute for Analytical Sciences*, vol. 78, pp. 4403-4419, 2008.

[5] S. J. Lee and S. Y. Lee, "Micro total analysis system (μ-TAS) in biotechnology," *Applied Microbiology and Biotechnology*, vol. 64, pp. 289-299, 2004.

[6] H. Andersson and A. van den Berg, "Microfluidic devices for cellomics: a review," *Sensors and Actuators B: Chemical*, vol. 92, pp. 315-325, 2003.

[7] R. M. Johann, "Cell trapping in microfluidic chips," *Analytical and Bioanalytical Chemistry*, vol. 385, pp. 1618-2642, 2006.

[8] E. Delamarche, D. Juncker, and H. Schmid, "Microfluidics for processing surfaces and miniaturizing biological assays," *Advanced Materials*, vol. 17, pp. 2911-2933, 2005.

[9] S. N. Bhatia, M. L. Yarmush, and M. Toner, "Controlling cell interactions by micropatterning in co-cultures: Hepatocytes and 3T3 fibroblasts," *Journal of Biomedical Materials Research*, vol. 34, pp. 189-199, 1997.

[10] L. Kim, Y.-C. Toh, J. Voldman, and H. Yu, "A practical guide to microfluidic perfusion culture of adherent mammalian cells," *Lab on Chip*, vol. 7, pp. 681-694, 2007.

[11] A. Khademhosseini, J. Yeh, G. Eng, J. Karp, H. Kaji, J. Borenstein, O. Farokhzad, and R. Langer, "Cell docking inside microwells within reversibly sealed microfluidic channels for fabricating multiphenotype cell arrays," *Lab on a Chip*, vol. 5, pp. 1380-1386, 2005.

[12] D. R. Albrecht, G. H. Underhill, A. Mendelson, and S. N. Bhatia, "Multiphase electropatterning of cells and biomaterials," *Lab on a chip*, vol. 7, pp. 702-209, 2007.

[13] P. R. C. Gascoyne and J. Vykoukal, "Particle separation by dielectrophoresis," *Electrophoresis*, vol. 23, pp. 1973-1983, 2002.

[14] H. A. Pohl, *Dieletrophoresis the behavior of neutral matter in nonuniform electric fields*. New York: Cambridge Univeristy Press., 1978.

[15] X.-B. Wang, Y. Huang, P. R. C. Gascoyne, and F. F. Becker, "Dielectrophoretic manipulation of particles," *IEEE Transactions on industry applications*, vol. 33, pp. 660-669, 1997.
[16] A. Rosenthal and J. Voldman, "Dielectrophoretic traps for single-particle patterning," *Biophysical Journal*, vol. 88, pp. 2193-2205, 2005.
[17] A. Ashkin, J. M. Dziedzic, and T. Yamane, "Optical trapping and manipulation of single cells using infrared laser beams," *Nature*, vol. 330, pp. 769-771, 1987.
[18] M. Evander, L. Johansson, T. Lilliehorn, J. Piskur, M. Lindvall, S. Johansson, M. Almqvist, T. Laurell, and J. Nilsson, "Noninvasive acoustic cell trapping in a microfluidic perfusion system for online bioassays," *Analytical Chemistry*, vol. 79, pp. 2984-2991, 2007.
[19] D. Bazou, L. A. Kuznetsova, and W. T. Coakley, "Physical enviroment of 2-D animal cell aggregates formed in a short pathlength ultrasound standing wave trap," *Ultrasound in Medicine & Biology*, vol. 31, pp. 423-430, 2005.
[20] J. H. Koschwanez, R. H. Carlson, and D. R. Meldrum, "Easily fabricated magnetic traps for single-cell applications," *Review of Scientific Instruments*, vol. 78, pp. 044301-5, 2007.
[21] A. Winkleman, K. L. Gudiksen, D. Ryan, G. M. Whitesides, D. Greenfield, and M. Prentiss, "A magnetic trap for living cells suspended in a paramagnetic buffer," *Applied Physics Letters*, vol. 85, pp. 2411-2413, 2004.
[22] A. Abbott, "Cell culture: Biology's new dimension," *Nature*, vol. 424, pp. 870-872, 2003.
[23] M. V. Risbud and M. Sittinger, "Tissue engineering: advances in in vitro cartilage generation," *Trends in Biotechnology*, vol. 20, pp. 351-356, 2002.
[24] S. Michael V, "Functional considerations in tissue-engineering whole organs," *Annals of the New York Academy of Sciences*, vol. 961, pp. 198-200, 2002.
[25] W.-G. Koh and M. V. Pishko, "Fabrication of cell-containing hydrogel microstructures inside microfluidic devices that can be used as cell-based biosensors," *Analytical and Bioanalytical Chemistry*, vol. 385, pp. 1389-1397, 2006.
[26] E. Leclerc, Y. Sakai, and T. Fujii, "Cell culture in 3-dimensional microfluidic structure of PDMS (polydimethylsiloxane)," *Biomedical Microdevices*, vol. 5, pp. 109-114, 2003.
[27] N. Pereira Rodrigues, Y. Sakai, and T. Fujii, "Cell-based microfluidic biochip for the electrochemical real-time monitoring of glucose and oxygen," *Sensors and Actuators B: Chemical*, vol. In Press, Corrected Proof, 2007.
[28] S. Raty, E. M. Walters, J. Davis, H. Zeringue, D. J. Beebe, S. L. Rodriguez-Zas, and M. B. Wheeler, "Embryonic development in the mouse is enhanced via microchannel culture," *Lab on a Chip*, vol. 4, pp. 186-190, 2004.
[29] Y. Tanaka, K. Sato, M. Yamato, T. Okano, and T. Kitamori, "Cell culture and life support system for microbioreactor and bioassay," *Journal of Chromatography A*, vol. 1111, pp. 233-237, 2006.
[30] A. P. Golden and J. Tien, "Fabrication of microfluidic hydrogels using molded gelatin as a sacrificial element," *Lab on Chip*, vol. 7, pp. 720-725, 2007.

[31] P. J. Hung, P. J. Lee, P. Sabounchi, R. Lin, and L. P. Lee, "Continuous perfusion microfluidic cell culture array for high-throughput cell-based assays," *Biotechnology and Bioengineering*, vol. 89, pp. 1-8, 2005.
[32] B. Alberts, A. Johnson, J. Lewis, M. Raff, K. Roberts, and P. Walter, *Molecular Biology of the Cell*, 3 ed. New York: Garland Publishing, 1994.
[33] G. M. Cooper, *The Cell A Molecular Approach*, 2 ed. Sunderland, Massachusetts: Sinauer Associates, Inc., 2000.
[34] "Stem Cell Basics," The National Institutes of Health resource for stem cell research, 2008.
[35] M. Richards, C.-Y. Fong, W.-K. Chan, P.-C. Wong, and A. Bongso, "Human feeders support prolonged undifferentiated growth of human inner cell masses and embryonic stem cells," *Nature Biotechnology*, vol. 20, pp. 933-936, 2002.
[36] H.-Q. Wang, L. Bai, B.-R. Shen, Z.-Q. Yan, and Z.-L. Jiang, "Coculture with endothelial cells enhances vascular smooth muscle cell adhesion and spreading via activation of [beta]1-integrin and phosphatidylinositol 3-kinase/Akt," *European Journal of Cell Biology*, vol. 86, pp. 51-62, 2007.
[37] S. R. Biggar and G. R. Crabtree, "Cell signaling can direct either binary or graded transcriptional responses," *The EMBO Journal*, vol. 20, pp. 3167-3176, 2001.
[38] G. M. Walker, M. S. Ozers, and D. J. Beebe, "Insect Cell Culture in Microfluidic Channels," *Biomedical Microdevices*, vol. 4, pp. 161-166, 2002.
[39] C. Yi, C.-W. Li, S. Ji, and M. Yang, "Microfluidics technology for manipulation and analysis of biological cells," *Analytica Chimica Acta*, vol. 560, pp. 1-23, 2006.
[40] H. Andersson and A. v. d. Berg, "Microfabrication and microfluidics for tissue engineering: state of the art and future opportunities," *Lab on a Chip*, vol. 4, pp. 98-103, 2004.
[41] N. W. Choi, M. Cabodi, B. Held, J. P. Gleghorn, L. J. Bonassar, and A. D. Stroock, "Microfluidic scaffolds for tissue engineering," *Nature Materials*, vol. 6, pp. 908-915, 2007.
[42] H. A. v. Recum, S. W. Kim, A. Kikuchi, M. Okuhara, Y. Sakurai, and T. Okano, "Novel thermally reversible hydrogel as detachable cell culture substrate," *Journal of Biomedical Materials Research*, vol. 40, pp. 631-639, 1998.
[43] S. R. Khetani, G. Szulgit, J. A. D. Rio, C. Barlow, and S. N. Bhatia, "Exploring interactions between rat hepatocytes and nonparenchymal cells using gene expression profiling," *Hepatology*, vol. 40, pp. 545-554, 2004.
[44] R. Johann and P. Renaud, "Microfluidic patterning of alginate hydrogels," *Biointerphases*, vol. 2, pp. 73-70, 2007.
[45] R. H. Li and D. H. A. F. T. Gentile, "Transport characterization of hydrogel matrices for cell encapsulation," *Biotechnology and Bioengineering*, vol. 50, pp. 365 - 373, 1995.
[46] S. Jean D, "Tissue engineering and reparative medicine," *Annals of the New York Academy of Sciences*, vol. 961, pp. 1-9, 2002.
[47] N. Wade, "In Tiny Cells, Glimpses Of Body's Master Plan," in *New York Times*, 2001.
[48] J. Lee, M. J. Cuddihy, and N. A. Kotov, "Three-dimensional cell culture matrices: State of the Art," *Tissue Engineering Part B: Reviews*, vol. 14, pp. 61-86, 2008.

[49] J. L. Drury and D. J. Mooney, "Hydrogels for tissue engineering: scaffold design variables and applications," *Biomaterials*, vol. 24, pp. 4337-4351, 2003.
[50] M. van der Rest and R. Garrone, "Collagen family of proteins," *FASEB J.*, vol. 5, pp. 2814-2823, 1991.
[51] M. Mitsuiki, A. Mizuno, and M. Motoki, "Determination of molecular weight of agars and effect of the molecular weight on the glass transition," *Journal of Agricultural and Food Chemistry*, vol. 47, pp. 473-478, 1999.
[52] Y. Ling, J. Rubin, Y. Deng, C. Huang, U. Demirci, J. M. Karp, and A. Khademhosseini, "A cell-laden microfluidic hydrogel," *Lab on a Chip*, vol. 7, pp. 756 - 762, 2007.
[53] M. S. Shoichet, R. H. Li, M. L. White, and S. R. Winn, "Stability of hydrogels used in cell encapsulation: An in vitro comparison of alginate and agarose," *Biotechnology and Bioengineering*, vol. 50, pp. 374-381, 1996.
[54] H. Uludag, P. De Vos, and P. A. Tresco, "Technology of mammalian cell encapsulation," *Advanced Drug Delivery Reviews*, vol. 42, pp. 29-64, 2000.
[55] A. D. Augst, H. J. Kong, and D. J. Mooney, "Alginate hydrogels as biomaterials," *Macromolecular Bioscience*, vol. 6, pp. 623-633, 2006.
[56] T. Maguire, A. E. Davidovich, E. J. Wallenstein, E. Novik, N. Sharma, H. Pedersen, I. P. Androulakis, R. Schloss, and M. Yarmush, "Control of hepatic differentiation via cellular aggregation in an alginate microenvironment," *Biotechnology and Bioengineering*, vol. 98, pp. 631-644, 2007.
[57] M. Peirone, C. J. D. Ross, G. Hortelano, J. L. Brash, and P. L. Chang, "Encapsulation of various recombinant mammalian cell types in different alginate microcapsules," *Journal of Biomedical Materials Research*, vol. 42, pp. 587 - 596, 1998.
[58] A. Mizrahi, "Pluronic polyols in human lymphocyte cell line cultures," *Journal of Clinical Microbiology*, vol. 2, pp. 11-13, 1975.
[59] N. Ma, J. J. Chalmers, J. G. Aunins, W. Zhou, and L. Xie, "Quantitative studies of cell-bubble interactions and cell damage at different Pluronic F-68 and cell concentrations," *Biotechnology Progress*, vol. 20, pp. 1183-1191, 2004.
[60] D. F. Stamatialis, H. H. M. Rolevink, and G. H. Koops, "Transdermal timolol delivery from a Pluronic gel," *Journal of Controlled Release*, vol. 116, pp. e53-e55, 2006.
[61] V. Bazargan, "Micro Flow Control Using Thermally Responsive Polymer Solutions," in *Mechanical Enginnering*, vol. Master of Applied Science. Vancouver University of British Columbia, 2008, pp. 151.
[62] J. E. Matthew, Y. L. Nazario, S. C. Roberts, and S. R. Bhatia, "Effect of mammalian cell culture medium on the gelation properties of Pluronic® F127," *Biomaterials*, vol. 23, pp. 4615-4619, 2002.
[63] M.-C. Jones and J.-C. Leroux, "Polymeric micelles - a new generation of colloidal drug carriers," *European Journal of Pharmaceutics and Biopharmaceutics*, vol. 48, pp. 101-111, 1999.
[64] F. Cellesi, N. Tirelli, and J. A. Hubbell, "Materials for cell encapsulation via a new tandem approach combining reverse thermal gelation and covalent crosslinking," *Macromolecular Chemistry and Physics*, vol. 203, pp. 1466-1472, 2002.

[65] H. G. Schild, "Poly (N-isopropylacrylamide) : experiment, theory and application," *Progress in polymer science*, vol. 17, pp. 163-249, 1992.
[66] Q. Chang-Yun, S. Yun-Xia, C. Han, C. Si-Xue, Z. Xian-Zheng, and Z. Ren-Xi, "Thermosensitive P(NIPAAm-co-PAAc-co-HEMA) nanogels conjugated with transferrin for tumor cell targeting delivery," *Nanotechnology*, pp. 275102, 2008.
[67] J. Yongmei, L. Yang, M. Yun, L. Xiaoli, Q. Zongyi, Z. Meifang, and H. J. Adler, "Novel Interpenetrating Networks (IPNs) Hydrogels Prepared In Situ by Liquid-Phase Photopolymerization," *Macromolecular Symposia*, vol. 264, pp. 95-99, 2008.
[68] J. E. Chung, M. Yokoyama, M. Yamato, T. Aoyagi, Y. Sakurai, and T. Okano, "Thermo-responsive drug delivery from polymeric micelles constructed using block copolymers of poly(N-isopropylacrylamide) and poly(butylmethacrylate)," *Journal of Controlled Release*, vol. 62, pp. 115-127, 1999.
[69] M. Jasionowski, K. Krzyminski, W. Chrisler, L. M. Markille, J. Morris, and A. Gutowska, "Thermally-reversible gel for 3-D cell culture of chondrocytes," *Journal of Materials Science: Materials in Medicine*, vol. 15, pp. 575-582, 2004.
[70] H.-F. Lu, E. D. Targonsky, M. B. Wheeler, and Y.-L. Cheng, "Thermally induced gelable polymer networks for living cell encapsulation," *Biotechnology and Bioengineering*, vol. 96, pp. 146-155, 2007.
[71] B. Amsden and N. Turner, "Diffusion characteristics of calcium alginate gels," *Biotechnology and Bioengineering*, vol. 65, pp. 605-610, 2000.
[72] "Control Release Application Guide," FMC Biopolymer, 2003.
[73] G. E. Jones, *Human Cell Culture Protocals*. Totowa, New Jersey: Humana Press, 1996.
[74] R. H. McDowell, *Properties of Alginate*, 2 ed. London: Alginate Industries Limited, 1957.
[75] A. Krtolica, C. O. d. Solorzano, S. Lockett, and J. Campisi, "Quantification of epithelial cells in coculture with fibroblasts by fluorescence image analysis.," *Cytometry*, vol. 49, pp. 73-82, 2002.
[76] J. C. McDonald, D. C. Duffy, J. R. Anderson, D. T. Chiu, H. Wu, O. J. A. Schueller, and G. M. Whitesides, "Fabrication of microfluidic systems in poly(dimethylsiloxane)," *Electrophoresis*, vol. 21, pp. 27-40, 2000.
[77] B.-H. Jo, L. M. V. Lerberghe, K. M. Motsegood, and D. J. Beebe, "Three-dimensional micro-channel fabrication in polydimethylsiloxane (PDMS) elastomer," *Journal of microelectromechanical systems*, vol. 9, pp. 76-81, 1999.
[78] W. W. Y. Chow, K. F. Lei, G. Shi, W. J. Li, and Q. Huang, "Microfluidic channel fabrication by PDMS-interface bonding," *Smart materials and structures*, vol. 15, pp. S112-S116, 2006.
[79] C. Jungfer, T. Schwartz, and U. Obst, "UV-induced dark repair mechanisms in bacteria associated with drinking water," *Water Research*, vol. 41, pp. 188-196, 2007.
[80] L. F. Wang, Q. Ji, T. E. Glass, T. C. Ward, J. E. McGrath, M. Muggli, G. Burns, and U. Sorathia, "Synthesis and characterization of organosiloxane modified segmented polyether polyurethanes," *Polymer*, vol. 41, pp. 5083-5093, 2000.

[81] J. Flueckiger, "Realization of a mcirofluidic chip for optical detection of glucose/oxygen," in *Microsystems Laboratory*, vol. Mater of applied science. Lausanne: EPFL, 2007, pp. 113.
[82] C. O'Donovan, J. Hynes, D. Yashunski, and D. B. Papkovsky, "Phosphorescent oxygen-sensitive materials for biological applications," *Royal Society of Chemistry Journals*, vol. 15, pp. 2946-2951, 2005.
[83] D. C. Duffy, J. C. McDonald, O. J. A. Schueller, and G. M. Whitesides, "Rapid prototyping of microfluidic systems in Poly(dimethylsiloxane)," *Analytical Chemistry*, vol. 70, pp. 4974-4984, 1998.
[84] D. J. Campbell, K. J. Beckman, C. E. Calderon, P. W. Doolan, R. H. Moore, A. B. Ellis, and G. C. Lisensky, "Uses of Polydimethylsiloxane (PDMS) elastomer," *Journal of Chemical Education*, vol. 76, pp. 537, 1999.
[85] A. O'Neill, J. S. Hoo, and G. Walker, "Chips & Tips: Rapid Curing of PDMS For Microfluidic Applications," in *Lab on a Chip*, vol. 2008: Lab on a Chip, 2006.
[86] M. Wu, J. Urban, Z. Cui, and Z. Cui, "Development of PDMS microbioreactor with well-defined and homogenous culture environment for chondrocyte 3-D culture," *Biomedical Microdevices*, vol. 8, pp. 331-340, 2006.
[87] S. G. Charati and S. A. Stern, "Diffusion of gases in silicone polymers: Molecular Dynamics Simulations," *Macromolecules*, vol. 31, pp. 5529-5535, 1998.
[88] T. C. Merkel, V. I. Bondar, K. Nagai, B. D. Freeman, and I. Pinnau, "Gas sorption, diffusion, and permeation in poly(dimethylsiloxane)," *Journal of Polymer Science Part B: Polymer Physics*, vol. 38, pp. 415-434, 2000.
[89] Y. Nahmias, Y. Kramvis, L. Barbe, M. Casali, F. Berthiaume, and M. L. Yarmush, "A novel formulation of oxygen-carrying matrix enhances liver specific function of cultured hepatocytes," *The FASEB Journal*, vol. 20, pp. 2531-2533, 2006.
[90] J. Bustamante, M. Galleano, E. E. Medrano, and A. Boveris, "Adriamycin effects on hydroperoxide metabolism and growth of human breast tumor cells," *Breast Cancer Research and Treatment*, vol. 17, pp. 145-153, 1990.
[91] L. Liu and H. Sheardown, "Glucose permeable poly (dimethyl siloxane) poly (N-isopropyl acrylamide) interpenetrating networks as ophthalmic biomaterials," *Biomaterials*, vol. 26, pp. 233-244, 2005.
[92] F. Mizutani, S. Yabuki, and S. Iijima, "Use of polydimethylsiloxane for constructing amperometric glucose-sensing enzyme electrode with low interference level," *Electroanalysis*, vol. 13, pp. 370-374, 2001.
[93] G. C. Randall and P. S. Doyle, "Permeation-driven flow in poly(dimethylsiloxane) microfluidic devices," *Proceedings of the National Academy of Sciences of the United States of America*, vol. 102, pp. 10813-10818, 2005.
[94] J. M. K. Ng, I. Gitlin, A. D. Stroock, and G. M. Whitesides, "Components for integrated poly(dimethylsiloxane) microfluidic systems," *Electrophoresis*, vol. 23, pp. 3461-3473, 2002.
[95] S. Bhattacharya, A. Datta, J. M. Berg, and S. Gangopadhyay, "Studies on surface wettability of poly(dimethyl) siloxane (PDMS) and glass under oxygen-plasma treatment and correlation with bond strength," *Microelectromechanical Systems*, vol. 14, pp. 590- 597, 2005.

[96] H. Hillborg and U. W. Gedde, "Hydrophobicity changes in silicone rubbers," *IEEE Transactions on Dielectrics and Electrical Insulation*, vol. 6, pp. 703 - 717, 1999.
[97] S. Bhattacharya, G. Yuanfang, V. Korampally, M. T. Othman, S. A. Grant, S. B. Kleiboeker, K. Gangopadhyay, and S. Gangopadhyay, "Optimization of design and fabrication processes for realization of a PDMS-SOG-Silicon DNA amplification chip," *Microelectromechanical Systems*, vol. 16, pp. 401-410, 2007.
[98] G. K. Fedder, "Mems fabrication," presented at Test Conference, 2003. Proceedings. ITC 2003. International, 2003.
[99] M. J. Madou, *Fundamentals of Microfabrication The science of Miniaturization 2nd Edition*. Boca Raton US: CRC Press LLC, 2002.
[100] H. Lorenz, M. Despont, N. Fahrni, N. LaBianca, P. Renaud, and P. Vettiger, "SU-8: a low-cost negative resist for MEMS," *Journal of Micromechanics and Microengineering*, pp. 121, 1997.
[101] F. R. and F. R.J., "Influence of processing conditions on the thermal and mechanical properties of SU8 negative photoresist coatings " *Journal of Micromechanics and Microengineering*, vol. 13, pp. 80-88, 2003.
[102] D. Van Steenwinckel, J. H. Lammers, T. Koehler, R. L. Brainard, and P. Trefonas, "Resist effects at small pitches," *Journal of Vacuum Science & Technology B: Microelectronics and Nanometer Structures*, vol. 24, pp. 316-320, 2006.
[103] M. S. Jane, D. G. Jeffrey, C. L. Nancy, E. C. Will, and J. H. Steven, "Negative photoresists for optical lithography," *IBM Journal of Research and Development*, vol. 41, pp. 81-94, 1997.
[104] H. Ito, C. G. Willson, and J. M. J. Frechet, "Positive and Negative Working Resist Compositions with Acid-Generating Photoinitiator and Polymer with Acid-Labile Groups Pendant From Polymer Backbone," U. S. Patent, Ed., G03C 160; G03C 168 ed. USA: International Business Machines Corporation, 1985.
[105] A. L. Bogdanov and S. S. Peredkov, "Use of SU-8 photoresist for very high aspect ratio x-ray lithography," *Microelectronic Engineering*, vol. 53, pp. 493-496, 2000.
[106] C. J. Jackson and M. Nguyen, "Human microvascular endothelial cells differ from macrovascular endothelial cells in their expression of matrix metalloproteinases," *The International Journal of Biochemistry & Cell Biology*, vol. 29, pp. 1167-1177, 1997.
[107] E. M. Purcell, "Life at low Reynolds number," *American Journal of Physics*, vol. 45, pp. 3-11, 1977.
[108] B. H. Weigl, R. L. Bardell, and C. R. Cabrera, "Lab-on-a-chip for drug development," *Advanced Drug Delivery Reviews*, vol. 55, pp. 349-377, 2003.
[109] P. Ander, L. Leung-Louie, and F. Silvestri, "Polycations. 1. Sodium, Calcium, and Sulfate Ion Diffusion Coefficients in Aqueous Salt Solutions Containing Ionene Bromides," *Macromolecules*, vol. 12, pp. 1204-1207, 1979.
[110] Y. J. Chuang, F. G. Tseng, and W. K. Lin, "Reduction of diffraction effect of UV exposure on SU-8 negative thick photoresist by air gap elimination," *Microsystem Technologies*, vol. 8, pp. 308-313, 2002.

[111] A. Vancha, S. Govindaraju, K. Parsa, M. Jasti, M. Gonzalez-Garcia, and R. Ballestero, "Use of polyethyleneimine polymer in cell culture as attachment factor and lipofection enhancer," *BMC Biotechnology*, vol. 4, pp. 23, 2004.
[112] M. Guerra-Crespo, J. L. Charli, V. H. Rosales-Garcia, G. Pedraza-Alva, and L. Perez-Martinez, "Polyethylenimine improves the transfection efficiency of primary cultures of post-mitotic rat fetal hypothalamic neurons," *Journal of Neuroscience Methods*, vol. 127, pp. 179 - 192, 2003.
[113] D. G. Anderson, A. Akinc, N. Hossain, and R. Langer, "Structure/property studies of polymeric gene delivery using a library of poly([beta]-amino esters)," *Molecular Therapy*, vol. 11, pp. 426-434, 2005.
[114] B. Gao, P. Jiang, F. An, S. Zhao, and Z. Ge, "Studies on the surface modification of diatomite with polyethyleneimine and trapping effect of the modified diatomite for phenol," *Applied Surface Science*, vol. 250, pp. 273-279, 2005.
[115] O. Boussif, F. Lezoualc'h, M. A. Zanta, M. D. Mergny, D. Scherman, B. Demeneix, and J. P. Behr, "A versatile vector for gene and oligonucleotide transfer into cells in culture and in vivo: polyethylenimine," *The Proceedings of the National Academy of Sciences USA*, vol. 92, pp. 7297 - 7301, 1995.
[116] S. Sangribsub, P. Tangboriboonrat, T. Pith, and G. Decher, "Hydrophobization of multilayered film containing layer-by-layer assembled nanoparticle by Nafion adsorption," *Polymer Bulletin*, vol. 53, pp. 425-434, 2005.
[117] V. Médout-Marère, A. El Ghzaoui, C. Charnay, J. M. Douillard, G. Chauveteau, and S. Partyka, "Surface Heterogeneity of Passively Oxidized Silicon Carbide Particles: Hydrophobic-Hydrophilic Partition," *Journal of Colloid and Interface Science*, vol. 223, pp. 205-214, 2000.
[118] S. H. Behrens and D. G. Grier, "The charge of glass and silica surfaces," *The Journal of Chemical Physics*, vol. 115, pp. 6716-6721, 2001.
[119] M. Flury and H. Fluhler, "Tracer characteristics of Brilliant Blue FCF," *Soil Science Society of America Journal*, vol. 59, pp. 22-27, 1995.
[120] J. Germán-Heins and M. Flury, "Sorption of Brilliant Blue FCF in soils as affected by pH and ionic strength," *Geoderma*, vol. 97, pp. 87-101, 2000.
[121] "Food Color Facts," U. S. F. a. D. Administration, Ed.: U. S. Food and Drug Administration, 1993.
[122] *Food Chemicals Codex*, 5 ed: National Academies Press, 2003.
[123] W.-J. Chang, D. Akin, M. Sedlak, M. R. Ladisch, and R. Bashir, "Poly(dimethylsiloxane) (PDMS) and silicon hybrid biochip for bacterial culture," *Biomedical Microdevices*, vol. 5, pp. 281-290, 2003.
[124] M. Butler, *Animal Cell Culture & Technology*, 2 ed. New York: Garland Science/BIOS Scientific, 2004.
[125] I. Meyvantsson and D. J. Beebe, "Cell culture models in microfluidic systems," *Annual Review of Analytical Chemistry*, vol. 1, pp. 423-449, 2008.
[126] W. Tan and T. A. Desai, "Microscale multilayer cocultures for biomimetic blood vessels," *Journal of Biomedical Materials Research Part A*, vol. 72A, pp. 146-160, 2005.
[127] E. C. Beuvery, J. B. Griffiths, and W. P. Zeijlemaker, *Animal cell technology: Developments Towards the 21st Century*. Boston: Kluwer Academic Publishers, 1995.

[128] Invitrogen, "LIVE/DEAD® Viability/Cytotoxicity Kit *for mammalian cells," Invitrogen, 2005.
[129] S. Hockley, V. Arlt, D. Brewer, I. Giddings, and D. Phillips, "Time- and concentration-dependent changes in gene expression induced by benzo(a)pyrene in two human cell lines, MCF-7 and HepG2," *BMC Genomics*, vol. 7, pp. 260, 2006.
[130] N. B. Javitt, "Hep G2 cells as a resource for metabolic studies: lipoprotein, cholesterol, and bile acids," *FASEB Journal*, vol. 4, pp. 161-168, 1990.
[131] A. Bader, I. H. B. Rinkes, E. I. Closs, C. M. Ryan, M. Toner, J. M. Cunningham, R. G. Tompkins, and M. L. Yarmush, "A stable long-term hepatocyte culture system for studies of physiologic processes: cytokine stimulation of the acute phase response in rat and human hepatocytes," *Biotechnology Progress*, vol. 8, pp. 219-225, 1992.
[132] R. A. Roberts and A. R. Soames, "Hepatocyte Spheroids: Prolonged Hepatocyte Viability for in Vitro Modeling of Nongenotoxic Carcinogenesis," *Fundamental and Applied Toxicology*, vol. 21, pp. 149-158, 1993.
[133] W. Dunham, "Report sees 7.6 million global 2007 cancer deaths," in *American Cancer Society*, 2007.
[134] F. Bray, P. McCarron, and D. M. Parkin, "The changing global patterns of female breast cancer incidence and mortality," *Breast Cancer Research*, vol. 6, pp. 229 - 239, 2004.
[135] A. Kamb, S. Wee, and C. Lengauer, "Why is cancer drug discovery so difficult?," *Nature Reviews Drug Discovery*, vol. 6, pp. 115-120, 2007.
[136] M. Bontenbal, A. M. Sieuwerts, H. A. Peters, W. L. J. v. Putten, J. A. Foekens, and J. G. M. Klijn, "Uptake and distribution of doxorubicin in hormone-manipulated human breast cancer cells in vitro," *Breast Cancer Research and Treatment*, vol. 51, pp. 139-148, 1998.
[137] F. A. Fornari, J. K. Randolph, J. C. Yalowich, M. K. Ritke, and D. A. Gewirtz, "Interference by doxorubicin with DNA unwinding in MCF-7 breast tumor cells," *Molecular Pharmacology*, vol. 45, pp. 649-656, 1994.
[138] N. R. Bachur, F. Yu, R. Johnson, R. Hickey, Y. Wu, and L. Malkas, "Helicase inhibition by anthracycline anticancer agents," *Molecular Pharmacology*, vol. 41, pp. 993-998, 1992.
[139] M. Abramowitz and M. W. Davidson, "Fluorochrome Data Tables Excitation/Emission Wavelengths Listed by Fluorochrome," Olympus Microscopy Resource Center, 2008.
[140] P. O. Gendron, F. Avaltroni, and K. Wilkinson, "Diffusion Coefficients of Several Rhodamine Derivatives as Determined by Pulsed Field Gradient–Nuclear Magnetic Resonance and Fluorescence Correlation Spectroscopy," *Journal of Fluorescence*, vol. 18, pp. 1093-1101, 2008.
[141] A. T. Hubbard, *Encyclopedia of Surface And Colloid Science*, vol. 4, 2 ed. New York: Taylor and Francis, 2006.
[142] Q. Zhao, B. Han, Z. Wang, C. Gao, C. Peng, and J. Shen, "Hollow chitosan-alginate multilayer microcapsules as drug delivery vehicle: doxorubicin loading and in vitro and in vivo studies," *Nanomedicine: Nanotechnology, Biology and Medicine*, vol. 3, pp. 63-74, 2007.

[143] M. Rajaonarivony, C. Vauthier, G. Couarraze, F. Puisieux, and P. Couvreur, "Development of a new drug carrier made from alginate," *Journal of Pharmaceutical Sciences*, vol. 82, pp. 912-917, 1993.
[144] G. Malich, B. Markovic, and C. Winder, "The sensitivity and specificity of the MTS tetrazolium assay for detecting the in vitro cytotoxicity of 20 chemicals using human cell lines," *Toxicology*, vol. 124, pp. 179-192, 1997.
[145] E. M. Lucchetta, M. S. Munson, and R. F. Ismagilov, "Characterization of the local temperature in space and time around a developing Drosophila embryo in a microfluidic device," *Lab on a Chip*, vol. 6, pp. 185-190, 2006.
[146] E. Leclerc, A. Corlu, L. Griscom, R. Baudoin, and C. Legallais, "Guidance of liver and kidney organotypic cultures inside rectangular silicone microchannels," *Biomaterials*, vol. 27, pp. 4109-4119, 2006.
[147] F. Lin and E. C. Butcher, "T cell chemotaxis in a simple microfluidic device," *Lab on a Chip*, vol. 6, pp. 1462 - 1469, 2006.
[148] J. Park, T. Bansal, M. Pinelis, and M. M. Maharbiz, "A microsystem for sensing and patterning oxidative microgradients during cell culture," *Lab on a Chip*, vol. 6, pp. 611-622, 2006.
[149] D. Beebe, M. Wheeler, H. Zeringue, E. Walters, and S. Raty, "Microfluidic technology for assisted reproduction," *Theriogenology*, vol. 57, pp. 125-135, 2002.
[150] K. Sato, A. Egami, T. Odake, M. Tokeshi, M. Aihara, and T. Kitamori, "Monitoring of intercellular messengers released from neuron networks cultured in a microchip," *Journal of Chromatography A*, vol. 1111, pp. 228-232, 2006.
[151] M. C. Liu, D. Ho, and Y.-C. Tai, "Monolithic fabrication of three-dimensional microfluidic networks for constructing cell culture array with an integrated combinatorial mixer," *Sensors and Actuators B: Chemical*, vol. 129, pp. 826-833, 2008.
[152] A. Prokop, Z. Prokop, D. Schaffer, E. Kozlov, J. Wikswo, D. Cliffel, and F. Baudenbacher, "Nanoliterbioreactor: long-term mammalian cell culture at nanofabricated scale," *Biomedical Microdevices*, vol. 6, pp. 325-339, 2004.
[153] X. Zhang, H. Yin, J. M. Cooper, and S. J. Haswell, "A microfluidic-based system for analysis of single cells based on Ca2+ flux," *Electrophoresis*, vol. 27, pp. 5093-5100, 2006.
[154] J. W. Allen, S. R. Khetani, and S. N. Bhatia, "Invitro zonation and toxicity in a hepatocyte bioreactor," *Toxicological Sciences*, vol. 84, pp. 110-119, 2005.
[155] N. Ye, J. Qin, W. Shi, X. Liu, and B. Lin, "Cell-based high content screening using an integrated microfluidic device," *Lab Chip*, vol. 7, pp. 1696 - 1704, 2007.
[156] I. Inoue, Y. Wakamoto, H. Moriguchi, K. Okano, and K. Yasuda, "On-chip culture system for observation of isolated individual cells," *Lab on a Chip*, vol. 1, pp. 50-55, 2001.
[157] S.-Y. Cheng, S. Heilman, M. Wasserman, S. Archer, M. L. Shuler, and M. Wu, "A hydrogel-based microfluidic device for the studies of directed cell migration," *Lab on a Chip*, vol. 7, pp. 763-769, 2007.
[158] D. Irimia, G. Charras, N. Agrawal, T. Mitchison, and M. Toner, "Polar stimulation and constrained cell migration in microfluidic channels," *Lab on a Chip*, vol. 7, pp. 1783-1790, 2007.

[159] A. P. Wong, R. Perez-Castillejos, J. Christopher Love, and G. M. Whitesides, "Partitioning microfluidic channels with hydrogel to construct tunable 3-D cellular microenvironments," *Biomaterials*, vol. 29, pp. 1853-1861, 2008.
[160] R. Gomez-Sjoberg, A. A. Leyrat, D. M. Pirone, C. S. Chen, and S. R. Quake, "Versatile, fully automated, microfluidic cell culture system," *Analytical Chemistry*, vol. 79, pp. 8557-8563, 2007.
[161] W. Tan and T. A. Desai, "Layer-by-layer microfluidics for biomimetic three-dimensional structures," *Biomaterials*, vol. 25, pp. 1355-1364, 2004.
[162] T. Braschler, R. Johann, M. Heule, L. Metref, and P. Renaud, "Gentle cell trapping and release on a microfluidic chip by in situ alginate hydrogel formation," *Lab on a chip*, vol. 5, pp. 553-559, 2005.
[163] V. L. Workman, S. B. Dunnett, P. Kille, and D. D. Palmer, "On-Chip Alginate Microencapsulation of Functional Cells," *Macromolecular Rapid Communications*, vol. 29, pp. 165 - 170, 2007.
[164] Y. Nakashima and T. Yasuda, "Cell differentiation guidance using chemical stimulation controlled by a microfluidic device," *Sensors and Actuators A: Physical*, vol. 139, pp. 252-258, 2007.
[165] T. Kaneko, K. Kojima, and K. Yasuda, "An on-chip cardiomyocyte cell network assay for stable drug screening regarding community effect of cell network size," *Analyst*, vol. 132, pp. 892 - 898, 2007.
[166] S.-M. Ong, C. Zhang, Y.-C. Toh, S. H. Kim, H. L. Foo, C. H. Tan, D. van Noort, S. Park, and H. Yu, "A gel-free 3D microfluidic cell culture system," *Biomaterials*, vol. 29, pp. 3237-3244, 2008.

Appendices

A. Status of Cell Culture Inside Microdevices

Cell Type	Material for Extra Cellular Matrix	Description
Mouse Embryos	None	• Mammalian embryos were cultured in microchannels without continuous media supply [28].
Drosophila melanogaster embryo	None	• Fruit fly embryos were immobilized with double-coated tape to study the dynamics of biochemical networks as cells respond to changes in temperature. [145].
Embryonic liver and kidney explants	None	• Study cellular responses in terms of migration/proliferation on PDMS surface [146]. Cells were subject to shear stress.
Human peripheral blood T lymphocytes (hPBT)	None	• T cells were used to study the cellular response to single and competing gradients of chemokine CCL19 and CXCL12 [147]. Cells were subject to shear stress.
Spodoptera frugiperda (Sf9)	None	• One of the earliest cellular study using microchannel. Insect cells were cultured with in static microfluidic environment [38].
Human Carcinoma	None	• Long term culture inside micro-environment for further study [31]. Cells were subject to shear stress.
Rate C2C12 myoblasts	None	• Cells were cultured in static microenvironment to characterize the device which generates a precise dose of dissolved oxygen [148].

Bacillus subtilis bacteria	None	• Bacillus subtilis were cultured within static microenvironment to demonstrate dynamic aerotaxis assays driven by oxygen microgradients [148].
Embryos / Oocytes	None	• One of the earliest cellular study using microchannel. Manipulate and culture embryos and oocytes to improve efficiencies in assisting reproduction [149]. Cells were subject to shear stress when changing media.
Rate hippocampal nerve	None	• Hippocampus was cultured to form neural networks for biological studies [150]. Cells were subject to shear stress when changing media.
B35 rat neuroblastoma	None	• Neuroblastoma cells were cultured to prove the microfluidic chip coated with parylene C could sustain cell growth [151]. Cells were subject to shear stress when changing media.
Fibroblast (CRL-10225, ATCC)	None	• Mechanical sieves were used [152]. Cells were subject to shear stress during trapping and culturing.
CHO Epithelial	None	• Monitor the cell activities inside Nanoliter Bioreactors [152]. Cells were subject to shear stress. • CHO cells were immobilized for *in situ* monitoring of the calcium flux response to agonists [153]. Cells were subject to shear stress.
Hepatocytes (Hep G2)	None	• Studies oxygen and nutrient consumption , and the synthesis of albumin and urea in microchip environment [26, 27]. Cells were subject to shear stress. • Test for drug screening and toxicology [154]. Cells were subject to shear stress.

		• Cells were trapped with mechanical sieves [152]. • Multiple drug gradient generator is integrated for drug discovery application [155]. Cells were subject to shear stress.
Rat Hepatocytes (AML-12)	None	• Demonstrate the possibility of cell culture in microchannel [29]. Cells were subject to shear stress.
	Agarose	• Cells were cultured in a microfluidic device that was made of agarose gel [52]. Cells were in contact with 70°C agarose solution.
E Coli	None	• Study E Coli cell growth rate and cell division time in a single cell culture environment [156]. • A steady gradient of α-methyl-DL-aspartate (attractant) was applied to carry out chemotaxis experiment [157]. Cells were subject to shear stress.
Human promyelocytic leukemia cells (HL-60)	None	• A steady gradient of formyl-Met-Leu-Phe (f-MLP, attractant) is applied to carry out the chemotaxis experiment [157]. Cells were subject to shear stress. • HL-60 cell line is used for studying chemotaxis that is induced by chemoattractants [158].
LADMAC / BAC 1.2F5	None	• Separate microchannel using matrigel to achieve co-culture (LADMAC and BAC cells) [159]. Cells were subject to shear stress.
Hepatocyte / Fibroblast	None	• Co-culture these two cell types to produce an *in vitro* model of zonation [154]. Cells were subject to shear stress.

	poly(ethylene glycol) (PEG)	• Perform cytotoxicity assays to the cultured cell line and demonstrate the possibility of co-culture more than one cell type [25]. Cells were exposed with UV light
Human primary mesenchymal stem cells (hMSCs)	Pluronic F-127	• Demonstrate the possibility of culture hMSCs in an automated microfluidic device and monitor the effect of osteogenic differentiation factors on cell motility [160].
Fibroblast (IMR-90) / Vein smooth muscle cells (HUVSMC) / Vein endothelial cells (HUVEC)	Collagen, Collagen-chitosan, matrigel and fibrin	• Co-culture multiple cell types together to form layer-by-layer tissue like 3-tunic structure [161]. Cells were subject to low temperature (0°C)
Yeast cell	Alginate	• Yeast cells were cultured to demonstrate the possibility and versatility of reversible cell trapping using alginate [44, 162].
HEK293 (CRL-1573, ATCC)	Alginate	• Encapsulated in microbeads inside microdevice [163].
U-2 OS	Alginate	• Demonstrate the possibility of encapsulating cells inside microbeads [163].
Adrenal pheochromocytoma (PC12)	Alginate	• Study the function of cells inside alginate microbeads [163].
	None	• Nerve growth factor is introduced in the microchannel through microvalves to study the cell differentiation and axon elongation [164].
Chondrocyte	Agarose	• Compare the metabolic activity (lactate production rate) and matrix (glycosaminoglycan) production of chondrocytes between microscale and larger culture scale [86]. Cells were in contact with agarose

		solution at higher temperature.
Cardiomyocytes	Agarose	• The beating state of cardiomyocytes is studied for drug (Haloperidol) testing [165]. Cells were cultured in static condition.
Human lung epithelial (A549, ATCC)	Aldehydes + inter-cellular polymeric linker	• Cells were modified with aldehydes to demonstrate the possibility of gel-free 3-D culture [166].
Human liver cell line (C3A, ATCC)	Aldehydes + inter-cellular polymeric linker	• After modified with aldehydes, cell clumps were formed without the use of gel encapsulation [166].
Rat primary progenitor cells (BMSCs)	Aldehydes + inter-cellular polymeric linker	• Demonstrate the possibility of 3-D culture without the use of hydrogel after modify the cell surface with aldehydes [166].

B. Chip Fabrication Recipe

Step N°	Description	Equipment	Program / Parameters	Target	Actual	Remarks
1	WAFER PREPARATION					
1.2	Wafer preparation	PECVD	Oxigen Plasma, Descum,	500mT pressure 150W power 300 sec time 100 sccm O2		PECVD and dehydration bake @ 200C for 10min
		Wet Bench	Piranha solution, wet etch, Oxygen Plasma			5:1 of H2SO4:H2O2 in Pyrex beaker exothermic reaction, 10min and then 20min of dehydration @ 200C on hot plate + Oxygen Plasma, 150W, 300s
2	PHOTOLITHOGRAPHY - Mask					
2.2	PR coating	Wet Bench	ramp + 100 rpm/s 2100 rpm 40 s	100 um		SU-8 2075, Microchem
2.3	Relaxation					Wait 2 min
2.4	PR pre-bake	Hotplate	ramp 10°C/min @ 65 °C 3 min ramp 10°C/min @ 95 °C 5 min ramp 10°C/min @ 65 °C 2 min	3min @ 65 C 10min @ 95 C 2min @ 65 C	5min @ 65 °C 10min @ 95 °C 3min @ 65 °C	Each sample has one dedicated hotplate to prevent sudden change of temerpature.
2.5	PR expose	Canon mask aligner	Hard contact,	2x40s	2x40s	The glass mask is pressend onto the transparent and the Su-8 surface -> hard contact. Exposure dose : 215- 240 mJ/cm^2
2.6	PR post-bake	Hotplate	ramp 10°C/min @ 65 °C 2 min ramp 10°C/min @ 95 °C 7 min ramp 10°C/min @ 65 °C 2 min	2min @ 65 C 7min @ 95C 2min @ 65C	2min @ 65 °C 7min @ 95 °C 2min @ 65 °C	Each sample has one dedicated hotplate to prevent sudden change of temerpature.
2.7	PR develope	Wet Bench	SU-8 developper Microchem	7-10 min	10 min	The develop time varies from sample to sample
2.9	Rinsing	wet Bench	Isopropanol / N2 dry			
3	PDMS BONDING GLASS					
3.1	Sample preparation	Dry Bench	Ethyl Alcohol Oven			Sample rinsed with Ethyl Alcohol and placed inside oven for 20 min at 50°C
3.2	PDMS Bonding	PECVD	Oxygen Plasma, Discum	500mT pressure 30W power 13 sec time 100 sccm O2		

C. Mammalian Cell Suspension Preparation Protocol

1. Suck out / Pipette out the media (make sure the needle does not touch the plane of the flask with cells, suck out / pipette out the liquid by tilting the flask - thus all the liquid is in the corner)
2. Wash cells with PBS (3ml)
3. Suck out / Pipette out PBS
4. Add Trypsin + EDTA (2ml)
5. Bang flask on all 4 sides to loosen up the cells
6. Incubate the cells for 2-3 minutes and check under microscope to see if all the cells have detached (i.e. all the cells will appear to be moving and floating on the liquid)
7. Add 2 ml of culture media (+FBS) to the flasks
8. Pipette up and down for the at lest 10 times – this ensures cells are evenly suspended and there are no clumps
9. Transfer the cells into a 15 ml conical tube
10. Centrifuge the tube for about 5 min
11. Discard the supernatant
12. Re-suspend the cells in about 2 ml of media – pipette up at least 10 times to ensure even suspension
13. Take out 10µl of the cell suspension and count under microscope using a Hemocytometer, calculate the concentration of cells and amount of cell suspension needed for the experiment
14. Make the required suspension – diluting or concentrating the stock (if necessary)

D. Drug Testing with LCC6/Her2 and Doxorubicin

Control: Cells in chip + gel + media (no DMSO, no drugs)
Cells in chip + gel + media + DMSO (no drugs)
Cells in wells + no drug
Cells in wells + DMSO (no drug)
Cells in wells + drug
Cells in wells + gel + no drug
Cells in wells + gel + DMSO (no drug)
Cells in wells + gel + drug

Test: Cells in chip + gel + drug

Day 0: All the cells loaded
Control chip dyed

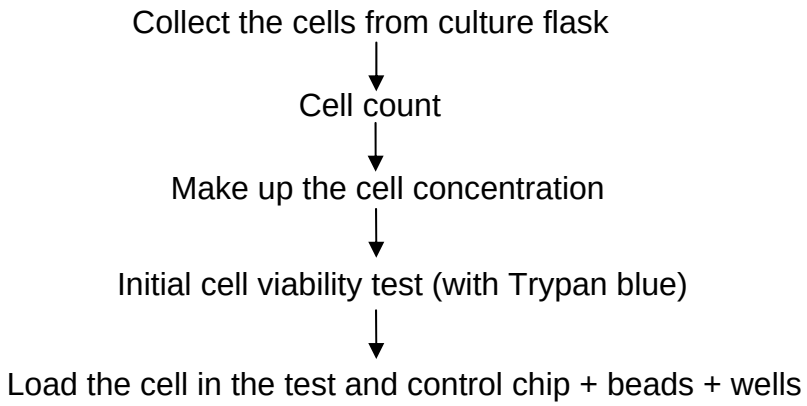

Day 1: Overall check up of the wells and the chips + dying one of the control chips (Live/Dead kit) for initial viability test
Day 2: Put in the drug (0.8 μM and 1.5 μM)
Day 3: One (or two) of the chips with the drug to be dyed (Live/Dead kit) for 24 hr viability test + One of the control chips
Day 4: One (or two) of the chips with the drug to be dyed (Live/Dead kit) for 48 hr viability test + One of the control chips (one not dyed before)
Day 5: One (or two) of the chips with the drug to be dyed (Live/Dead kit) for 72 hr viability test + One of the control chips (one not dyed before)